Choroidal-scleral cell interplay and the regulation of scleral biomechanics

Candidate: Yuyi Ren

Supervisor: Professor Maryse Bailly

Institution: Institute of Ophthalmology, UCL

Thesis degree: Master of Philosophy

Date: 2022

Declaration

I, Yuyi Ren, confirm that the work presented in this thesis is my own. Where information has been derived from other sources, I confirm that this has been indicated in the thesis. The content of my thesis is the work I have carried out since the commencement of my MPhil degree and does not include a substantial part of work that has been quantified for any other degree in any university or institution.

Abstract

Worldwide prevalence and severity of myopia have increased dramatically nowadays. High myopia and its irreversible associated eye elongation increase the risk of sight-threatening conditions. However, the exact mechanisms that drive myopia progression are still unknown. Myopia almost exclusively occurs in childhood, suggesting the adult sclera is functionally different from the young sclera. During myopia progression, the sclera becomes thinner and more elastic, and the composition of its scleral extracellular matrix changes. Similarly, the choroid is thinner and accommodation-induced choroidal secreted factors are linked to tissue biomechanics that may regulate scleral remodelling and eye elongation. Thus, we hypothesize that signals from the choroid are crucial to the regulation of scleral biomechanics. In addition, light exposure and subsequent dopamine release may regulate scleral remodelling and eye elongation, and myopia development and progression could be induced by near work.

We used human primary fibroblasts isolated from the sclera and choroid of donor eyes from different ages and antero-posterior positions to test our hypothesis. We found that paediatric scleral fibroblasts embedded in the 3D collagen gels had greater contractility than adult ones, particularly those from the anterior part of the sclera. Scleral fibroblasts' ability to contract collagen gels was enhanced following stimulation with the choroid-conditioned medium, and this promotion was not due to an increase in proliferation or change in a-SMA expression. Furthermore, the ability of choroid conditioned medium to stimulate scleral fibroblasts was completely abolished when choroid cells were treated with dopamine. This suggests that normal scleral development is regulated by a balance

between positive biochemical signals from the choroid, and negative signals resulting from a direct effect of retina-derived dopamine on the choroid cells. These findings may help improve clinical practice to control myopia development and progression in the future.

Impact Statement

Vision is one of the essential senses that raise us to experience the beauty of the world, but 50% of the world's population is estimated to suffer from myopia in 2050. Myopic patients experience irreversible blurred vision, and struggle with the elongated axial length of the eye, as it increases the risk of myopia-complicated eye diseases and even blindness. Although current interventions are capable of correcting refractive errors of myopia, no medication to control myopia progression has been licensed yet due to its poorly understood exact mechanisms. The sclera and choroid are associated with myopia progression, and sclera biomechanics is critical to maintaining normal eye growth. This study aimed to investigate if the choroid could secrete growth factors to regulate sclera biomechanics in vitro, and how this regulation could be affected by dopamine applied to choroid cells. This study also developed a functional 3D biomimetic retina, choroid and sclera interfaces to mimic an actual back of the eye.

To the best of my knowledge, this is the first study in vitro using primary human scleral fibroblasts and choroid cells that presents the discovery: choroid cell-secreted factors promote scleral fibroblast contractility, and this stimulatory effect could be inhibited by dopamine applied to choroid cells. In addition, we first developed the functional 3D biomimetic RPE monolayer, choroid and sclera interfaces in vitro. Studies from this thesis motivate us to explore the following 4 directions: 1) which molecular components of scleral fibroblasts are regulated by choroid-secreted factors. 2) which growth factors secreted by choroid cells regulate scleral biomechanics. 3) how mechanical stimulation applied to choroid cells could affect scleral biomechanics. 4) optmise the 3D biomimetic

model to explore cellular component interactions. This work inspires us in these new directions to reveal the exact mechanism of myopia, and potentially prevent and treat myopia in the future.

Despite this study is performed by MPhil student Yuyi Ren and supervisors Professor Maryse Bailly and Dr Annegret Dahlmann-Noor, this project attracted the interest and collaboration of other labs. For example, Dr Jack Hopkins (Professor Shin-Ichi Ohnuma's lab, Institute of Ophthalmology, UCL) provided PRELP protein as a potential scleral fibroblast contraction marker. Dr Victoria Tovell (Professor Pete Coffey's lab, Institute of Ophthalmology, UCL) provided IPSC-derived RPE cells to establish the retina layer of the 3D biomimetic model. Dr Clare Thompson (Prof Martin Knight's lab, School of Engineering and Materials Sciences, QMUL) would provide the support to test the mechanical stimulation's effect on choroid cells to regulate scleral biomechanics in the future. This will broaden the impact and directions of current study, and potentially to have multidisciplinary collaborations.

Table of Content

List of Abbreviations

bFGF: basic fibroblast growth factor

CCM: choroid conditioned medium

D: dioptre

dopamine-CCM: conditioned medium generated from dopamine treated choroid cells

ECM: extracellular matrix

FDM: form-deprivation myopia

FGF: fibroblast growth factor

MMP: matrix metalloproteinase

PDGF: platelet-derived growth factor

RPE: retinal pigment epithelium

SDS: sodium dodecyl sulfate

SE: spherical equivalent

TGF-β: transforming growth factor-β

TIMP: tissue inhibitor of metalloproteinase

TPA: 12-O-tetradecanoyl-phorbol-13 acetate

tPA: tissue plasminogen activator

List of Figures

List of tables

Introduction

1. Anatomy of the eye

As human beings, we live on five senses, smell, touch, taste, hearing and sight, amongst which, our daily life/experience is more heavily reliant on vision than ever before. The sense organ for sight/vision is the eye, which acquires a global shape essential for its function (**Error! Reference source not found.***)*. When light rays reflect off an object and enter the eyes through the anterior part to the retina, vision is produced, and the object could be seen. To explain this process in detail, the cornea (outer surface of the front eye) refracts the light onto the lens by light passing through the pupil. Then the lens “refracts” (bends) the light onto the retina through the vitreous chamber, and the retina finally sends messages to the optic disc by transforming the visual signal into electrical energy to produce the sense of vision that is processed by the brain ultimately. The retina is the light-sensitive tissue which forms the inner most layer of the eyeball, and the choroid forms the middle vascular layer which provides oxygen and nutritious support to the normal function of the retina. To ensure a perfect and precise focus on the retina, the shape of the ocular globe is of great importance. To provide such structural support and maintenance, the sclera forms the outer white layer which warps the eyeball that connecting to the edge of cornea.

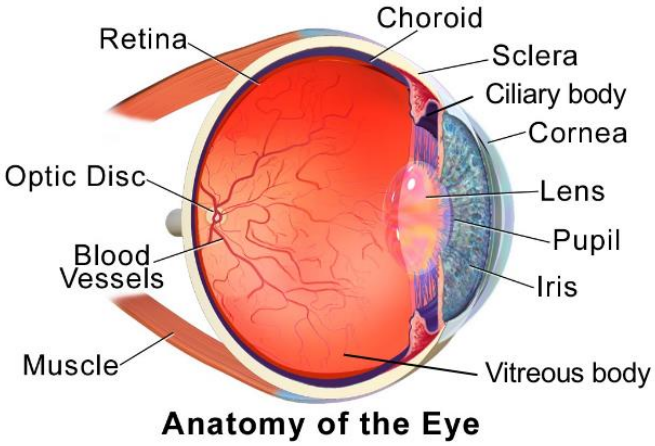

Figure 1. Anatomy of the eye. The sclera forms the outer white layer at the outmost layer of the eye, the choroid is the middle layer between the sclera and retina, and the retina is the inner layer of the eye globe. Adapted from Blausen.com staff (2014).

2. Postnatal Eye growth

With the development of medical sciences in several fields, and the increasing awareness of ophthalmic health problem, a number of eye disorders have been found to cause blurred vision. In terms of refractive error-caused blurred vision, it includes simply refractive errors, such as axial myopia and hyperopia, as well as other pathological disorders causing refractive errors, such as cataract and corneal diseases. During normal eye growth, the axial length of the eye is important in ensuring a precise focus of light onto the retina, hence it is essential to know how axial length changes in the eye growth processes. In the myopic eye, axial length elongation is usually observed, and dopamine was found to slow down this axial elongation, which will be introduced specifically in the following subsections.

2.1. Normal eye growth

2.1.1. Axial length of the eye

The axial length of the eyeball is a classic geometric parameter to describe eye size, it is the distance from the anterior cornea to the posterior retina (Schmid et al. 1996). During normal eye growth, the axial length at birth is about 16.8mm, then reaches to 22-25mm by the age of 16-18 and remains constant in adulthood, see *Figure* 2 (Bhardwaj and Rajeshbhai 2013; Hussain, Shahid, and Woodruff 2014). To monitor this process of axial length elongation, there were various studies recruited children and/or teenagers to analyse their annual axial elongation in the emmetropic eye condition. For example, the large-scale collaborative Longitudinal Evaluation of Ethnicity and Refractive Error (CLEERE) study recruited 6-14-year-old children with normal vision conditions and monitored their eye axial length for 10 years. In this observational study, they found that the axial length of the eye started from 22.7mm, and grew by approximate 0.1mm per year to reach 23.7mm in this population of emmetropic children, see

Figure *3* (Mutti et al. 2007). Moreover, the Orinda Longitudinal Study of Myopia (OLSM) also recruited 6-14-year-old emmetropic children in the United States from both white and Asian, the Singapore Cohort Study of the Risk Factors for Myopia (SCORM) recruited 6-12-year-old emmetropic children in Singapore, and both these two studies reported 0.1mm to 0.24mm per year axial elongation rate in the emmetropic groups in their 3-year observations (Chamberlain et al. 2021). This rate of axial length of the eye

increases plays a critical role in acquiring focused precise vision, an ideal refractive state named emmetropization, which presents with perfect vision when light rays precisely focus on the retina (Troilo et al. 2019). In both animal models and humans, the eyes exhibited refractive errors (blurred vision) at birth, and such errors would minify during early postnatal development and maintain emmetropia afterwards under normal conditions (Troilo et al. 2019).

2.1.2. Mechanisms of controlling eye growth

Although the exact mechanism of eye growth remains unclear, many hypotheses have been suggested. It is generally assumed that two mechanisms control eye growth in animal models, visually guided and shape-related hypotheses. One suggests that when visual manipulations are ceased from causing ametropia by monocular visual form deprivation or complete darkness feeding, such as unilateral myopia and bilateral hyperopic, the eye guided the vitreous chamber growth towards achieving emmetropia (Troilo and Wallman 1991). The other mechanism suggests that the eye shape slowly acts towards changing normal size and shape of the eye to remain emmetropization (Troilo and Wallman 1991; Smith, Hung, and Arumugam 2014). Furthermore, visually guided eye growth initially occurs in the retina and cascades in the choroid and sclera by transferring locally generated chemical messages, ultimately remodelling scleral extracellular matrix (ECM) remodelling (Wallman et al. 1995; Rada and Palmer 2007). In animal models, scleral remodelling occurred with visual stimuli. For example, matrix metalloproteinase (MMPs) expression increased in tree shrew and primate scleras, but the synthesis of collagen and proteoglycan decreased when the sclera grew in response to visual stimuli (Norton

and Rada 1995; Rada, Nickla, and Troilo 2000; Moring, Baker, and Norton 2007; Guggenheim and McBrien 1996).

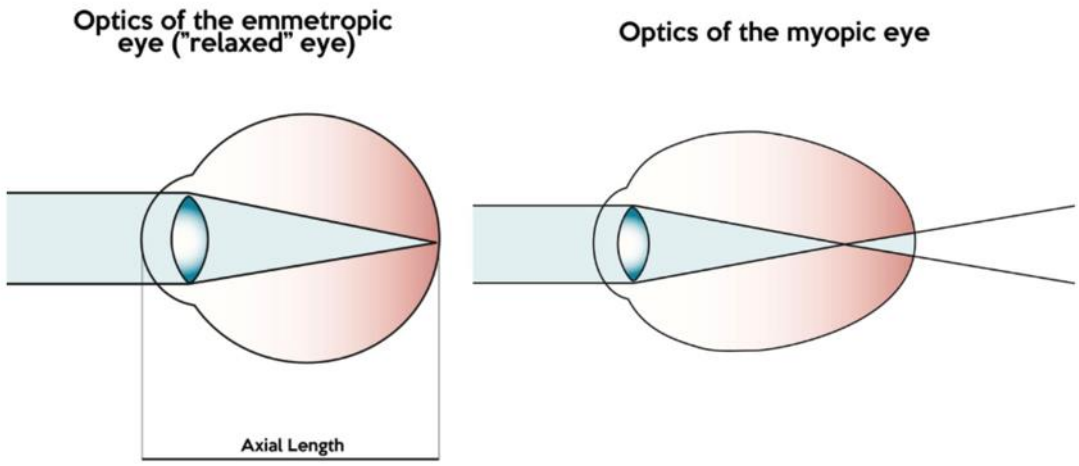

Figure 2. Schematic emmetropic and myopic eye. Adapted from Organisation of Plano, Singapore, 2018, say my(no)pia: prevent myopia from developing into high myopia, https://plano.co/say-mynopia-prevent-myopia-from-developing-into-high-myopia/. In the emmetropic eye, the parallel rays of distant objects are focused on the retina. In the myopic eye, the axial length of the eye increased due to the elongated eye shape, and the light from distant objects is focused in front of the retina.

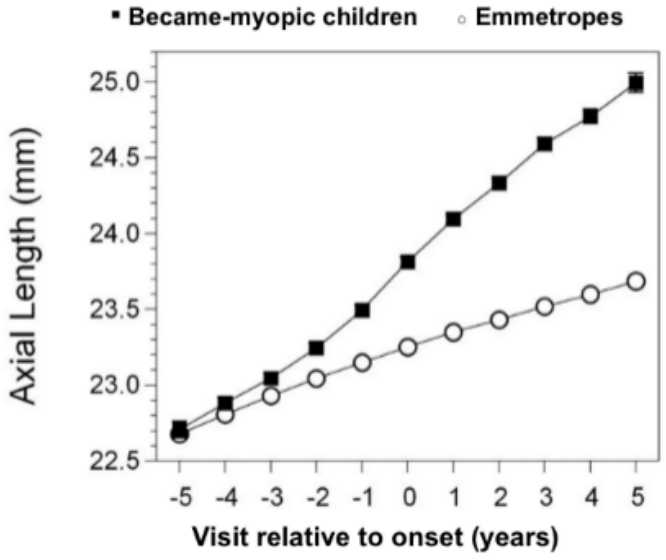

Figure 3. The difference in axial length between myopes and emmetropes. Adapted from Mutti, D. O. et al., 2007. The year 0 was defined when the emmetrope at least one visit before a visit during myopia was diagnosed, one year before onset was -1 and so on to 5 years prior was -5, while one year after onset was year 1 and up to year 5 in s similar fashion.

2.2. Myopia

2.2.1. Definition, prevalence, severity, and treatment

Myopia is a common eye disorder, usually due to the elongated axial length of the eye. It also called near-sightedness or short-sightedness, and myopic patients usually have blurred vision when the distant light from an object focused in front of the retina (*Figure 2).* The WHO (World Health Organisation) officially stated in 2021 that the leading global causes of vision impairment are uncorrected refractive errors, cataracts, age-related macular degeneration, and glaucoma. Myopia is one common type of uncorrected refractive error, attracting more attention gradually. In clinical practice, myopia is generally classified into three classifications depending on visual acuity: low, moderate and high myopia. For example, it is widely accepted to define three classifications by a spherical equivalent (SE) system in clinical use, and the SE is the spherical power when the circle of least confusion of a sphero-cylindrical lens is coincident with the focal point. It defines low myopia < -3.0 dioptres (D), high myopia > 6.0 dioptres (D), and moderate myopia (-3.0 Dioptres to -6.0 Dioptres). The number of dioptre indicates the severity of myopia, the larger the number is, the severer the refractive error.

In recent decades, myopia has become the most common uncorrected refractive error worldwide, particularly in Asia. For

example, the prevalence of myopia in the adult population in many countries is 10-30%, and 80-90% in young adults in partial regions of East and Southeast Asia, such as Singapore, China, and South Korea (Baird et al. 2020). In South Korea, 96.5% of 19-year-old young adults are myopic (Baird et al. 2020). In the UK, 23% of 12-13-year-old children were estimated to require glasses for myopia by applying NICER (The Northern Ireland Childhood Errors of Refraction) study data (McCullough, O'Donoghue, and Saunders 2016; Breslin, O'Donoghue, and Saunders 2013). By 2050, it is predicted that approximately 5 billion people (50% world's population) will be myopic, while it was estimated that 1.5 billion myopes (23% world's population) in 2000 (Holden et al. 2016). The importance of myopia study is not only due to the increasing prevalence, but also the severity of progressive myopia and its complications. Myopia can increase the risk of sight-threatening complications, especially when progressing to high myopia (Haarman et al. 2020). It was estimated that 20% of the myopic population has high myopia, which increases the risk for vision loss due to retinal detachment, choroidal neovascularization, cataracts, glaucoma, macular degeneration, and macular atrophy (Wu et al. 2016; Haarman et al. 2020). Moreover, myopia onset and progression almost exclusively occur during childhood and young adolescence, which enables myopia to keep progressing to high myopia from young age, increasing the risk of irreversible elongated eye and sight-threatening conditions (Baird et al. 2020; Williams et al. 2015).

Up to now, there are several prescriptions in clinical practice to improve the blurred vision of myopic patients, such as eyeglasses, contact lenses, refractive surgery, and implantable contact lenses that correct the refractive error by modifying the focus onto the retina. The dual focus contact lenses slowed myopia progression as the

refractive error and axial elongation in the myopic eye were changed less compared to using single-vision glasses (Anstice and Phillips 2011; Chamberlain et al. 2022), but the mechanism of slowing myopia progression remained unclear. Also, all these current prescriptions cannot reverse the axial length elongation of the eye or cure myopia in essence, but only change the refractive index of either cornea or lens for light rays precisely focus on the retina. Orthokeratology is the specially designed and fitted contact lens, that temporarily reshapes the cornea to correct refractive errors by refracting light rays to focus on the retina. Although orthokeratology showed partial efficiency in slowing the axial eye elongation by steeping the mid-peripheral cornea, as it slows down myopia progression rate from 0.2 to 0.3 dioptres per year spherical refractive error change compared to 0.4 to 0.5 dioptres per year with single-vision glasses correction (Lee, Wang, and Chiu 2017). It is not widely used as it requires specially trained skills for fitting, and it leads to discomfort when worn overnight (Huang et al. 2016). Recently, there are some pharmacological interventions for myopia control have been applied in the clinical trial, including atropine and pirenzepine. In particular, low-dose (0.01%) atropine for children's myopia progression control has been reported to exhibit the efficiency to slow down refractive error change and axial length elongation in several clinical trials, such as ATOM2 (Atropine for the Treatment of Myopia 2) study, LAMP (Low Concentration Atropine for Myopia Progression) study (Fu et al. 2020; Khanal and Phillips 2020). These pharmaceuticals showed effective suppression of refractive error and slowed the progression of irreversible eye elongation, but the exact mechanism of myopia progression and how pharmacological interventions work are still unclear (Baird et al. 2020; Huang et al.

2016; Upadhyay and Beuerman 2020; Wu et al. 2019; Siatkowski et al. 2004).

2.2.2. Mechanisms of myopia development and progression

The axial length elongation of the eye is the classic manifestation of myopia, it is essential to unveil how this abnormal elongation progresses to understand myopia development and progression.

Figure *3 shows* the CLEERE study found just before the myopia onset (year 0) in the became-myopia group, the axial eye grew in the fastest pattern by 0.33mm per year, then 0.2-0.27mm growth per year after onset during the myopia progression. This axial length of the eye showed a distinct annual growth rate in this became-myopia children to reach 25mm, compared to the emmetropic children ultimately reach about 23.7mm. In addition, some studies observed the axial length of the myopic eye in adulthood, which exceeds 26.5mm in adults (Saka et al. 2010; Ohno-Matsui et al. 2021). Although limited studies uncovered the underlying mechanism of this axial elongation in the myopic eye, earlier work suggested that near work and related increased accommodation were key factors to promote myopia development (Morgan and Rose 2005). Gwiazda and colleagues suggested when the near objects were presented in front of the emmetropic eye, the eye accommodated bringing the objective light rays to precisely focus on the retina. In the myopic eye, less accommodation was functionally working to fail in focusing on the retina, which is called the “lag of accommodation”. The “lag of accommodation” is the quantification of the difference between

accommodative stimuli and measured accommodative response, and a larger lag of accommodation in cooperation with near work operated myopia development and progression (Gwiazda et al. 2004). For example, hyperopic defocus, is the condition that reduced accommodative response during nearwork leads to a lag accommodation vice versa (Chen et al. 2020). However, these findings were all about clinical manifestations, the exact mechanism underlying myopia development and progression still remains unknown.

2.3. Signal effect on eye growth

The eye is a vision sense organ like all the other organs in the body, functionally developing throughout life. The authoritative American Optometric Association (AOA) also states that the axial length of the eye usually starts to grow in the first two years of life and reaches the fastest growth rate in puberty, until steadies in adulthood (AOA 2022), which indicates eye growth is a long-term process. Hence, it is also important to uncover the mechanism that affects eye growth, either acting as a positive signal to promote eye growth or a negative signal to inhibit it.

2.3.1. Accommodation promotes eye growth

The vision is produced in a complicated cooperation of eye tissues, thereby there are several hypotheses about how these tissues affect the others in eye accommodation. For example, some earlier work hypothesized that the ciliary muscle was critical to deform the lens to adjust eye accommodation for achieving object light rays precisely focus onto the retina (Jeon et al. 2012; Buckhurst et al. 2013). The ciliary body consists of the ciliary muscle, which is anteriorly

controlling the lens contraction. Fisher and colleagues found that human lens accommodation response exhibited a positive correlation with ciliary muscle stretching *in vitro* (Fisher 1977). In the testing of human eyes *in vivo*, Domkin and colleagues computed ciliary muscle contraction force from lens accommodation referred to Fisher's formula to track refraction during computer mouse work, and they found when relevant near viewing was employed, a small "lag of accommodation" in the eye lens was shown, exhibiting a hyperopic refraction (light rays focus behind the retina) when relevant far viewing was employed (Domkin, Forsman, and Richter 2019). The ciliary body not only connects to lens, but also continuously connects to the anterior choroid at its posterior part. In the chicken model of form-deprivation myopia (FDM), the chicken's eye is covered with a frosted diffuser, which prevents the eye from receiving a clear vision, leading to myopia development. In this model, the choroidal thickness of young chicks acutely decreased during eye accommodation and myopia development (Nickla and Wallman 2010; Wildsoet and Wallman 1995). In human model *in vivo*, some unpublished preliminary work conducted by Dr Annegret Dahlmann-Noor in our lab used OCT (optical coherence tomography) measurement to find that the mean subfoveal choroidal thickness of children's healthy eyes decreased from 320 to 300um with accommodative effort, which was similar to the chicken FDM model in terms of choroidal thickness decrease during myopia progression. It is possible this choroidal thickness decrease was due to the mechanical stretching (accommodation) exerted from the adjacent posterior ciliary body stretching. And mechanical stretching (accommodation) might serve as a positive signal to promote eye growth.

2.3.2. Light exposure inhibits eye growth

Evidence has shown that children who spend more time in outdoor activity have a lower incidence and slower progression of myopia (Wu, Chen, Lin, et al. 2018; Rose et al. 2008). Recent studies suggested that this light exposure and subsequent dopamine release are important components that regulate axial eye elongation via the dopaminergic retina-sclera signalling pathway (Feldkaemper and Schaeffel 2013; Zhou et al. 2017). In an observational study that monitored the axial eye length for 18 months, school-aged children were found to have less axial eye growth when they had a greater light exposure which collected from a wrist-worn light sensor device (Read, Collins, and Vincent 2015). In the animal models *in vivo*, the ambient light inhibited the progression of form-deprivation myopia in chicks and rhesus monkeys (Stone et al. 2016; Karouta and Ashby 2014; Smith, Hung, and Huang 2012). In these FDM models, dopamine release was found to be down-regulated by measuring its precursor L-DOPA concentration in the histochemistry method, suggesting dopamine played an inhibition role in the axial eye growth (Iuvone et al. 1989; Megaw, Morgan, and Boelen 1997). In addition to developing myopia in animal models by covering eyes to achieve form-deprivation myopia, placing the minus spectacle lenses in front of the eye also can achieve myopia model. The spectacle lenses serve as a complementary lens in front of the cornea, they refract the light to focus behind the retina. With sufficient stimuli, the eyeball accommodates to elongate axial length to move the focal plane (retina) forward to achieve a good vision, which leads to axial elongation like a myopic eye as a myopia model. In this spectacle lenses-induced myopia animal model *in vivo*, some studies used intravitreal injections of dopamine receptor agonists to see how dopamine could influence eye growth. These researchers found that

choroidal thickness was increased transiently with the injection of non-specific and D2 agonists (apomorphine and quinpirole), whilst D1 agonist SKF 38393 did not increase choroidal thickness. (Nickla and Wallman 2010). Since choroidal thickness decreased during eye accommodation and myopia progression, which was opposite to dopamine agonists had an effect on increasing choroidal thickness. Hence, these researchers suggested dopamine had a negative effect on eye accommodation and myopia progression, and they further hypothesized that dopamine was possibly related to the inhibition of axial eye growth. Moreover, in studies in the FDM rabbit model, the scleral thickness of form-deprivation myopic eyes increased with dopamine treatment, whilst the control form-deprivated myopic eye without dopamine treatment exhibited decreased scleral thickness. In this FDM rabbit model, researchers also found collagen fibril diameter in the sclera was increased with dopamine treatment (Lin et al. 2008). These findings suggested that dopamine release essentially serves as a negative signal to keep normal sclera development and maintain normal eye growth.

3. Sclera

The sclera is the connective tissue, wrapping the eyeball at the outmost layer, structurally playing an essential role in maintaining eye shape and defining the axial length of the eye. This structural integrity is provided by the scleral extracellular matrix of collagen and proteoglycans, as well as scleral fibroblasts embedded in the extracellular matrix. On the one hand, the scleral extracellular matrix and cellular components contribute to supporting and maintaining scleral biomechanics, which enables the sclera to remain good strength and elasticity for controlling the eye growth (Metlapally and

Wildsoet 2015). On the other hand, scleral thickness decreases, and scleral remodelling happens during myopia development and progression, such as the collagen are reduced and proteoglycan synthesis decreased in chick model (Norton and Rada 1995). Hence, sclera biomechanics is of great importance to regulate eye growth, the following subsections will introduce them in detail.

3.1. Sclera composition and properties

3.1.1. Structure

The sclera is the outmost layer of the eyeball *(Figure 4)*, it sits anteriorly to the cornea, and posteriorly to the optic nerve***(Error! Reference source not found.)***. The sclera constitutes about 90% of the connective tissue coat of the eye, and provides support and maintenance for the shape of the eye globe. In most mammals, the visible sclera of the eye is the same colour as its iris. However, all the healthy human sclera is white no matter what kind of colour of the iris. In the human eye, the thickness of the sclera varies from 0.3mm to 1mm, regionally different in eye orientation (frontal/maxilla and nasal/temporal) (Troilo et al. 2019; Norman et al. 2010). At the corneal scleral limbus, scleral thickness is about 0.5mm, and increases to about 1mm near the optic nerve (Olsen et al. 1998). The sclera mainly consists of collagen and elastic fibre, predominantly containing collagen type I (90%), as well as a small proportion of collagen type III (Bailey 1987; Keeley, Morin, and Vesely 1984). This dense collagenous structure regulates scleral stiffness (Wang et al. 2020), and the composition and stiffness of the sclera are spatially compartmented, with antero-posterior position differences, presenting higher structural stiffness and thickness in the peripapillary at the posterior sclera (Seko et al. 2017; Xi et al. 2017; Read et al. 2016). The scleral stiffness and thickness differences are

not only in different antero-posterior position, but also in different ages. The growing sclera in the children's eye is thinner than the adult ones, and the sclera becomes stiffer with aging (Read et al. 2016; Friberg and Lace 1988).

3.1.2. Biomechanical property

In the human eye, Young's modulus of the posterior sclera is about 1.8 MPa, and the anterior sclera is about 2.9MPa(Asejczyk-Widlicka et al. 2007), which indicates that the elasticity of sclera also exhibited antero-posterior position differences like scleral thickness and stiffness. The creep rate is another mechanical property parameter, it is the time rate of deformation of a material subject to stress at a constant temperature. During myopia development and progression, some studies have shown that scleral biomechanics changed a lot. For example, the elasticity and creep rate of the sclera increased in the myopic eye, matrix composition changed as collagen content reduced, and the sclera became thinner during myopia progression, particularly at the posterior pole; (McBrien, Jobling, and Gentle 2009; Hayashi et al. 2013; Troilo et al. 2019). Moreover, the tensile properties of the sclera, in conjunction with normal intraocular pressure, contribute to resistance to internal and external forces during normal eye growth (McBrien, Jobling, and Gentle 2009).

3.1.3. Cell population

In connective tissue, fibroblasts are the most common type of cells. Fibroblasts stem from a mesenchymal origin, usually presenting elongated spindle-shape or stellate shape and projections (Dick, Miao, and Limaiem 2022). Fibroblast contributes to the synthesis of collagen and extracellular matrix, providing a structural framework

(“stroma”) for tissues, and playing a critical role in wound healing (Bainbridge 2013). It is generally accepted that fibroblasts have two states with different structures, active fibroblasts and inactive fibroblasts, helping tissue maintenance and metabolism. Active fibroblasts are characterized by their abundant rough endoplasmic, and inactive fibroblasts are recognized by their smaller, spindle-shape and less rough endoplasmic reticulum (Dick, Miao, and Limaiem 2022). Some studies also suggested fibroblasts have two subtypes with different metabolic activities: quiescent (inactive) and proliferating (active) cells. Quiescent fibroblasts are in the reversible state to retain the ability to re-enter cell proliferation but do not divide, and they refer to small, dense cells passively exiting from the cell cycle, exhibiting high metabolic activity, whilst commonly referred fibroblasts are proliferating cells that replicate the entire cellular components to divide (Lemons et al. 2010; Chen et al. 2012). In the human sclera, resident cells appear elongated and closely apposed to the collagen bundles, primarily scleral fibroblasts. Scleral fibroblasts are stellate or spindle-shaped cells with a larger nucleus and relatively scanty (thin, lymphocyte-like) cytoplasm appearance (Watson and Young 2004). Myofibroblast is one type of cell typically differentiated from fibroblast by mechanical stress induction, or cell signally factors stimulation, such as transforming growth factor-beta(TGF-β) (McBrien, Jobling, and Gentle 2009). Myofibroblasts typically express a-smooth muscle actin (a-SMA), characterized as contractile non-muscle cells for possessing secretory features of fibroblasts, and contractile features like smooth muscle cells, playing an important role in the wound healing response (Yuan et al. 2018; Tomasek et al. 2002). In the human sclera, the proportion of myofibroblasts increases with aging, which suggests that fewer

scleral myofibroblasts are in the sclera when the eye is growing rapidly at a young age (Poukens, Glasgow, and Demer 1998).

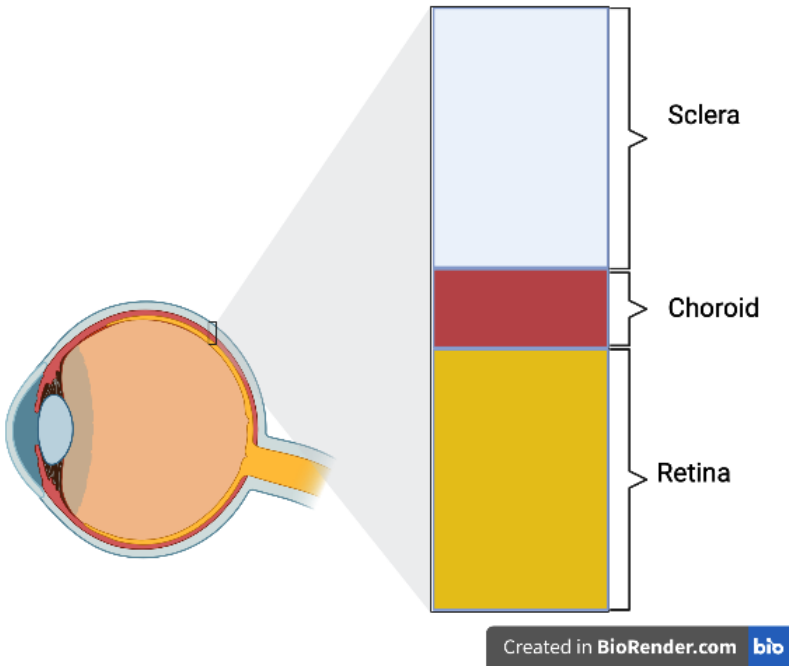

Figure 4. Schematic diagram of eyeball layer. The sclera is adjacent to the choroid at the outmost layer, and the retina is adjacent to the choroid at the inner layer of the eyeball.

3.2. Scleral biomechanics regulation

The scleral extracellular matrix is critical in regulating scleral biomechanics. The sclera extracellular matrix (ECM) is mainly composed of a scaffold of protein fibrils, collagen, elastin, and interfibrillar proteoglycans. It presents type I and III collagen, but predominantly presents the type I collagen (Watson and Young 2004). Scleral ECM remodelling was hypothesized to be associated with visually guided eye growth. With visually guided eye growth, a cascade of locally generated chemical messages initiated from the retina, and transited to the sclera, which contributed to scleral ECM remodelling. (Wallman et al. 1995; Rada and Palmer 2007). The visual environment significantly influenced the synthesis and

turnover of proteoglycans in the sclera. In particular, the synthesis of proteoglycans in the posterior sclera was related to maintaining emmetropic refraction (perfect focus) and normal ocular size (Rada et al. 2000). Furthermore, the collagen and proteoglycan synthesis of scleral ECM are controlled by some specific growth factors, suggesting scleral ECM remodelling is also assumed to be controlled by these specific growth factors. For example, scleral proteoglycan synthesis increased significantly in later adulthood, which was related to age, suggesting that scleral growth might be associated with systemic growth factors, such as insulin-like growth factors (Rada, Nickla, and Troilo 2000). Jobling and colleagues also found that sclera remodelling was regulated by fibroblast growth factor (FGF-2) and transforming growth factor-β (TGF-β). FGF-2 is an inhibitor of collagen synthesis, and TGF-β plays an important role in controlling fibroblast proliferation, synthesis of collagen, proteoglycan and matrix metalloproteinase-2 (MMP2) in the extracellular matrix (Jobling et al. 2004). MMPs are also important components in the extracellular matrix, serving as enzymes to process or degrade collagen and other proteins (Sternlicht and Werb 2001). MMPs are induced by several functional cytokines, such as interleukin (IL)-1a and tumour necrosis factor (TNF) (Di Girolamo et al. 1997). Tissue inhibitor of metalloproteinase-1 (TIMP-1) is secreted by connective tissue cells such as fibroblasts, which is also involved in scleral ECM remodelling by inhibiting MMPs (Liu, Chen, and Lilly 2008). Moreover, scleral ECM also could be degraded by reactivation of basic fibroblast growth factor (bFGF) and cytokines, such as interferon γ, platelet-derived growth factor (PDGF), and thymocyte derived growth factors (Watson and Young 2004; Schache and Baird 2012).

In addition to the scleral ECM, cellular components of the sclera also contribute to scleral biomechanics as fibroblasts are mechanosensitive cells that predominantly produce scleral ECM (Duffy 2011). With elevated intraocular pressure-induced mechanical strain, myofibroblasts are differentiated from fibroblasts in the sclera, playing a critical role in regulating ECM synthesis, secretion and remodelling (Qu et al. 2015). As mechanical stretching promotes not only eye growth, but also fibroblasts differentiation, suggesting it is possibly that the proportion of myofibroblasts increases during eye growth. In the FDM mouse model, recent studies identified that the sclera had distinct fibroblasts populations in the FDM mouse eye, exhibiting “fibroblasts” shifted to “myofibroblast-like” in the myopic mouse sclera (Wu, Chen, Zhao, et al. 2018; Morgan, Ashby, and Nickla 2013). In tree shrew myopia models developed by light/dark cycles, recent studies also found that the a-SMA expression level in the sclera cells was increased during myopia development, suggesting the number of myofibroblasts may be increased in this myopia development process (Jobling et al. 2009; Backhouse and Phillips 2010). Hence, different fibroblasts subpopulations that include fibroblasts and myofibroblasts may be co-existing in the sclera to coordinate biomechanical properties and growth of the sclera.

4. Choroid

Earlier work demonstrated that with visual signal stimuli, the ciliary muscles, and lens were in cooperation with the choroid to adjust, which ensured the light focused precisely on the retinal plane (Wallman et al. 1995). It initially suggested that the choroid may be relevant to controlling eye growth. On the one hand, with ciliary body mechanical stretching, the eye lens could be contracted to adjust eye

accommodation, which may play a positive signal role in promoting eye growth. In consideration of the choroid position, it connects to the ciliary body anteriorly, and its thickness decreased during myopia development and progression (Nickla and Wallman 2010; Wildsoet and Wallman 1995), the choroid might be of great importance in promoting eye growth. On the other hand, dopamine is released from the retina, and dopamine may serve as a negative signal to inhibit eye growth. In this signal pathway, the choroid possibly sends biochemical messages from the retina to the sclera due to its adjacent position between the retina and sclera, contributing to inhibiting eye growth. Hence, it is essential to know more information about the choroid.

4.1. Structure

The choroid is the vascular layer of the eye, containing connective tissues but made up of a significant amount of blood vessels, lying between the retina and the sclera *(Figure 4).* The choroid anteriorly forms the ciliary body, and extends posteriorly to the optic nerve, see ***Error! Reference source not found.***. It also forms the uveal tract along with the ciliary body and iris, supplying oxygen and nourishment to the outer layer of the retina. The thickness of the choroid varies from 0.1mm in the peripheral areas to 0.2mm at the far extreme posterior of the eye. The choroid consists of five different layers, including Bruch's membrane from the inner layer to Choriocapillaris (layer of tiny blood vessels), Sattler's layer (layer of medium blood vessels), Haller's layer (layer of large blood vessels), and suprachoroid at the outer layer of the choroid. In normal human eyes, the Heel modulus of the Bruch's membrane/choroid complex (BMCC) was 370KPa, while sclera was found to be much stiffer with a Heel modulus of 4400KPa, and the elasticity of the choroid was

found to decrease with older age (Ferrara et al. 2021). During eye accommodation, the choroidal thickness acutely decreases, suggesting the choroid significantly changes during visual manipulations (Zhang and Wildsoet 2015; Nickla and Wallman 2010). Although the change of choroid thickness may partly result from choroidal blood flow variation and vascular permeability (Novais et al. 2015; Zhang et al. 2019), some studies hypothesized that choroidal tissue thickness could be modulated by secretion of osmotically active proteoglycans, or by contracting nonvascular stromal smooth muscle cells (Nickla and Wallman 2010). In healthy children's eyes, the mean subfoveal choroidal thickness decreased significantly with accommodative effort, which was much more significant than that in adult eyes (Daniel et al. 2018), highlighting the difference in tissue mechanics in children compared to adults. In chick FDM eyes, the choroidal thickness increased in response to myopic defocus (elongated eye) by moving the retina towards the image plane and compensating for imposed refractive error, and its thickness oppositely decreased in response to hyperopic defocus (shortened eye) (Wallman et al. 1995). This finding suggests that the choroid might participate in modulating eye growth by adjusting the refractive state.

4.2. Cell population

The choroid is a highly vascularized layer of the connective tissue of the eye, its blood vessels are critical to delivering nutrients, and oxygen to supply the retina. The blood vessels contain epithelial cells, endothelial cells, pericytes, and vascular smooth muscle cells (Espinosa-Heidmann et al. 2005; Kur, Newman, and Chan-Ling 2012; Scholfield, McGeown, and Curtis 2007). However, besides the vascular cells, the choroid cellular component is also a mixture of

various nonvascular resident cells, including predominant fibroblasts which form the choroid stroma., Melanocytes are also presented in the choroid stroma, secreting melanin pigment which absorbs light and protects choroidal blood vessels from light toxicity (Sohn et al. 2014). In addition, non-vascular smooth muscle cells and immunocompetent cells are in cooperation with fibroblasts and melanocytes, forming the choroid stroma to modulate intraocular pressure and accommodation (Nickla and Wallman 2010).

4.3. Choroid secretome

The choroid consists of abundant blood vessels and stroma, it has the function of secreting various growth factors to develop choroid growth and maintain choroidal vasculature. For example, choroidal endothelial and stromal cells secret bFGF, vascular endothelial growth factor (VEGF), and hepatocyte growth factor (HGF), which promote and/or inhibit endothelial cells differentiation, migration and proliferation to maintain choroidal vasculature (Saint-Geniez, Maldonado, and D'Amore 2006; Frank et al. 1996; Ogata et al. 1996; Grierson et al. 2000). Moreover, choroid cells could also secret MMPs (MMP1, MMP2, MMP3, MMP9) and their tissue inhibitors (TIMP3) (Nickla and Wallman 2010), TGF-β and t-PA (tissue plasminogen activator), and these growth factors are involved in maintaining choroidal capillaries and developing choroidal stroma (Zhang and Wildsoet 2015; Steen et al. 1998).

5. Choroidal-scleral interplay

A variety of studies have demonstrated that during myopia progression, the thickness and elasticity of the sclera decreased (Friberg and Lace 1988; McBrien, Jobling, and Gentle 2009; Read et al. 2016; Asejczyk-Widlicka et al. 2007), as well as the choroidal

thickness, which decreased acutely in the myopic eye (El-Shazly et al. 2017). Since choroid and sclera are involved in myopia development, both of them exhibit decreased thickness, suggesting the choroid and sclera might function as a block or interact in the same direction during the eye growth (Metlapally and Wildsoet 2015; Zhang and Wildsoet 2015).

The biomechanical property of the sclera is essential to control eye accommodation, as it ensures the scleral integrity to structurally support the eyeball. In both animal models and human eyes, structural biochemical changes in the scleral extracellular matrix are associated with the high myopia progression (Troilo et al. 2019; Hayashi et al. 2013). Some studies have demonstrated that scleral biomechanics was not only simply changed by tissue redistribution since the sclera accommodates to stretch in response to the elongated eye, but also associated with the physical loss of the scleral extracellular matrix (Gentle et al. 2003; McBrien, Lawlor, and Gentle 2000). For example, a number of studies stated that secretion of matrix components (such as collagen) decreased during myopia progression, but the levels of remodelling proteins such as MMPs (Harper and Summers 2015; Metlapally and Wildsoet 2015; Liu et al. 2017) increased. The choroid is thought to regulate scleral metabolism during visually guided eye growth, as its position is directly adjacent to the sclera, and it has the function to secrete some growth factors to regulate the scleral remodelling (Wallman et al. 1995; Summers Rada and Hollaway 2011).

There are several growth factors that could be synthesized by the choroid, such as bFGF, TGF-β, MMPs and TIMPs, and these growth factors are also implicated in the scleral ECM remodelling (Zhang and Wildsoet 2015; Steen et al. 1998; Nickla and Wallman 2010). A microarray gene profiling applied to retinal pigment epithelium

(RPE)/choroid preparations from marmosets undergoing visual manipulations has revealed altered expression of a significant number of genes, including secreted growth factors linked to tissue mechanics such as TGF-β and FGF-2 (Shelton et al. 2008). It suggested that choroid could also secret TGF-β and FGF-2, which contributes to scleral ECM remodelling. Furthermore, some studies co-cultured scleral tissue with choroid tissue from form-deprivated myopic eyes, and found that scleral glycosaminoglycans (GAG) synthesis from the myopic sclera was significantly increased compared to normal eyes (Rada, Thoft, and Hassell 1991; Rada et al. 1992). Since the GAG is another component of the scleral ECM, it is assumed that these findings suggested choroid have the effect on scleral grwoth. Moreover, scleral proteoglycans synthesis can also be regulated by choroidal retinoic acid (Zhang and Wildsoet 2015). And in the FDM animal models, proteoglycan synthesis was differentially modulated by choroidal fluid removed from eyes undergoing recovery following experimentally induced myopic defocus compared to the myopic eye (without recovery) and emmetropic eye (Rada and Palmer 2007). Hence, altogether suggests that choroid might secret some growth factors, which regulate scleral ECM remodelling.

6. Retina

The retina is the innermost tissue layer of the eye (***Error! Reference source not found.****),* playing an important role in light perception, which translates images to the brain. Most importantly, what comes into an interest in this project, is that dopamine is released from the retina in the eye, and it is adjacent to the choroid *(Figure 4),* completing our hypothesis about the dopamine from light-mediated signals involved in eye growth by diffusing to choroid and

sclera ultimately. In terms of histology, the retina consists of ten individual layers, including an inner limiting membrane from the innermost, then nerve fibre layer, ganglion cell layer, inner plexiform layer, inner nuclear layer, outer plexiform layer, outer nuclear layer, outer limiting membrane, segments of photoreceptors, and retinal pigment epithelium (RPE) at the outermost which is closest to the choroid *(Figure 5).* The RPE is a single layer of pigmented cells which forms a barrier between the retina and choroid, playing an important role in absorbing scattered light to improve the visual image quality and diminish the photo-oxidative stress (Strauss 2005). In the eye, dopamine is released by amacrine cells and D1 and D2 dopamine receptors are distributed in the retina, playing an important role in messaging chemicals for light adaption (Witkovsky 2004). The vitreous body is adjacent to the inner retina, while the choroid is oppositely adjacent to the outer retina, see *Figure 1*. A corollary about a dopamine diffusion model from the retina to the vitreous chamber was presented by Wistkovsky and his colleagues, they suggested that the vitreous chamber represented a sink for diffused 'liquids' from the retina, and its dopamine content was proportional to the net release rates from the retina (Witkovsky 2004; Witkovsky et al. 1993). Although it is unclear if the dopamine in the retina could diffuse to the choroid, which is oppositely diffuse to the vitreous chamber, dopamine has been found to influence the choroid, such as increasing the choroid blood flow. In the rabbit model *in vivo*, intravitreal injection of dopamine was found to increase choroid blood flow by laser doppler flowmetry measurement, and selective D1/D5 receptor stimulation decreased choroidal vascular resistance and intraocular pressure (Reitsamer, Zawinka, and Branka 2004).

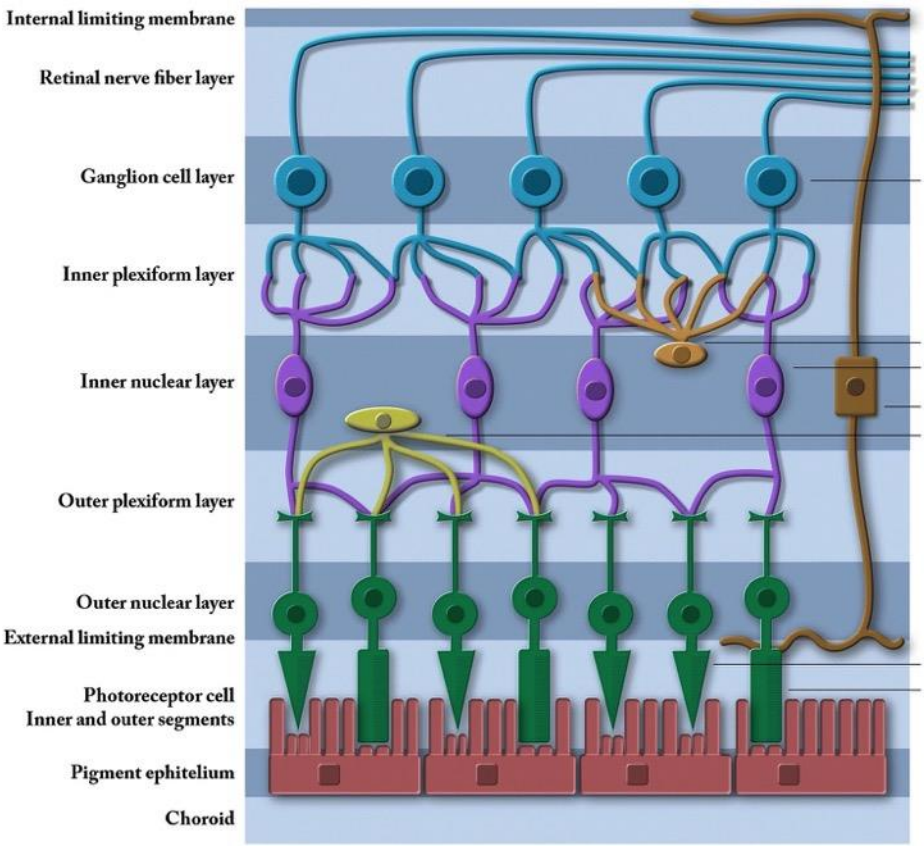

Figure 5. Ten layers in the retina. Cited from Andrea Cerveró et al. 2021.

7. Hypothesis and objectives

We hypothesize that signals from the choroid are crucial to the regulation of scleral biomechanics. The choroid may be central to regulating the sclera growth, integrating signals from light (retinal-mediated dopamine release), and controlling the scleral growth and eye growth (*Figure 6).* In our hypothesis, light exposure stimulates dopamine release from the retina. Dopamine diffuses to the choroid and stimulates the synthesis of choroidal secreted factors, which play an inhibitiory role in scleral growth, exhibiting a negative biochemical signal to stop eye growth.

In this study, we aim to test our hypothesis by looking at the interplay between choroid cells and scleral fibroblasts *in vitro* using

primary cells isolated from human paediatric and adult donor tissue. Our objectives are proposed as follows:

1). Investigate the effect of choroid cell-secreted factors on biomechanical properties of scleral fibroblasts, and how this is affected by biochemical stimulation (dopamine) applied to choroid cells.

2). Engineer a functional 3D biomimetic retina, choroid, and sclera interfaces to mimic an actual back of the human eye.

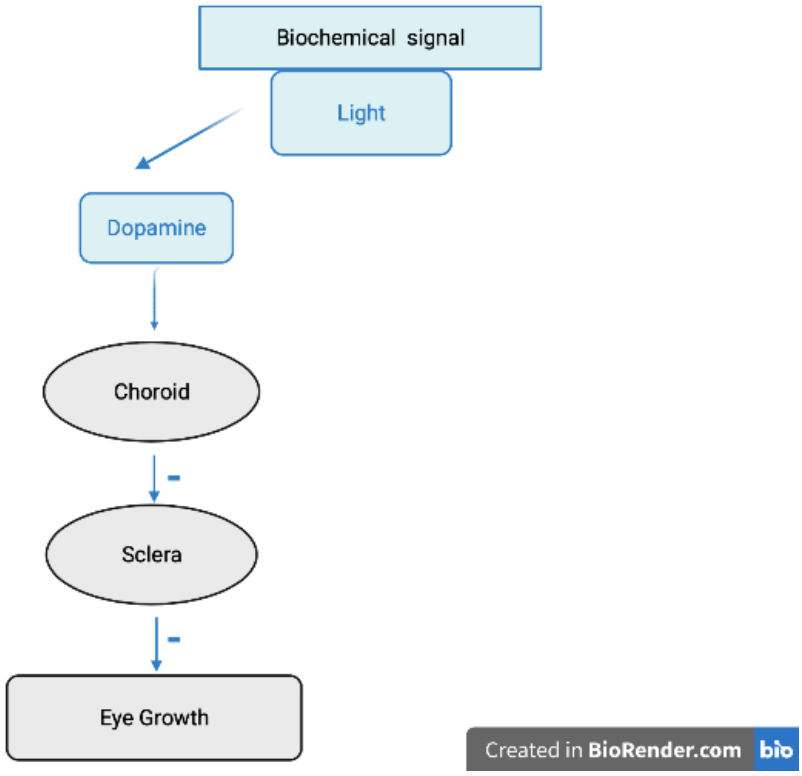

Figure 6. Schematic of hypothesis on how choroid signals regulate sclera biomechanics and eye growth. Light-mediated dopamine released from the retina acts on the choroid to inhibit/counteract the growth-promoting signals, The blue line is a negative signal pathway.

Method

1. Cell Culture

1.1. Primary cell isolation

Human scleral fibroblasts (HSF) were isolated from sclera tissue of donor eyes and established as primary cultures by Professor Maryse Bailly. Donor eyes were collected from 2 different eye banks [NIIOS Amnitrans Eye Bank (AER), Rotterdam, the Netherlands, and NHSBT Eye Bank, Bristol, UK), specifically requested as to have no sign of prior eye issues, with consent and were approved by the Ethics committee. The sclera was symmetrically divided into 4 different quadrants (nasal, temporal, inferior, superior), and 3 different sections (anterior, equatorial, and posterior), as shown in *Figure 7*. Human scleral fibroblasts growing from the tissue fragments were trypsinized (0.05% Trypsin-EDTA, Sigma, UK) when confluent and cultured in T75 tissue culture flasks (Corning, USA) in the complete medium [Dulbecco's Modified Eagle's Medium (DMEM, 4.5 g/L glucose, Gibco, Life Technologies, UK) supplemented with fetal bovine serum (FBS, 10% vol/vol, Biosera, France), penicillin (100U/ml, Gibco, Life techniques), streptomycin (100 ug/ml, Gibco, Life techniques), and L-glutamine (2mM, Gibco, Life Technologies, UK)], and incubated at 37^{o}C, 5% CO_2. The culture medium changed every two days for routine cell culture, and the flasks were split 1:3 when confluent. The isolated primary human scleral fibroblasts were named HSF (anonymised donor number), with the right (L) or left (R) eye, their original quadrants (Q1-Q4) and positions (A, E or P) in the sclera tissue. With regards to the position of those isolated cells, only those cells positioned in the anterior and posterior were used in the experiments but excluded those in the equatorial position were due to limited time. The human scleral fibroblasts used for all experiments in this project are listed in *Table 1* with donor information. All cells were used between passage 4 and 12 for all the experiments.

Primary human choroid cells were isolated from choroid tissue of the donor human eye through primary cultures, by Professor Maryse Bailly. Donor eyes were collected from one eye bank (AER, NHSBT), specifically requested as to have no sign of prior eye issues, with consent and were approved by the Ethics committee. The choroid was separated from the sclera and the retina was removed. choroid cells cultured following the same protocol as scleral fibroblasts mentioned in method section 1,1. Choroid cells were used for all experiments in this project listed in with further information, seen in *Table 1.* These cells were used between passage 5 and passage 13 for all the experiments.

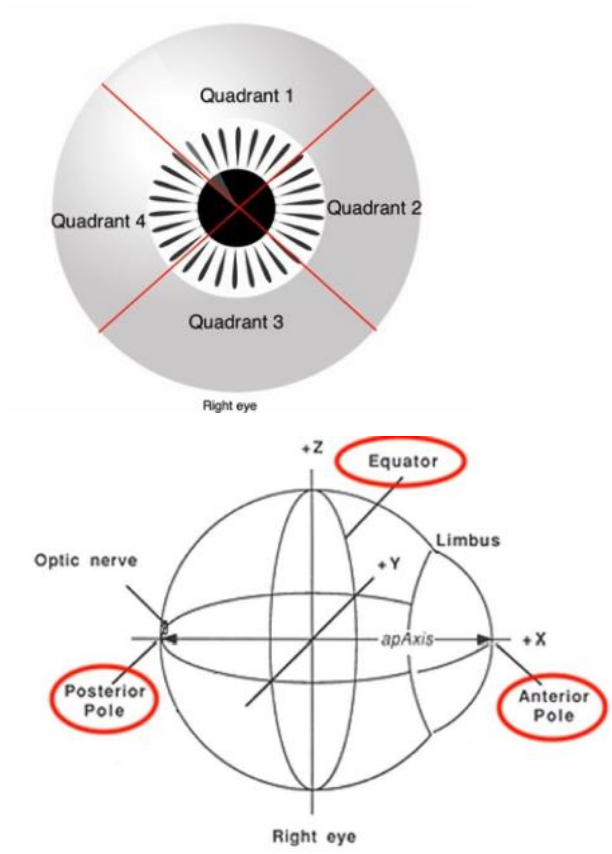

Figure 7. Illustration of the sclera tissue preparation. The left figure shows the right eye, divided into 4 quadrants symmetrically following the frontal, nasal, maxilla and temporal sides. The right figure shows the eye, divided into 3 parts, anterior, equatorial and posterior part.

Human Scleral Fibroblasts					
Donors	**Left/Right eye**	**Quadrant**	**Position**	**Donor Age**	**Gender**
HSF9	Left	1	anterior and posterior	3	Male
HSF14	Left	1	Anterior and posterior	3	Female
HSF1	Left	1	anterior and posterior	22	Male
R7312	Right	1	Anterior and posterior	40	Female
Choroid cell					
Donors	**Left/Right eye**	**Age**	**Gender**		
Choro-9R (matching scleral HSF9 above)	Right	3	Male		
Choro-10R	Right	35	Female		

Table 1. Details of human scleral fibroblasts and human choroid cells were used in this study.

1.2. Preparation of choroid conditioned medium

Choroid conditioned medium (CCM) was generated by incubating choroid cells for 24 hours with serum-free DMEM supplemented with 2mM L-glutamine (SF-Md) at 37ºC, 5% CO_2 incubator. The medium was collected and filtered with a 0.45 um filter (Sigma-Aldrich, UK) to remove cellular debris. Serum-free medium was placed in empty tissue culture T25 flasks (Corning, USA) in the incubator under the same conditions as a control.

Dopamine-treated choroid conditioned medium (dopamine-CCM) was generated by treating dopamine to treat choroid cells with dopamine prior to generating the conditioned medium. Briefly, dopamine hydrochloride powder (Sigma-Aldrich, UK) was dissolved in MilliQ H_2O at 100mM stock, and sterile filtered (0.22 filter, Sigma-

Aldrich, UK). Dopamine solution was diluted in MilliQ H_2O to 100uM as a substock, then further diluted in the complete medium to final dilutions of 10uM, 1uM, 100nM and 10nM. The choroid cells were cultured in the complete medium for one day, and on day2, the culture medium was replaced with the freshly made dopamine-containing medium and the cells were incubated for 96 hours. On day5, the medium was then removed and replaced with serum-free DMEM for 24 hours to generate the conditioned medium as the dopamine-CCM. When optimized dopamine treatment time, the choroid cells were cultured in the complete medium for 4 days and changed medium once on day2. On day4, the culture medium was replaced with the freshly made dopamine-containing medium and the cells were incubated for 24 hours. On day5, the medium was then removed and replaced with serum-free DMEM for 24 hours to generate the conditioned medium as the dopamine-CCM. In parallel, CCM was generated by culturing the choroid cells in the complete medium when the dopamine treatment group was incubated with the dopamine-containing medium under the same conditions, removing the complete medium and replacing the serum-free medium to starve cells 24 hours as control. Moreover, the serum-free medium was incubated in the tissue culture T25 flasks (Corning, USA) under the same condition as a control.

2. Collagen Contraction Assay

The collagen contraction assay was performed as previously published (Dahlmann-Noor et al. 2007). Briefly, scleral fibroblasts were trypsinised, counted, and $1x10^5$ cells were resuspended in100ul complete medium.-1ml rat tail collagen type I (2mg/ml in 0.6% acetic acid, First link Ltd., UK) was placed in a tube with 160ul of concentrated medium mix [1.4ml 10X DMEM (Sigma-Aldrich, UK),

140ul L-glutamine, and 360ul $NaHCO_3$ (Gibco, Life Technologies, UK)]. The mix was titrated with about 64ul of 1M NaOH to reach neutral pH. The cells were then added to the collagen and the mix was cast (150ul gel solution) into the well of the glass bottom MaTek dish (MaTek Corporation, USA). The gels were placed in the incubator to polymerize for 10 min. They were then detached from the well, and floated with the 2ml choroid conditioned medium. Photos of the gels were taken daily and analysed in the software ImageJ. For each photo of the gel, the actual gel size and microwell size were measured by tool “oval” in the ImageJ after setting measurement “area”, and their area size was ratioed following the formula contraction percentage (%) = (microwell size – gel size)/gel size, which was analysed as collagen gel contraction percentage. Photos of the gel were analysed on day1 and day4 with ImageJ. For choroid cell contraction, choroid cells were trypsinised, counted and resuspended with 100ul FBS. The gels were prepared as above and, floated in complete medium. All experiments use triplicate gels.

3. Cell Growth Rate (2D)

Cells were trypsinised, resuspended in the complete medium and counted. 1 ml of the cell suspension was seeded into the 24 well plates (Nunc, Thermo, UK) with 6,250 cells/ml/well, incubated at 37^{o}C, 5% CO_2 overnight. From day1 after overnight incubation, cells were trypsinised, pelleted and resuspended with 100ul complete medium for cell number counting with a hemocytometer. Cells were counted daily from day1 to day12, the culture medium was changed every 1-2 days. Duplicate wells were counted each day. Initially, we started with 24-well plates for young scleral fibroblasts (HSF9-A/P, HSF14-A/P), culturing in the medium supplemented with 10% serum, and counting cell numbers daily, as well as adult scleral fibroblasts

(R7312-A) for expanding assays in different ages. However, although cells were growing up to confluency in some areas (by eye observation) at the culture bottom of the 24-well plate, the overall cell number did not reach a plateau phase as expected, even after 12 days. The uneven culture area of the well in the 24-well plate might respond to this unexpected phenomenon, with cells gathering in the centre of the bottom cell culture area to inhibit cell proliferation. Thus, we moved to use 12-well plates with a larger cell culture area to avoid the cell gathering in the centre, while keeping the same initial amount of cells seeded for adult scleral fibroblasts, which had not been tested (R7312-A/P, HSF1-A/P). Although only one experiment was performed to culture HSF9-P in the 12-well plate, we found no significant difference in cell growth rate tendency of scleral fibroblasts in the 12-well plate and 24-well plate (*Figure 8).* In the 12 well plates, the same initial number of cells and volume of cell suspension in each well (6,250 cells/ml/well) were kept for cell seeding on the day0, all the others were as same as cell counting in the 24 well plates, but cells were counted every 2-3 days from day1 to day12.

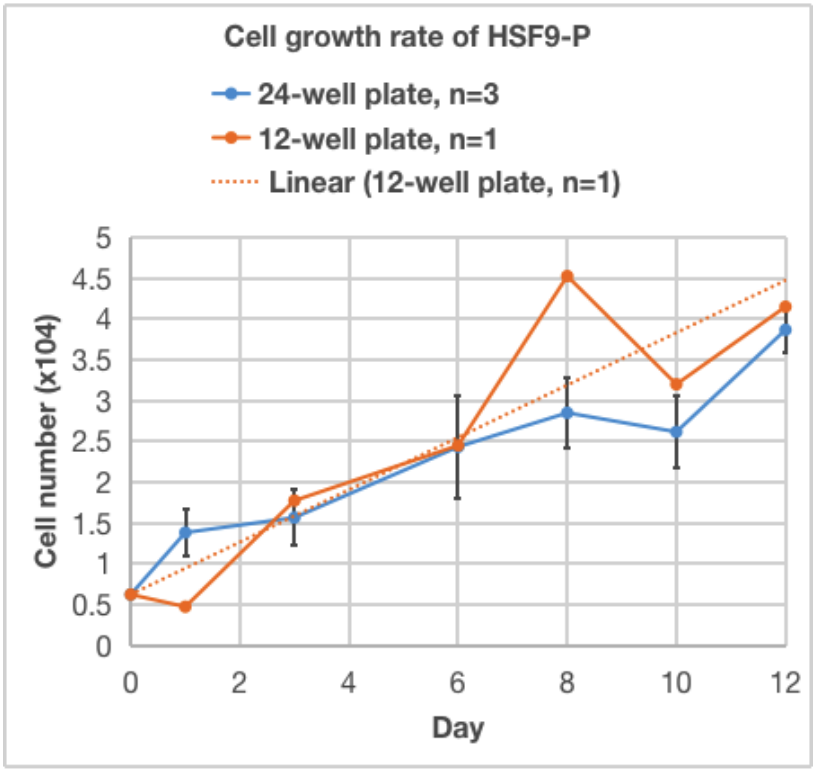

Figure 8. The cell growth rate of HSF9-P showed no significant difference in the 12-well plate and 24-well plate. Shown in the blue line is mean +/-SEM, n=3. Shown in the orange line n=1. The linear dot line showed the tendency of the cell growth rate of HSF9-P cultured in the 12-well plate,

4. Proliferation Assay (3D) scleral fibroblasts

Scleral fibroblasts embedded in the collagen gels were made to be floating in the MaTek dishes as described in method section2 of the collagen gel contraction assay. In parallel, one duplication was made for gel contraction control. After 1 day and 4 days, one set of gels was used to measure the gel contraction percentage as control, and another set of 3D collagen gels was used to measure the proliferation rate by cell viability scanning. Briefly, collagen gels were transferred from MaTek dishes to the 48-well plate, with 100ul matched conditioned medium as gels were in the MaTek dishes, added 10ul CCK8 reagent (Cell Counting Kit-8, Sigma-Aldrich, UK)

incubated at 37°C, 5% CO_2 for 2 hours. The 100ul incubated culture medium was transferred to the 96-well plate, and absorbance was measured at 450nm. In parallel, the conditioned medium without cells was incubated under the same condition for absorbance measurement as controls. Duplicate wells were measured to minimize variation.

5. LDH Cytotoxicity Assay

For cytotoxicity assay, choroid cells were trypsinised and counted. 4,000 cells were resuspended with 100ul complete medium for each well, and were seeded into the 96 well plates incubated at 37°C, 5% CO_2. After overnight incubation, dopamine diluted in the MilliQ water at different concentrations was added to wells. After 1 day and 4 days of dopamine treatment, the culture medium was processed using CyQuant LDH (Lactate Dehydrogenase) cytotoxicity assay kit (Invitrogen, Thermo Fisher Scientific, UK), following the manufacturer's protocol, and the cytotoxicity percentage was calculated following the formula, cytotoxicity percentage (%) = (compound-treated LDH activity – spontaneous LDH activity)/(maximum LDH activity – spontaneous LDH activity). Cells were lysed with lysis buffer as maximum LDH activity controls (100% cytotoxicity). Triplicate wells were measured to avoid bias.

6. Live/Dead Viability Assay

After 1 and 4 days, the 3D collagen gels in dopamine treated choroid conditioned medium were used to image cell viability, gels in matched choroid conditioned medium and serum-free medium as control. Collagen gels were transferred from MaTek dishes into 24-well plates, incubated with 2uM calcein AM and 4uM ethidium homodimer-1 Live/Dead Viability reagents (Life Technologies, UK)

at room temperature for 40 minutes. Images were taken by Zeiss LSM 700 confocal microscope with onboard Zen software with 10X objective.

7. Western Blot

For the lysates, cell suspension in RIPA lysis buffer [150 mM NaCl, 0.1% Triton X-100, 0.1% sodium dodecyl sulphate, 50 mM Tris-HCl PH8.0, 0.5% sodium deoxycholate, protease inhibitor (Roche, UK)] were centrifuged to collect the supernatant. Cells in the 2D monolayer culture environment were trypsinised, pelleted and resuspended in RIPA lysis buffer. Cells in the 3D collagen gel culture environment were digested with 0.05% collagenase-D (Roche, UK) until completely liquefied, and the cell pellet resuspended in RIPA lysis buffer was obtained by centrifuging the digest. Protein concentration was quantified by BCA assay (Thermo Fisher Scientific, UK), and the samples were denatured in sample buffer (5x sample buffer, made from 5% SDS, 50% glycerol, 0.1% bromphenol blue, 250mM Tris-HCl PH6.8) at 95^{o}C for 5 minutes. 5ug protein was loaded on 4-12% precast polyacrylamide gels (Blot^{TM}, Invitrogen, Thermo Fisher Scientific, UK) for SDS-PAGE. Proteins were transferred to PDVF membranes (Thermo Fisher Scientific, UK), and membranes were blocked in 5% skimmed milk [(made in 0.1% Tween-20 in TBS (TBST)] at room temperature for 1 hour before overnight incubation at 4 ^{o}C with primary antibody (a-SMA, 1:3000 dilution) in the blocking solution. Membranes were washed (3 times) with TBST before 1-hour incubation at room temperature for 1 hour with secondary antibody [Peroxidase-AffiniPure goat anti-mouse IgG (H+L), Jackson Immunoreaserch, USA] diluted (1:5000) in 5% skimmed milk (made in 0.1% TBST) at room temperature. After another washing (3 times) with TBST at room temperature,

membranes were developed using ECL (Pierce, Thermo Fisher Scientific, UK), and exposure with a chemillu machine (BioRad, USA). For loading control, after developing the membranes, membranes were reprobed with primary antibody GAPDH at 1:3000 in 5% skimmed milk (made in 0.1% TBST) with the following steps described above, after washing (0.1% TBST) and stripping (stripping buffer, made by 0.75g glycine, 1.5g NaCl, dissolved in 300ml MilliQ water, adjusted PH to 2.5 and topped up MilliQ water to 500ml)). Scanned membranes were analysed using ImageJ software, and band intensities of reference samples were ratioed to GAPDH in each matched loaded well for comparing all the cell stains and all independent experimental repeats.

8. Biomimetic Model

8.1 Physical weight-derived biomimetic model

Compressed gels by physical weight were as previously published protocol (Kozdon et al. 2020), this protocol generates a Tenon's capsule/ bulbar conjunctiva interface with an elastic modulus of 7.19+/-1.15 kPa, close to the conjunctiva stiffness. Because the sclera is a much stiffer tissue, with Young's modulus 1.8 to 2.9 MPa (Sergienko and Shargorogska 2012), we initially tried to generate stiffer sclera mimics by modifying this protocol with a longer compression time though we are not sure if longer compression time could achieve stiffer gels. Also, we used the Lonza collagen as it was generally used for cornea mimics in Professor Julie Daniels Lab (UCL Institute of Ophthalmology), but we initially did not pay attention to that the Lonza collagen might generate less stiff gels than the First Link collagen used in the published protocol (Kozdon et al. 2020), as it is half the collagen concentration (1mg/ml) of the First Link one (2mg/ml). Briefly, the

bottom layer of 3D collagen gel solution was mixed with 1.9ml rat tail collagen (type I collagen, 1mg/ml in 0.6% acetic acid, Lonza, Bioscience), 330ul of the concentrated medium, titrated with about 70ul 2M NaOH to reach the neutral pH, and 170ul FBS cell suspension ($2x10^5$ cells) to cast 300ul gel solution into the 10mm metal rings, then incubated at 37ºC, 5% CO_2 for 40 minutes. The gels were placed between 2 pieces of nylon curtain on 2 layers of Whatman® qualitative filter paper (Sigma-Aldrich, UK). A coverslip was placed on top, and the gels were compressed by placing a 58g weight (Thermo Fisher Scientific, Paisley, UK) on top. After 15 minutes, the weight was removed, and the compressed gels were peeled from the nylon mesh. The top layer of 3D gel solution was mixed with the standard volume described above but Lonza collagen, and 100ul cell suspension ($0.75x10^5$ cells, resuspended with 100ul FBS), then casted 150ul on the top of the bottom compressed layer of 3D collagen gel into the microwell of glass bottom in the MaTek dish, and left detached, added 2ml complete medium to float the 2-layer 3D construct.

8.2. RAFT-derived biomimetic model

Compressed gels by Real Architecture For 3D Tissues (RAFT) system were as previously published protocol (Kureshi et al. 2015), with reference to unpublished data following the protocol from Professor Julie Daniels Lab (UCL Institute of Ophthalmology). The Daniels' lab protocol used the RAFT system to make cornea mimics, with Young's modulus of 1+-/ 0.5 MPa in the cornea biomimetic. The Young's modulus of the human sclera is between 1.8 to 2.9 MPa(Sergienko and Shargorogska 2012), which is not too different from the stiffness of the cornea, thereby we initially followed Daniel's protocol to develop scleral mimics. However, we did not pay attention

to the collagen concentration as we used Lonza collagen (1mg/ml), whereas Daniel's protocol used Koken collagen (3mg/ml, native collagen, bovine dermis, Cosmo Bio Ltd, USA). Although we did not measure Young's modulus of our scleral mimics, it is highly likely that our scleral mimics were less stiff than Daniel's cornea mimics. Briefly, the bottom layer (sclera mimics) of 3D collagen gel solution was a mixture of 3.8ml rat tail collagen (type I collagen, 1mg/ml in 0.6% acetic acid, Lonza, Bioscience), 660ul of the concentrated medium (introduced in method section 3), titrated with about 70ul 2M NaOH to reach the neutral pH, and 340ul FBS resuspended cell suspension (4x105 cells) to cast 600ul gel solution into the glass bottom of the 24-well plate (Nunc, Thermo, UK), then incubated at 37^{o}C, 5% CO2 for 45 minutes. The gels were compressed by placing the RAFT absorber (Lonza, Bioscience) following the manufacturer's protocol at room temperature for 30 minutes. The RAFT absorber creates well-controlled and high-density collagen scaffolds of scleral fibroblasts by absorbing excess liquid from the collagen mix. The middle layer (choroid mimics) of the 3D gel solution was a mixture of the 2ml Lonza collagen, 360ul concentrated medium, titrated with about 140ul 1M NaOH to reach the neutral pH, and 100ul FBS resuspended cell suspension (1.5x105 cells) to cast 300ul gel solution on the top of the bottom compressed scleral mimics layer, in the glass bottom of the 24-well plate (Nunc, Thermo, UK). The bottom layer was detached from the glass bottom but the two layers maintained attachment, and 2ml complete medium was added for culturing the 2-layer 3D construct. The top monolayer (retina mimics) of RPE cells differentiated from IPSC-derived were provided and plated above the 2-layer 3D construct by Dr Victoria Tovell (Professor Pete Coffey's lab, Institute of Ophthalmology UCL).

9. Immunofluorescence

9.1. IF for cells in 2D

Immunofluorescence for cells in the 2D culture environment was as previously published protocol (Kozdon et al. 2015). Briefly, Coverslips (diameter 13mm) were prepared by acid washing with 1M HCl for 3-5 minutes, PBS wash, 70% ethanol for 1-2 minutes, and another PBS wash before seeding cells. Cells were trypsinised, counted for 0.5x 10^5 cells, and resuspended in 2ml complete medium for incubation at 37ºC, 5% CO_2. After overnight cell incubation, cells were fixed with 3.7% formaldehyde in PBS for 7 minutes, followed by 0.5% Triton -X 100 (Sigma-Aldrich, UK) in PBS permeabilization for 20 minutes and 0.1M Glycine (Sigma-Aldrich, UK) in PBS wash for 10 minutes. After 5 minutes of washing with 1% BSA in TBS pH8.0, coverslips were transferred to a humidified dark chamber, and blocked/stained for F-actin with Rhodamine-labeled Phalloidin (Molecular Probes, OR, USA) at 1:20 dilution in TBS-1% BSA-1% FBS at room temperature for 20 minutes. After removing the phalloidin, primary antibody (*Table 2)* was added at 1:100 in TBS-1% BSA and probed at room temperature for 1 hour. After washing (3 times) with 1% BSA in TBS pH8.0, cells were incubated in secondary antibody (Alexa Fluor 488-Conjugated AffiniPure donkey anti-mouse IgG, donkey anti-rabbit IgG, Jackson Immunoresearch Laboratories, PA, USA) at a dilution of 1:100 at temperature for 1 hour, and another washing (3 times) with 1% BSA in TBS pH8.0. Coverslips were transferred to microscope slides, mounted by Fluoroshield mounting medium with DAPI (Abcam, UK). Images were taken by EVOS M7000 microscope with onboard M7000 software with 10X objective.

Target protein	Dilution	Supplier	Cat.No
a-SMA	1:100	Sigma-Aldrich	A5228

Calponin-1	1:500	Abcam	Ab46794
Vimentin	1:1000	Abcam	Ab92547
NG2	1:200	Abcam	Ab83178
PDGFR	1:100	Abcam	Ab32570
CD31	1:20	Thermo Fisher	MA5-13188
CD144	1:100	Thermo Fisher	14-1449-82
VWF	1:50	Thermo Fisher	MA5-14029

Table 2. List of primary antibodies used in IF.

9.2. IF for cells in 3D

Immunofluorescence for cells in the 3D culture environment was as previously published protocol (Yang et al. 2019). Briefly, the biomimetic model gels were fixed with 3.7% formaldehyde in PBS for 30 minutes, followed by 0.5% Triton -X 100 (Sigma-Aldrich, UK) permeabilization for 30 minutes, 0.1M Glycine (Sigma-Aldrich, UK) wash for 30 minutes. For quick F-actin staining in the RAFT-derived biomimetic model, gels were then incubated with Rhodamine-phalloidin (1:20 in TBS- 2% FBS) for F-actin staining at room temperature in the dark for 1 hour after washing with TBS pH8.0 for 5 minutes. After removing the phalloidin, washing (3 times) with TBS PH8.0 for 30 minutes. Gels were transferred to MaTek dishes after aspirating the TBS, mounted by Fluoroshield mounting medium with DAPI (abcam, UK), images were taken by Stellaris5 confocal microscope with 10X objective, and 3D volumes were reconstructed with Volocity software. For physical weight-derived biomimetic model, gels were then incubated with Rhodamine-phalloidin (1:20 in TBS-1% BSA-1% FBS) for F-actin staining at room temperature in the dark for 30 minutes after washing with 1% BSA in TBS pH8.0 for 5 minutes. After removing the phalloidin, gels were incubated with primary antibody (a-SMA) diluted at 1:100 in TBS-1% BSA and probed at 4 ^{o}C overnight in the dark. After washing (3 times) with 1% BSA in TBS pH8.0 for 10 minutes, cells were incubated in secondary

antibody (donkey anti-mouse IgG) at the dilution of 1:100 at room temperature for 2 hours in the dark. After another washing (3 times) with 1% BSA in TBS pH8.0, gels were transferred to microscope slides, mounted by Fluoroshield mounting medium with DAPI (abcam, UK). Images were taken with the Zeiss LSM700 confocal with objective 10x, and 3D volumes were reconstructed with Volocity software.

10. Statistics

Most experiments were performed in triplicate, and with at least three independent repeats. Data presented in this study were the mean average +/- stand error of the mean (SEM) of at least three repeats, unless otherwise noted. Statistical analysis was performed using the two-tailed Student's t-test with Welch correction in Prism9 (GraphPad software) or Excel software. $P<0.05$ was considered to be statistically significant.

Results

1. Choroid-conditioned medium stimulates scleral fibroblasts contractility

We used scleral fibroblasts isolated from both paediatric (HSF9, HSF14) and adult (HSF1, R7312) donor tissue, and choroid cells isolated from paediatric and adult donors (Choro-9R, matching HSF9 sclerals, and Choro-10R, respectively) to investigate whether choroid-secreted factors could stimulate fibroblast contractility, and whether scleral fibroblasts from different ages and antero-posterior positions respond differently. We used the standard gel contraction assay developed in the lab, which has been shown to be a valid reflection of changes in fibroblast mechanical properties (Dahlmann-Noor et al. 2007). We found that paediatric scleral fibroblasts (HSF9-

A/P, HSF14-A/P) were spontaneously more contractile (in the absence of serum) than adult ones (HSF1-A/P, R7312-A/P), particularly the anterior ones. Conditioned medium from choroidal cell cultures [(Con-Md, Choro9R), (Con-Md, Choro10R)] stimulated contraction for all scleral fibroblasts (*Figure 9a*), suggesting that choroid cells produce specific factors that can modulate scleral fibroblast contractility as initially hypothesized. When the contraction percentage was ratioed to the control contraction in the serum-free medium, we found that paediatric posterior scleral fibroblasts (HSF9-P, HSF14-P) were more sensitive to the choroid cell cultured conditioned medium than paired anterior ones (HSF9-A, HSF14-A), and particularly more sensitive to the conditioned medium cultured from paediatric choroid cells. The HSF9-P were significantly stimulated more by paediatric choroid cell cultured conditioned medium (Con-Md, Choro9R) than the HSF9-A, and HSF14-P were significantly more sensitive to paediatric choroid cell cultured conditioned medium (Con-Md, Choro9R) than HSF14-A (*Figure 9b*). However, adult scleral fibroblasts (HSF1-A/P, R7312-A/P) did not show such a different sensitivity to the age-matched choroid conditioned medium, regardless of anterior and posterior positions (*Figure 9b*).

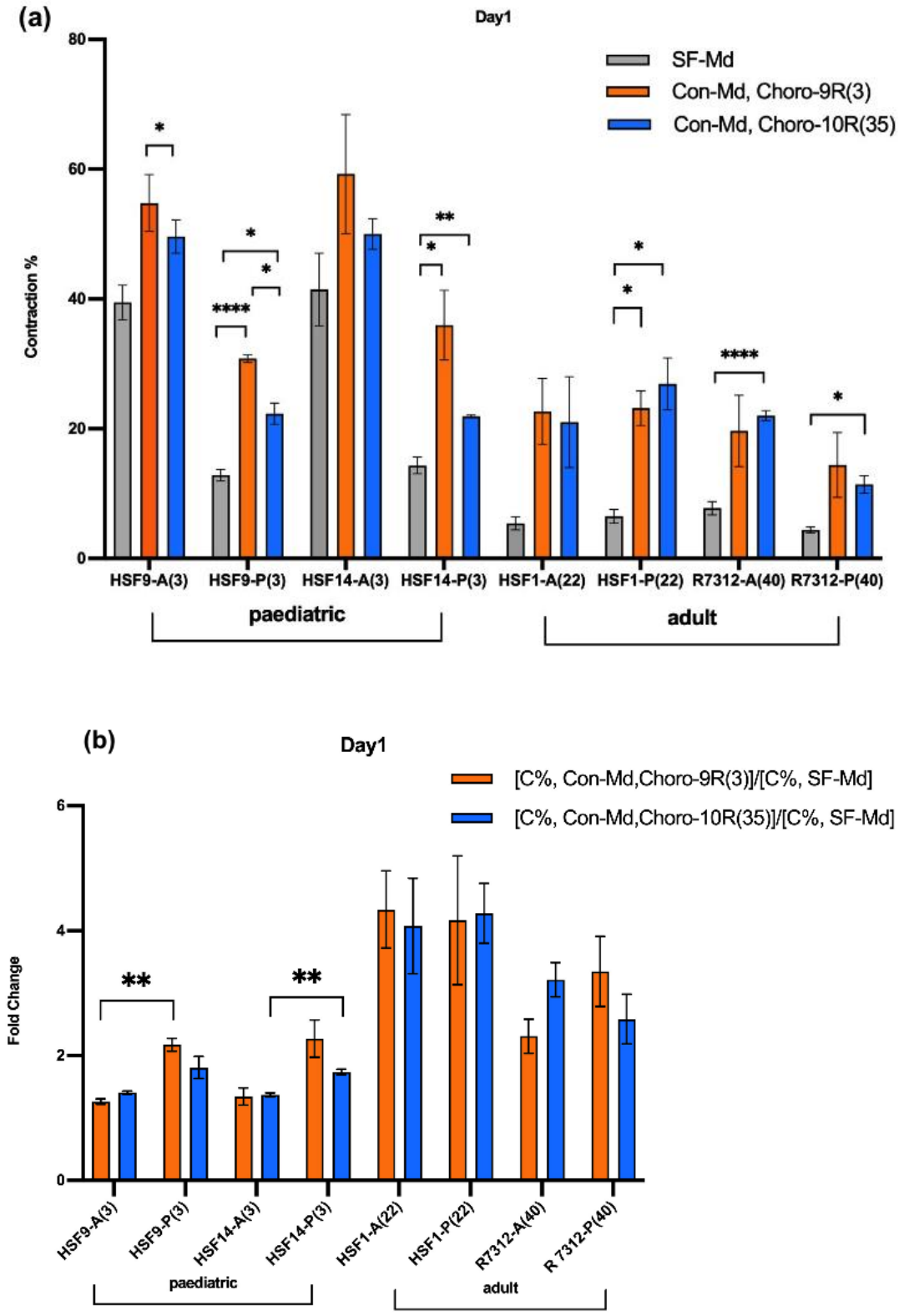

Figure 9. Choroid conditioned medium promoted scleral fibroblasts contraction. (a). Choroid cells secreted factors stimulate scleral fibroblasts contractility with age and position differences. Conditioned medium from peadiatric (Choro-9R) and adult (Choro-

10R) were used, and 2 sets of peadiatric and adult scleral fibroblasts were used. Scleral fibroblasts were embedded in collagen gels and contraction was measured after 1 day in the presence of the serum-free medium or choroid-conditioned medium. Shown is the mean contraction percent +/- SEM; [“SF-Md”, n=6, “Con-Md, Choro-9R (3)” and “Con-Md, Choro-10R (35)”, n=3. The number in the bracket shows the tissue donor age. * P<0.05, ** P<0.01, **** P<0.0001, t-test. (b). An indication that paediatric choroid-conditioned medium had more of an effect than adult choroids to stimulate the contractility of paediatric scleral fibroblasts from the posterior position. Shown is the contraction fold change of each choroid conditioned medium ratioed to serum-free control (mean +/- SEM). ** P<0.01, t-test.

2. Scleral fibroblast characterisation

2.1. Proliferation

2.1.1. Anterior scleral fibroblasts proliferate faster than posterior scleral fibroblasts

We observed differences in the growth rates of the scleral fibroblasts during routine cell culture, and we hypothesised that this might partly explain some of the differences we saw in the contraction assay. We thus decided to investigate the growth rate of fibroblasts. We found that "anterior" scleral fibroblasts proliferated faster than paired "posterior" ones, regardless of age (***Error! Reference source not found.****a*). To clarify, we combined the results to compare age differences and position differences in cell growth rate tendency, respectively. We found that age did not significantly affect the proliferation of scleral fibroblasts (***Error! Reference source not found.****b*). However, we found that anterior scleral fibroblasts had a greater cell growth rate tendency than posterior

scleral fibroblasts, regardless of age (***Error! Reference source not found.****c*). These findings suggested that age was not a key factor for scleral fibroblasts proliferation in the 2D cell culture environment, but antero-posterior location was.

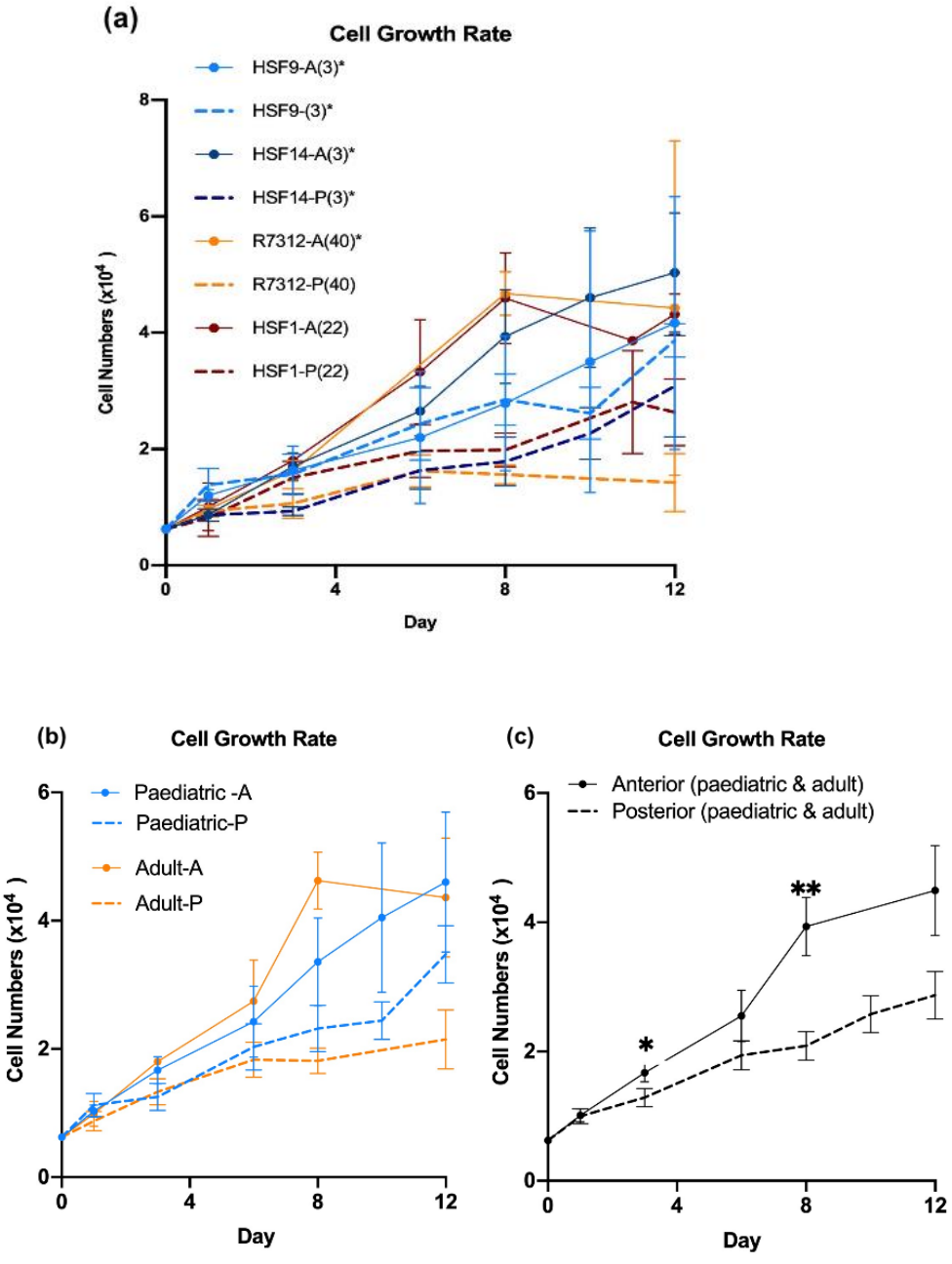

Figure 10. The scleral fibroblasts present different proliferation rates with respect to antero-posterior position. (a). The scleral fibroblasts cultured in 2D plates were counted daily for 12 days. Shown is mean cell number +/- SEM, n=3. (b). The scleral fibroblast growth rate is

not correlated to age, “Paediatric-A” indicates HSF9-A and HSF14-A, “Paediatric-P” indicates HSF9-P and HSF14-P, “Adult -A” indicates R7312-A and HSF1-A, “Adult -P” indicates R7312-P and HSF1-P. (c). Anterior scleral fibroblasts grow faster than posterior scleral fibroblasts, “Anterior (paediatric & adult)” indicates HSF9/14/1-A and R7312-A, “Posterior (paediatric & adult)” indicates HSF9/14/1-P and R7312-P. * P<0.05, ** P<0.01, t-test.

2.1.2. Scleral fibroblasts do not proliferate in 3D collagen gels.

We used the CCK8 proliferation assay to determine whether scleral fibroblasts proliferated differently in collagen gels, and whether this difference in proliferation could explain the response to the choroid condition medium. Initially, we evaluated the proliferation of paediatric anterior (HSF9-A) and posterior (HSF9-P) scleral fibroblasts using a 2 hours incubation for the assay on day0, 1 and 4. However, we found differences in the metabolic rates between anterior and posterior positions made it difficult to compare as anterior scleral fibroblasts (HSF9-A) overall had higher OD value readings than posterior ones (HSF9-P), and the OD value readings of posterior ones were too low to avoid bias, see *Figure 11a*. For comparable baseline results, we increased incubation time to 4 hours for all the posterior scleral fibroblasts (HSF9-P, HSF14-P, HSF1-P), but kept 2 hours incubation for the anterior scleral fibroblasts (HSF9-A, HSF14-A, HSF1-A). After one day, we found no significant difference in cell numbers of all fibroblasts cultured in serum-free medium or upon stimulation with choroid conditioned medium. Although different conditions of the medium still did not affect the cell numbers after 4 days, cell numbers were overall significantly decreased on day4 for all cell lines and conditions,

regardless of age and position differences of scleral fibroblasts or age differences of choroid cells cultured conditioned medium [(*Figure 11b(1-4*)]. In contrast, we found that all the scleral fibroblasts embedded in the 3D collagen gel had significantly increased contraction upon choroid conditioned medium stimulation than in the serum-free medium, on day1 and day4 as expected [*Figure 11c (1-4)].* However, we doubted if this CCK8 proliferation assay was accurate enough for cell number measurement on day4, which was possibly affected by cellular metabolism since the cell number of all the scleral fibroblasts decreased on day4, which was not as expected. Thus, we digested 3D collagen gel to count cell numbers to determine if the cell number decreased on day4 in this more direct measuring way. We found that the cell number of young posterior scleral fibroblasts (HSF9-P) decreased on day4 in serum-free medium or upon stimulation with choroid conditioned medium, respectively; and these counted cell numbers had no significant differences with different conditions on day0, day1 and day4, respectively (*Figure 11d*). Therefore, the CCK8 proliferation assay was confirmed to accurately measure the cell proliferation rate in the 3D collagen gel. Altogether these results suggest that the proliferation of scleral fibroblasts is unlikely to explain the contractility changes with choroid conditioned medium stimulation in the 3D collagen gel.

(a)

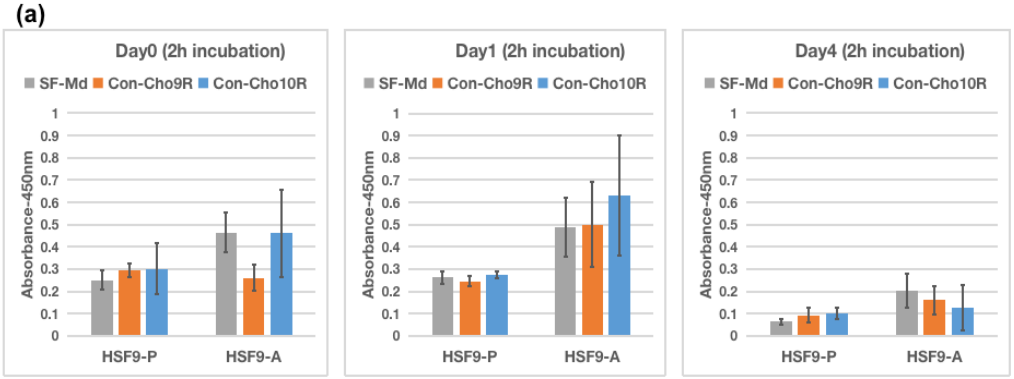
Day0 (2h incubation)
Day1 (2h incubation)
Day4 (2h incubation)
SF-Md Con-Cho9R Con-Cho10R
Absorbance-450nm
HSF9-P
HSF9-A

(b1)

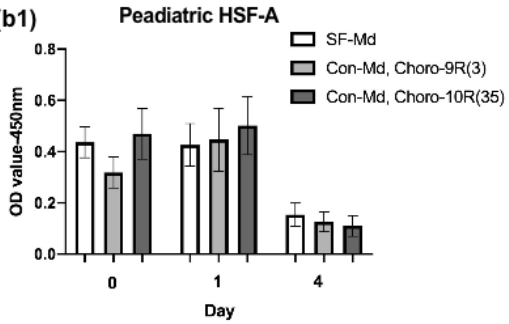
Peadiatric HSF-A
SF-Md
Con-Md, Choro-9R(3)
Con-Md, Choro-10R(35)
OD value-450nm
Day

(c1)

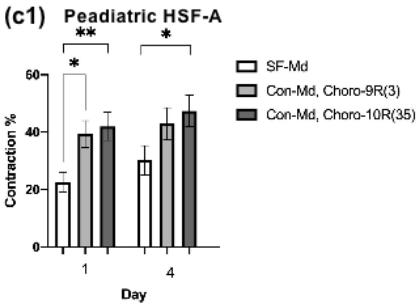
Peadiatric HSF-A
SF-Md
Con-Md, Choro-9R(3)
Con-Md, Choro-10R(35)
Contraction %
Day

(b2)

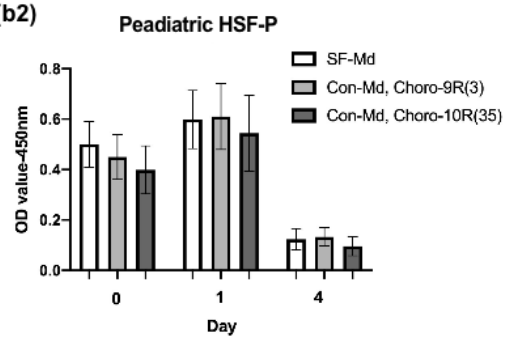
Peadiatric HSF-P
SF-Md
Con-Md, Choro-9R(3)
Con-Md, Choro-10R(35)
OD value-450nm
Day

(c2)

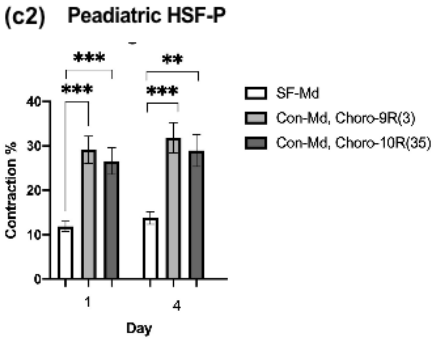
Peadiatric HSF-P
SF-Md
Con-Md, Choro-9R(3)
Con-Md, Choro-10R(35)
Contraction %
Day

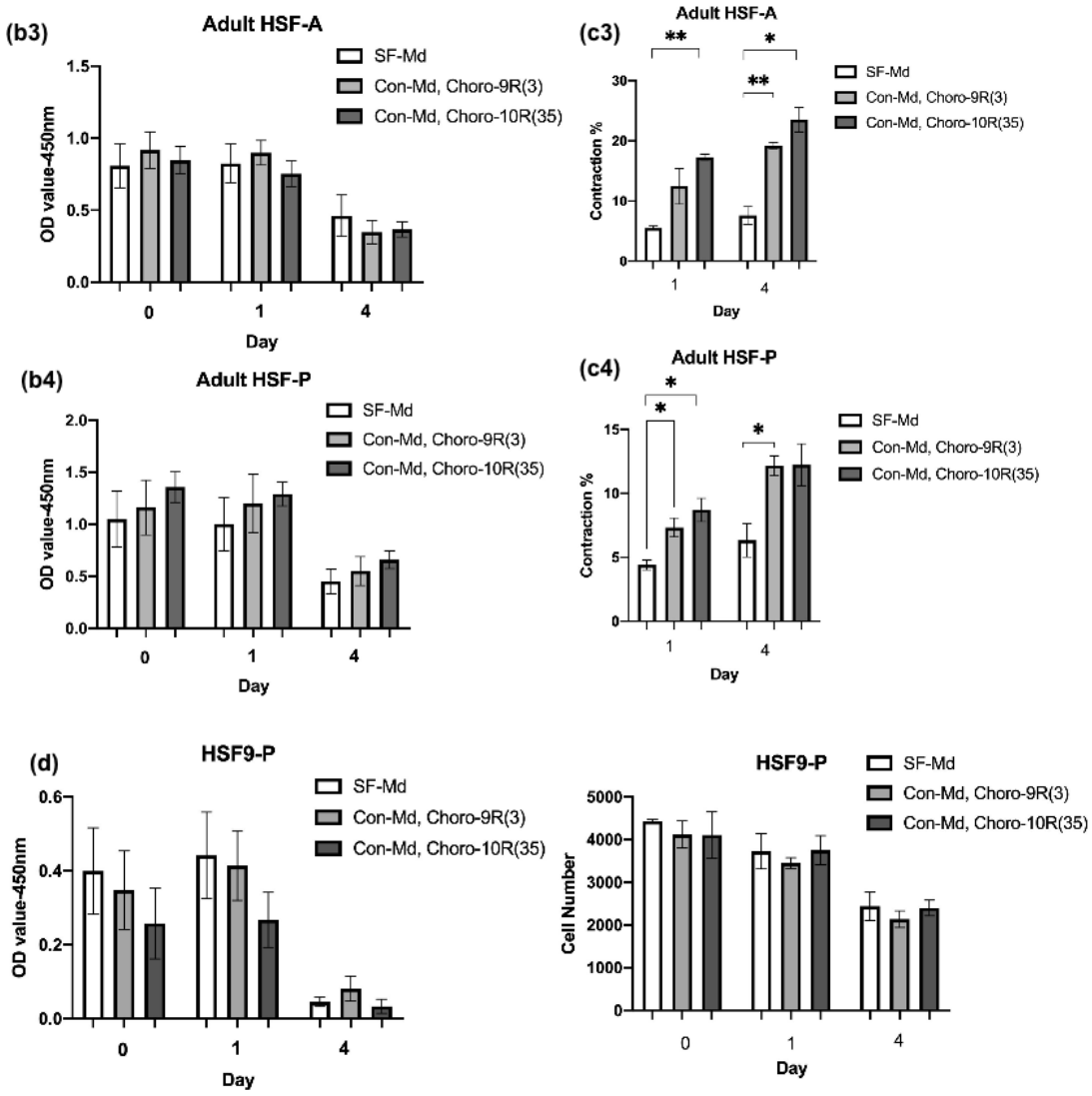

Figure 11. Scleral fibroblasts did not proliferate in 3D collagen gels. (a). Anterior scleral fibroblasts had different metabolic rates from posterior fibroblasts in the CCK8 proliferation assay. (b1-b4). Scleral fibroblasts did not proliferate in 3D collagen gels regardless of age and position differences. “Paediatric HSF” included HSF9 and HSF14, “Adult HSF” included HSF-1. “A” indicates position “anterior” and “P” indicates position “posterior”. (c1-c4). Scleral fibroblasts contracted in the 3D collagen gels upon stimulation of choroid conditioned medium. (d). Paediatric posterior scleral fibroblasts did not proliferate in the 3D collagen gels, as determined in both CCK8 proliferation assay and gel digested cell counting. Shown is mean +/- SEM, n>=3. The number in the bracket indicates donor age.

2.2. Scleral fibroblasts activation markers

2.2.1. Scleral fibroblasts express a-SMA with anterior/posterior position and age differences

Alpha-smooth muscle actin (a-SMA) is a classic marker of contractility, and a typical marker of "activated" myofibroblasts. Previous work in mouse models has identified a population of a-SMA-expressing cells in the normal sclera, which are expanding during the myopia progression (Wu, Chen, Zhao, et al. 2018). Generally, a-SMA expression is increased during myopia progression (Yuan et al. 2018), suggesting “activated” myofibroblasts may expand during myopia progression. We used western blot to analyse a-SMA levels in scleral fibroblasts to determine if this marker is linked to the “activated” fibroblast – myofibroblasts population, potentially stimulated by the choroid secreted factors. We initially found that paediatric scleral fibroblasts had a higher expression level of a-SMA than adult ones, and "posterior" scleral fibroblasts had a higher expression level of a-SMA than "anterior" ones (Figure *12*). It suggested that a-SMA expression level varied in antero-posterior position and age differences in the human sclera, expressing a higher level in "paediatric" age compared to "adult" age, as well as higher expression level in posterior position than the anterior ones. These results suggested that a-SMA expression might be a critical marker of the scleral fibroblast state (i.e., growing phase or stable adult differentiated phase).

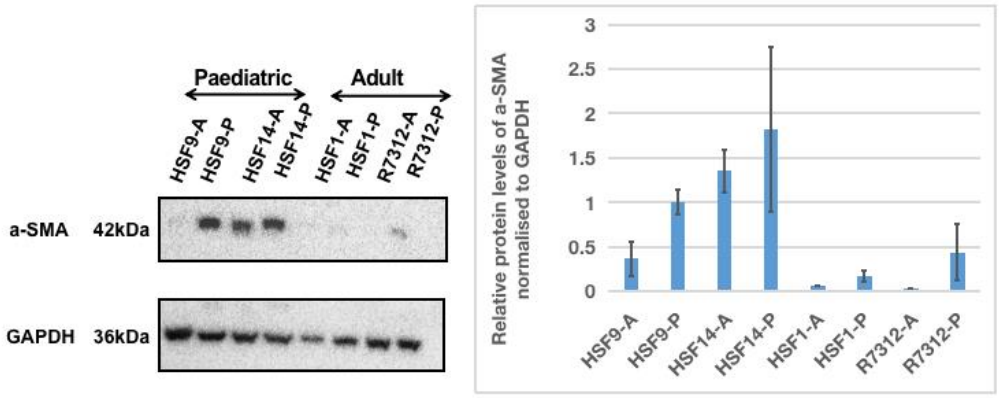

Figure 12. a-SMA expression is higher in paediatric scleral fibroblasts versus adult ones and posterior versus anterior sections of the sclera. Representative western blot and quantification of a-SMA level for scleral fibroblasts after 5-7 days culture in 10% serum. GAPDH, loading control. Shown is mean +/- SEM, n=3.

2.2.2. Choroid conditioned medium does not stimulate a-SMA expression in 2D monolayers

To further determine if the a-SMA was the key marker that responded to promoted scleral fibroblasts contraction potentially stimulated by the choroid secreted factors, we cultured scleral fibroblasts with the choroid conditioned medium in the 2D cell environment. To maximise potential effect, we chose paediatric scleral fibroblasts, as we anticipated that paediatric tissue would have the higher expression level of a-SMA than adult ones. We used western blot to analyse a-SMA levels in paediatric scleral fibroblasts (HSF9-A/P) cultured with serum-free medium for 24 hours or choroid conditioned medium (Choro-9R, Choro-10R) for 24 hours in standard 2D culture. We found paediatric scleral fibroblasts overall expressed low levels of a-SMA in the absence of serum, and no

increase after stimulation upon choroid conditioned medium, regardless of antero-posterior position differences (Figure *13*).

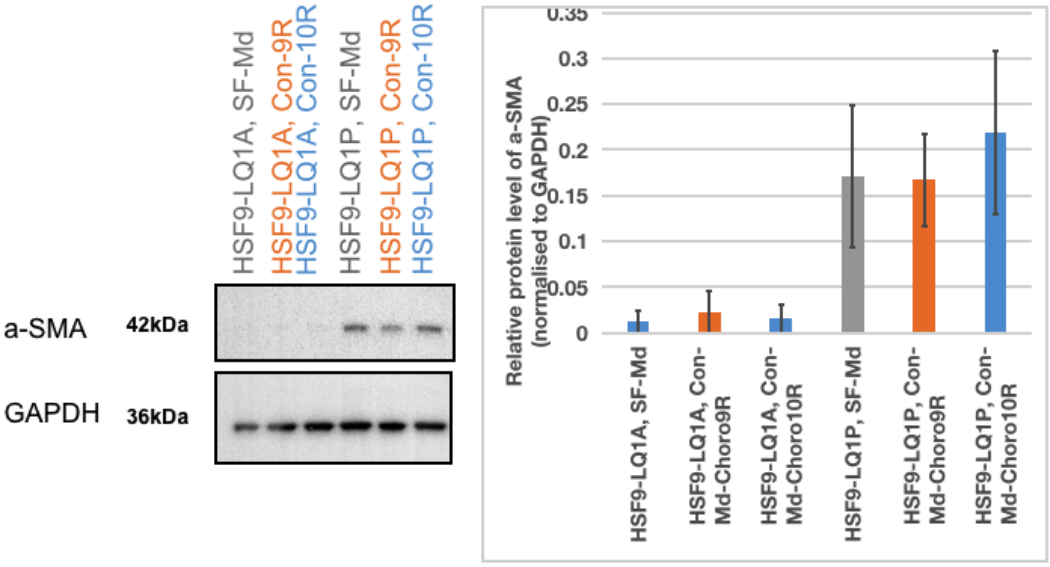

Figure 13. The expression levels of a-SMA of paediatric scleral fibroblasts in the serum-free medium or choroid-conditioned medium had no significant difference. Representative Western blot of and quantification of a-SMA level for paediatric scleral fibroblasts after 24h culture in 3 different conditions, SF-Md, Con-Md from Choro9R and Choro10R. GAPDH, loading control. Shown is mean +/- SEM, n=3

2.2.3. PRELP negatively regulates scleral fibroblast contraction

PRELP（Proline And Arginine Rich End Leucine Rich Repeat Protein) is associated with myopia progression (Majava et al. 2007), and preliminary work from Professor Shin-Ichi Ohnuma (Institute of Ophthalmology, UCL) implicated PRELP in cell dynamics. These suggest it might be a valuable marker of scleral fibroblast activation. We thus initiated a collaboration with the Ohnuma lab to investigate

the possible involvement of PRELP in scleral fibroblast contraction potential. A preliminary WB revealed that scleral fibroblasts seem to express little or no PRELP, but choroid cells showed significant levels. Thus, we hypothesized that PRELP might be one of the factors secreted by choroid cells which would affect scleral fibroblasts. We then set to look at the effect of PRELP on scleral fibroblast contraction, using as a PRELP source culture medium from HEK293T cells expressing a doxycycline inducible human PRELP construct. When we used the serum-free medium as the original medium to prepare the PRELP-rich and control medium (prepared by Jack Hopkins, Professor Shin-Ichi Ohnuma's lab), we found a negative effect of PRELP on contraction, although the difference was not significant. Similarly, in the standard medium with 10% serum, PRELP slightly decreased scleral fibroblast contraction, although still not significantly (***Error! Reference source not found.****a, b*). Altogether, these results suggested that PRELP was likely not one of the choroid factors stimulating scleral fibroblast contraction, although it may negatively affect scleral fibroblast activation. With little or no expression in the scleral fibroblasts, more work needs to be done to determine whether it may be a marker of growing sclera.

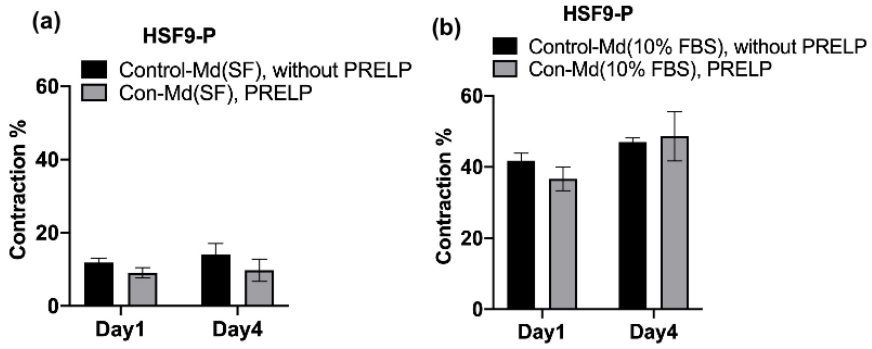

Figure 14(a-b). PRELP negatively affects scleral fibroblast contraction without significance. HSF9-P paediatric scleral

fibroblasts were cultured in collagen gel in the presence of (a) serum-free control medium or PRELP-rich serum-free medium, or (b) control medium with 10% serum with/without PRELP, and contraction was measured on day1 and 4. Shown is the mean +/- SEM, n=3. Control and PRELP-rich medium were 48-hour-conditioned media from HEK293 cells expressing doxycycline-inducible PRELP. Shown is mean +/- SEM, n=3.

3. Choroid cell characterization

3.1. Characterization of the choroid cell population

The choroid cells we used in this study were isolated from the whole choroid tissue so are presumed to be a mixed population of "fibroblastic" cells. They likely contained different cell populations, for example, fibroblasts, myofibroblasts, pericytes, smooth muscle cells, and endothelial cells (Nickla and Wallman 2010; Espinosa-Heidmann et al. 2005; Kur, Newman, and Chan-Ling 2012; Scholfield, McGeown, and Curtis 2007). Alpha-SMA is a marker for pericytes, smooth muscle cells that are presumed present in our mixed population of choroid cells, and it is also a key marker for fibroblasts and myofibroblasts. Preliminary western blot results indicated that choroid cells expressed high levels of a-SMA, compared to scleral fibroblasts (Figure *15a*), and both "paediatric" and "adult" choroid cells were very contractile in standard collagen gel contraction assays (*Figure 16*). We expanded the analysis of a-SMA expression level in more choroid cells, and we found that both “paediatric " and "adult" choroid cells express a-SMA, but the expression level was not correlated with age (Figure *15b*).

To confirm a-SMA and other cell population markers expression in choroid cells and determine the proportion of cells expressing the

protein, we used immunofluorescence. Generally, vimentin is used as a typical marker for fibroblasts, and also a marker for myofibroblasts (Chaurasia et al. 2009; Sliogeryte and Gavara 2019; Ostrowska-Podhorodecka et al. 2022). Calponin-1 is a specific marker for smooth muscle cells (Liu and Jin 2016; Feng et al. 2019). The NG2 and PDGFR are commonly used as markers for pericytes (Schultz et al. 2014; Braun et al. 2007), and CD31, CD144, and VWF are typical markers to identify endothelial cells (Braun et al. 2007; Flores-Nascimento et al. 2015; Shi et al. 2021). We found that both "paediatric" and "adult" choroid cells (Choro-9R, Choro-10R) expressed vimentin, a-SMA, and calponin-1 [*Figure 17(a-b)*]. For those cells, the proportions of double-positive expression of a-SMA and calponin-1 in both "paediatric " and "adult" choroid cells were close to 30%, confirming smooth muscle cells were present (*Figure 17d*). Myofibroblasts were included in choroid cells, as cells were positively expressed a-SMA and showed bundles of actin microfilaments which were not present in the fibroblasts, (*Figure 17c).* Myofibroblasts reached a proportion of 8% in those cells regardless of choroid donor ages (*Figure 17d*). These results indicated that fibroblasts were the predominant cell populations in the choroid cells, smooth muscle cells were presented in the second place, and a small proportion of myofibroblasts were also presented in this mixed population of primary choroid cells, regardless of choroid donor ages. However, choroid cells were negative for the expression of NG2, PDGFR, CD31, CD144 and VWF [*Figure 17(e-f)*], indicating pericytes and endothelial cells were not represented in this cell population mix. Altogether these results suggested our mixed population of choroid cells presented fibroblasts, smooth muscle cells and myofibroblasts.

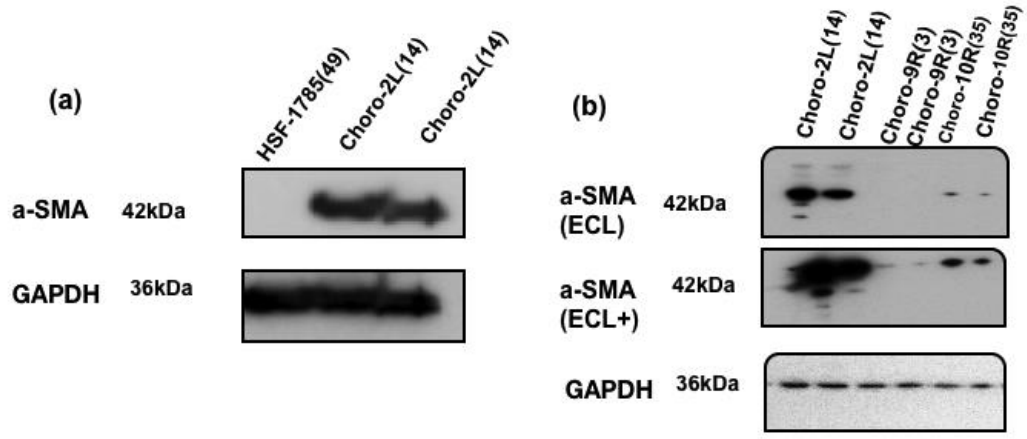

Figure 15. Choroid cells expressed a-SMA. (a). Representative western blot of a-SMA expression in choroid cells Choro-2L (14-year-old donor) cultured in 10% serum medium for 5-7 days, and adult scleral fibroblasts (HSF1785, 49-year-old donor). GAPDH is shown as a loading control. (b) Comparative a-SMA expression for 3 different choroid lines (donor age in brackets). 'ECL' reagent is the standard chemiluminescent substrate for western blot visualizing proteins, and 'ECL+' reagent generates stronger chemiluminescent signals than "ECL" with higher sensitivity.

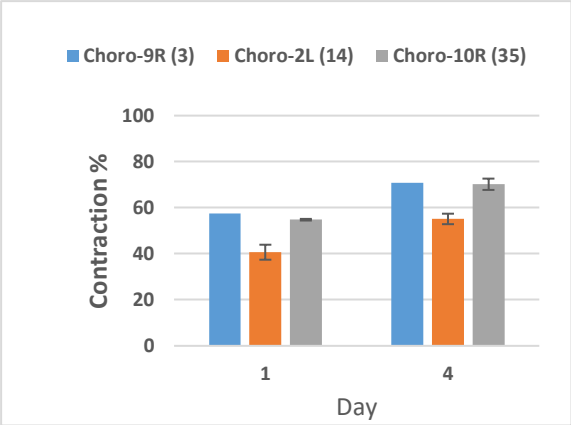

Figure 16. Choroid cells have a strong contraction potential. Choroid cells were cultured in collagen gel in the 10% serum medium and

contraction was measured on days 1 and 4. Shown is mean contraction percent +/- SEM, “Choro-9R”, n=1; “Choro-2L”, n=3; “Choro-10R”, n=3. The numbers in the bracket are the donor age.

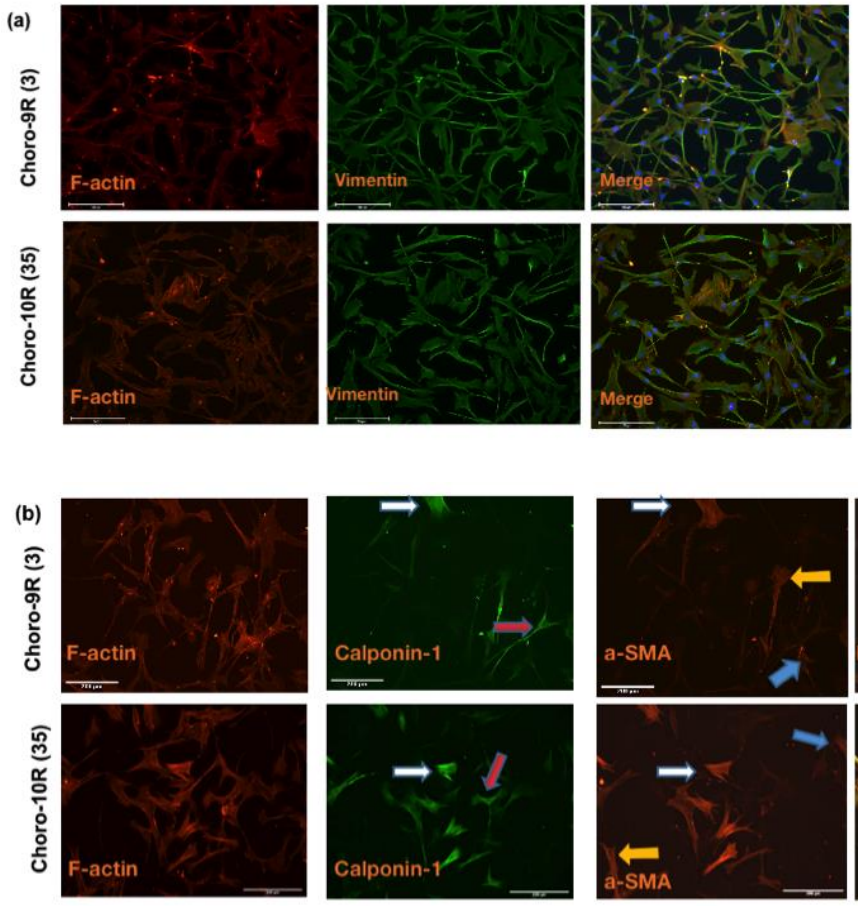

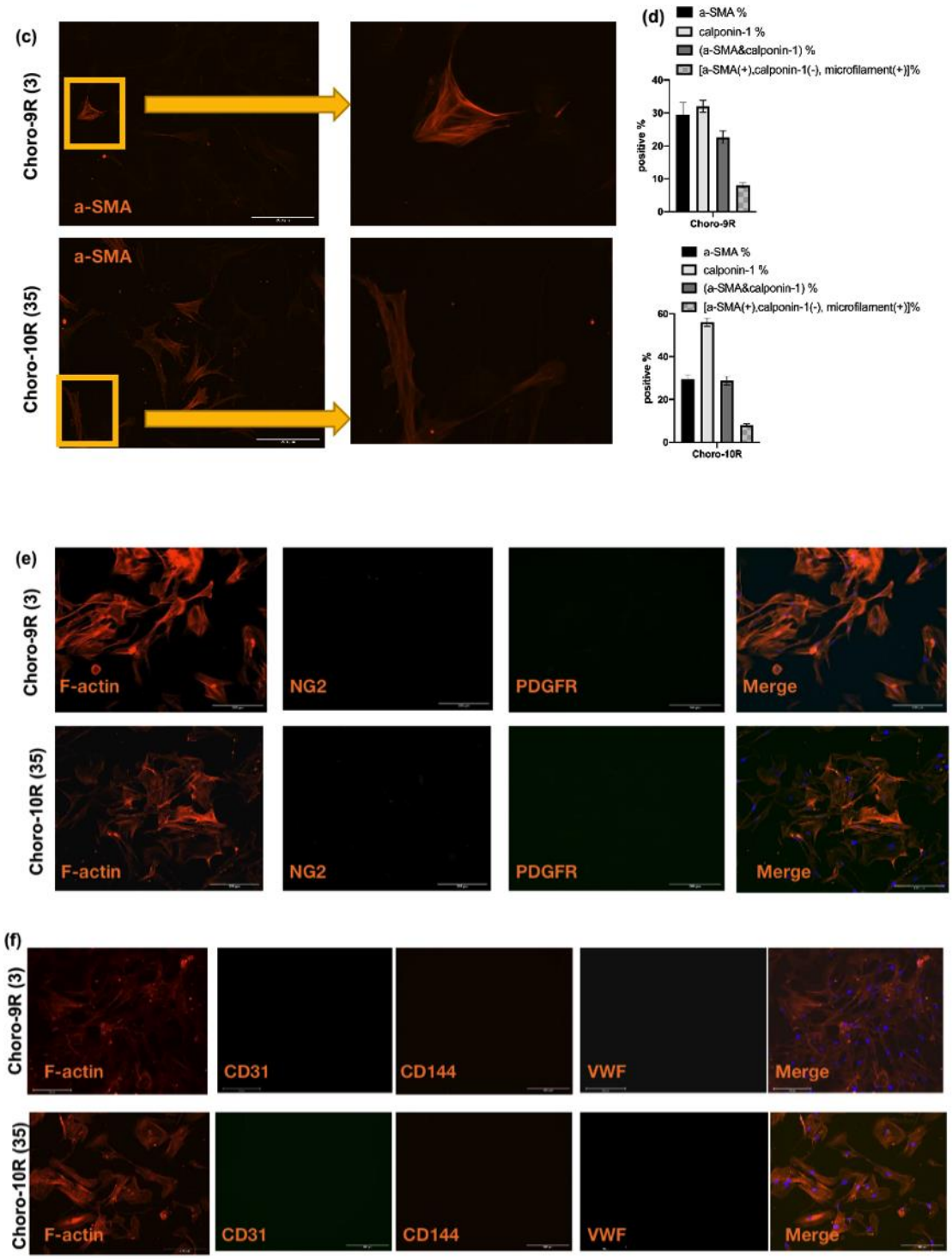

Figure 17(a-f). Choroid cells expressed vimentin, a-SMA and calponin-1. (a) Representative immunofluorescence images of choroid cells positively expressed vimentin. (b). Representative immunofluorescence images of choroid cells positively expressed a-SMA and/or calponin-1. The red arrow indicates a single positive

expression of calponin-1, the blue arrow indicates a single positive expression of a-SMA, the white arrow indicates double positive staining, and the yellow arrow indicates myofibroblast bundled with microfilaments. (c). Representative immunofluorescence images and zoomed-in images of myofibroblasts population in choroid cells. (d). Analysis of a-SMA and calponin-1 mono and or double staining cell percentage, shown is mean+/- SEM, n=20. “+” indicated positive expression, and “-” indicated negative expression. (e) Representative immunofluorescence images of choroid cells negatively expressed NG2 and PDGFR. (f). Representative immunofluorescence images of choroid cells negatively expressed CD31, CD144 and VWF. Choroid cells included both paediatric (Choro-9R) and adult (Choro-10R) ones, the number in the bracket indicated donor age. Cells were fixed and stained for F-actin (rhodamin-phalloidin) and imaged on an EVOS microscope using a 10X non-immersion objective. Scale bar= 200um.

3.2. Effect of dopamine treatment

3.2.1. Dopamine inhibits paediatric choroid cells’ ability to stimulate scleral fibroblast contractility

We hypothesise that dopamine inhibition of eye growth might be mediated through the choroid, relaying signals from the retina to the sclera. We exposed the choroid cells to dopamine to simulate downstream light-mediated signalling, and characterised the effects on scleral fibroblasts using the standard collagen gel contraction assay. Myopia usually exclusively occurred during childhood and young adolescence, thereby we chose paediatric scleral fibroblasts for the testing. To maximise potential effect, we chose paediatric scleral fibroblasts in the posterior position (HSF9-P) and paediatric

choroid cells (Choro-9R, in this case matching donor to the sclera), as we anticipated that posterior ones would be more receptive than anterior ones with choroid conditioned medium that resulted in the strongest contraction potential (see *Figure 9*). Some studies have reported that in both animal and human models, dopamine released from the retina was in the concentration of about 100nM to 3uM (Witkovsky 2004; Ohngemach, Hagel, and Schaeffel 1997; Frederick et al. 1982), and our previous lab work applied 100uM dopamine to scleral fibroblasts which showed significant toxicity. Thus, we treated the choroid cells with dopamine for 96 hours using five different concentrations (1nM, 10nM, 100nM, 1uM and 10uM dopamine), and prepared the 24-hour conditioned medium as before. We found that a dopamine concentration as low as 10nM completely abrogated the ability of the choroid conditioned medium to stimulate scleral fibroblast contraction (*Figure 18a*). To determine whether this effect was age-dependent, we also exposed “adult” choroid cells (Choro-10R, 35-year-old donor) to dopamine at 100nM, 1uM and 10uM, and prepared the conditioned medium under the same condition. We found that the adult choroid was an order of magnitude less sensitive to the dopamine treatment with only a partial effect at 10uM (*Figure 18b*), as opposed to full inhibition of the stimulatory effect for paediatric choroid at 10nM (*Figure 18*a). It suggested that dopamine critically and preferentially affected paediatric choroid cells’ ability to stimulate the contractility of scleral fibroblasts.

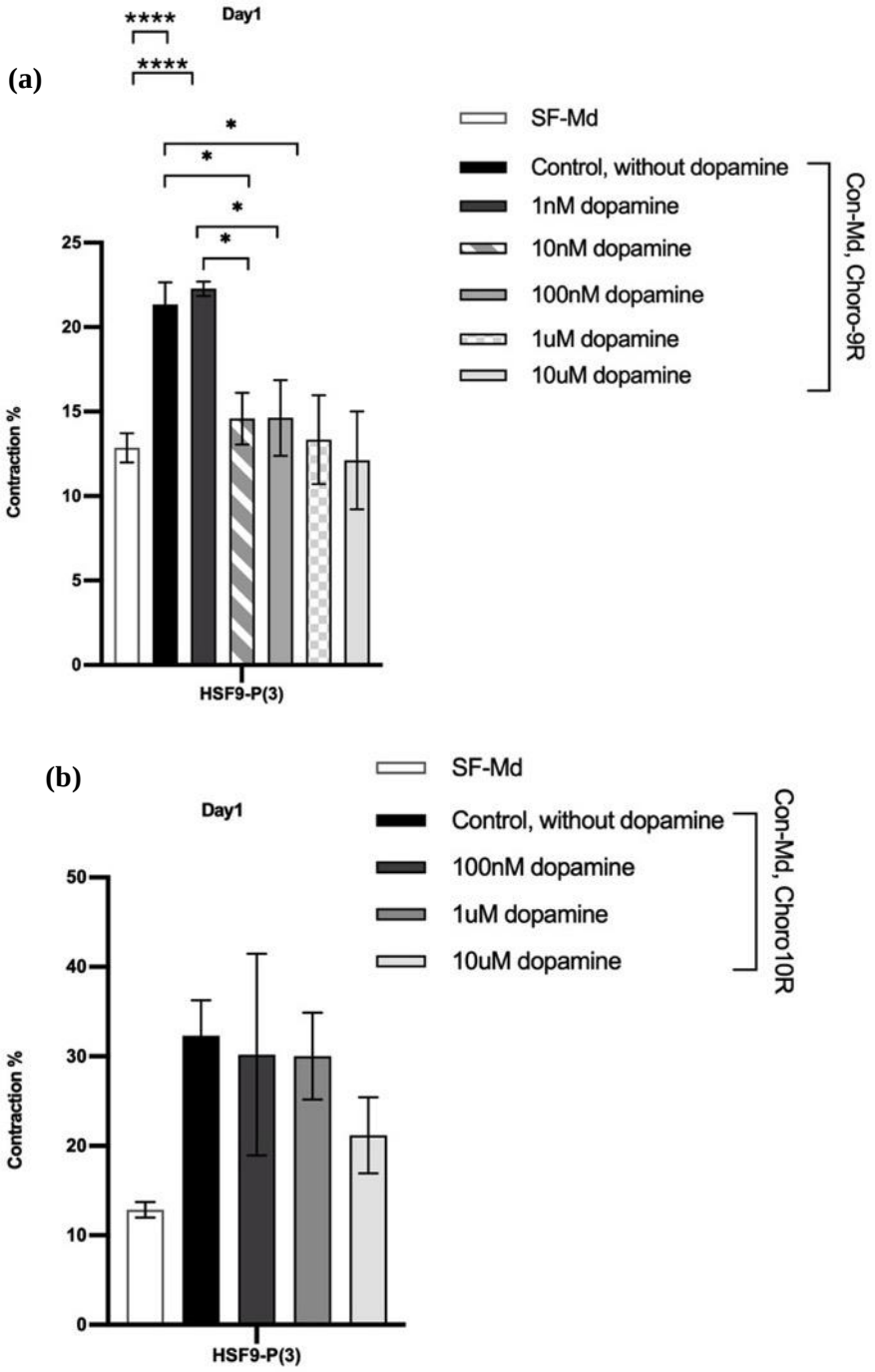

Figure 18. Dopamine treatment abrogated the stimulatory effect of paediatric choroid conditioned medium on scleral fibroblasts contraction. (a). Paediatric choroid cells (Choro-9R) were treated with/without dopamine for 96h (at different concentrations), and the medium was then replaced with the serum-free medium for 24 hours to generate conditioned medium. The choroid conditioned medium (with/without dopamine treatment) was then used to incubate scleral

fibroblasts (HSF9-P) for their contraction measurement after 1 day, the serum-free medium as control. (b). Adult choroid cells (Choro-10R) were treated with/without dopamine for 96h (at different concentrations), and the medium was then replaced with the serum-free medium for 24 hours to generate the conditioned medium to incubate scleral fibroblasts (HSF9-P) contraction measurement after 1 day. Shown is mean contraction percent +/- SEM, n>=3. *, P<0.5, ****, P<0.0001, t-test.

To optimise the dopamine treatment condition for inhibition of the choroidal conditioned medium effect on the sclera, we shortened the exposure time and applied effective concentration of dopamine to choroid cells. We kept using the most receptive scleral fibroblasts (HSF9-P) with the most responsive potential choroid cells (Choro-9R). We treated the choroid cells with dopamine for 24 hours at two concentrations (10nM, 100nM dopamine), and prepared the 24-hour conditioned medium as before. We found that a dopamine concentration as low as 10nM for 24 hours of treatment completely abrogated the ability of the choroid-conditioned medium to stimulate scleral fibroblast contraction (*Figure 19*). Altogether these results suggest that the dopamine concentration as low as 10nM treating choroid cells as little as 24 hours could effectively inhibit the ability of choroid conditioned medium to stimulate scleral fibroblasts contraction.

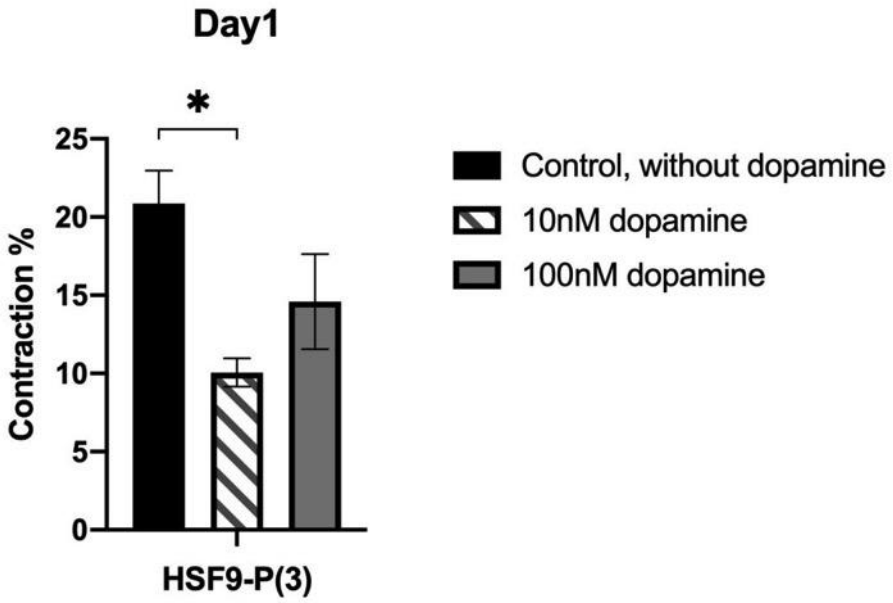

Figure 19. 24 hours dopamine treatment abrogates the stimulatory effect of paediatric choroid conditioned medium on scleral fibroblasts contraction. Paediatric choroid cells (Choro-9R) were treated with/without dopamine for 24h (at different concentrations), and the medium was then replaced with the serum-free medium for 24 hours to generate the conditioned medium. Scleral fibroblasts (HSF9-P) were embedded in collagen gels and exposed to either serum-free medium or choroid-conditioned medium (with/without dopamine treatment), and the contraction was evaluated after 1 day. Shown is mean contraction percent +/- SEM, in the “Control, without dopamine” group, n=6; in the “10nM dopamine” and “100nM dopamine” group, n=3. *, P<0.5, t-test.

3.2.2. Dopamine treatment is not toxic to choroid cells

To determine if the dopamine was toxic to choroid cells, we first looked at the morphology of choroid cells with or without dopamine treatment for 24 hours and found no obvious changes (*Figure 20a*). To further confirm dopamine was not toxic to choroid cells, we used the LDH assay to determine the cytotoxicity percentage in choroid

cells treated with dopamine in three different concentrations (10nM, 100nM and 1uM) and two different culture times (24 hours and 96 hours). We found almost no cytotoxicity of dopamine to choroid cells in all three different concentrations for 24 hours of incubation, though 96 hours of incubation slightly increased the cytotoxicity (*Figure 20b*). Altogether these results suggested that optimised 10nM dopamine treatment to paediatric choroid cells for 24 hours incubation was not toxic.

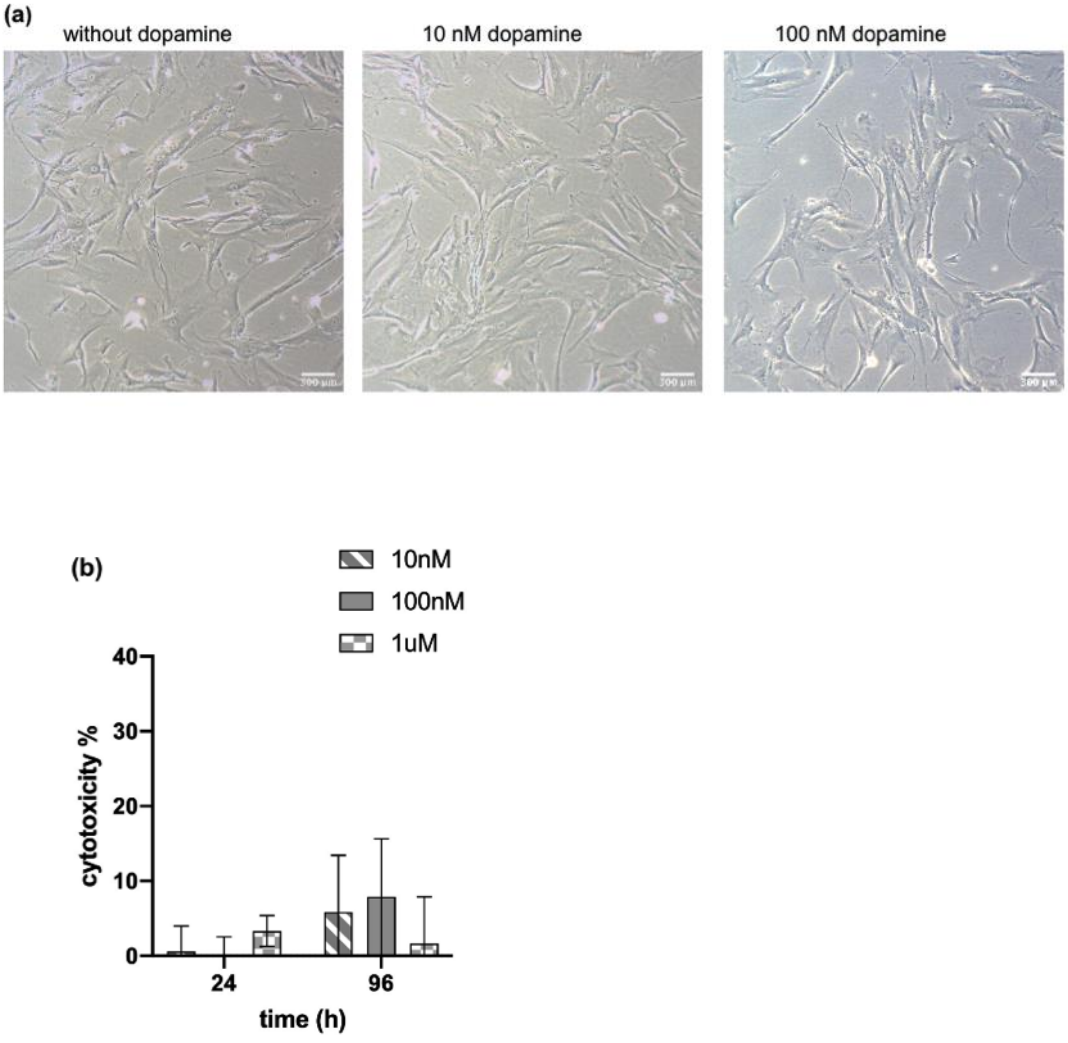

Figure 20. Dopamine is nontoxic to paediatric choroid cells. (a). Representative pictures of paediatric choroid cells (Choro-9R) with/without dopamine treatment for 24h at different concentrations.

Scale bar = 300um, (b) LDH assay showed minimal cytotoxicity of paediatric choroid cells (Choro-9R) treated with dopamine for 24h and or 96h (at different concentrations). Cytotoxicity percentage was normalized to 100% toxicity control, the shown is mean +/- SEM, n=3.

3.2.3. Dopamine-CCM prevents stimulating scleral fibroblasts contraction rather than toxication.

Dopamine is not toxic to paediatric choroid cells, but if the scleral fibroblasts stimulated contraction was prevented by conditioned medium from dopamine-treated choroid cells (dopamine-CCM) or inhibited by its toxicity remained unclear. We used CCK8 proliferation assay, direct cell counting after digesting gel, and live/dead assay to determine if the choroid conditioned medium treated with dopamine was affecting scleral fibroblast viability in collagen gels. We found no effect of the dopamine-CCM on cell numbers (CCK8 and cell counts, *Figure 21*). The OD values (indicating cell numbers) of scleral fibroblasts (HSF9-P) cultured with all three conditions were not significantly different each day respectively. Also, the cell counting from digested collagen gel remained similar to the OD value trendy. Although cell numbers decreased on day4, this trend matched the cell viability change trendy in the CCK8 proliferation assay.

Moreover, we used the live/dead assay to confirm further that the dopamine-CCM was not toxic to scleral fibroblasts in the 3D collagen gel. We found no significant increase in dead scleral fibroblasts with the “dopamine” CM, compared to CM without dopamine treatment (*Figure 22*).

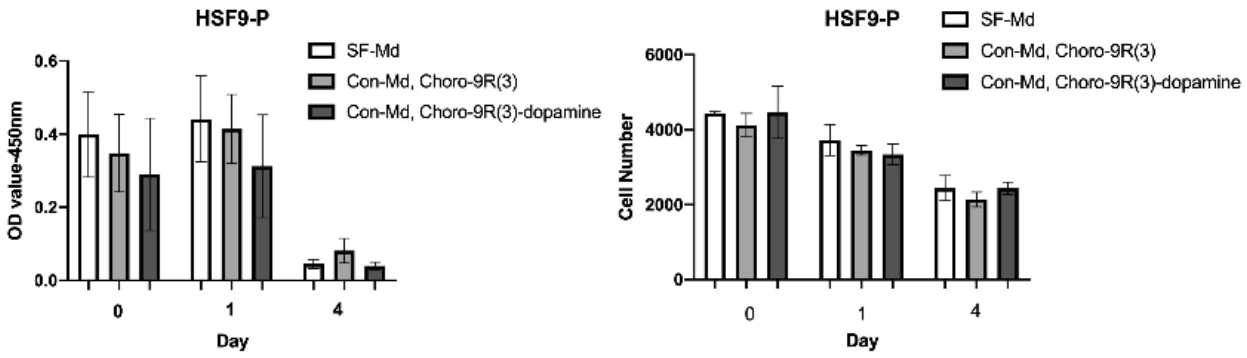

Figure 21. Conditioned medium from dopamine-treated choroid cells had no effect on scleral fibroblast viability in collagen gels. The left figure shows from day0 to day4, paediatric scleral fibroblasts (HSF9-P) viability in serum-free medium and with or without 10nM dopamine 24 hours-treated choroidal conditioned medium in the 3D collagen gel cultures are not changed on time-dependent manner, by CCK8 proliferation assay for 4 hours incubation. Shown is mean +/-SEM, in the “SF-Md, “Con-Md, Choro-9R” and “Con-Md, Choro-9R-dopamine treated” group, n>=4. The right figure shows the cell number of paediatric scleral fibroblasts (HSF9-P) with or without 10nM dopamine 24 hours-treated choroidal conditioned medium in the 3D collagen gel cultures are without significant difference. Shown is mean +/-SEM, n>=4. Three different mediums have no significant difference, respectively on the same day, p value = ns.

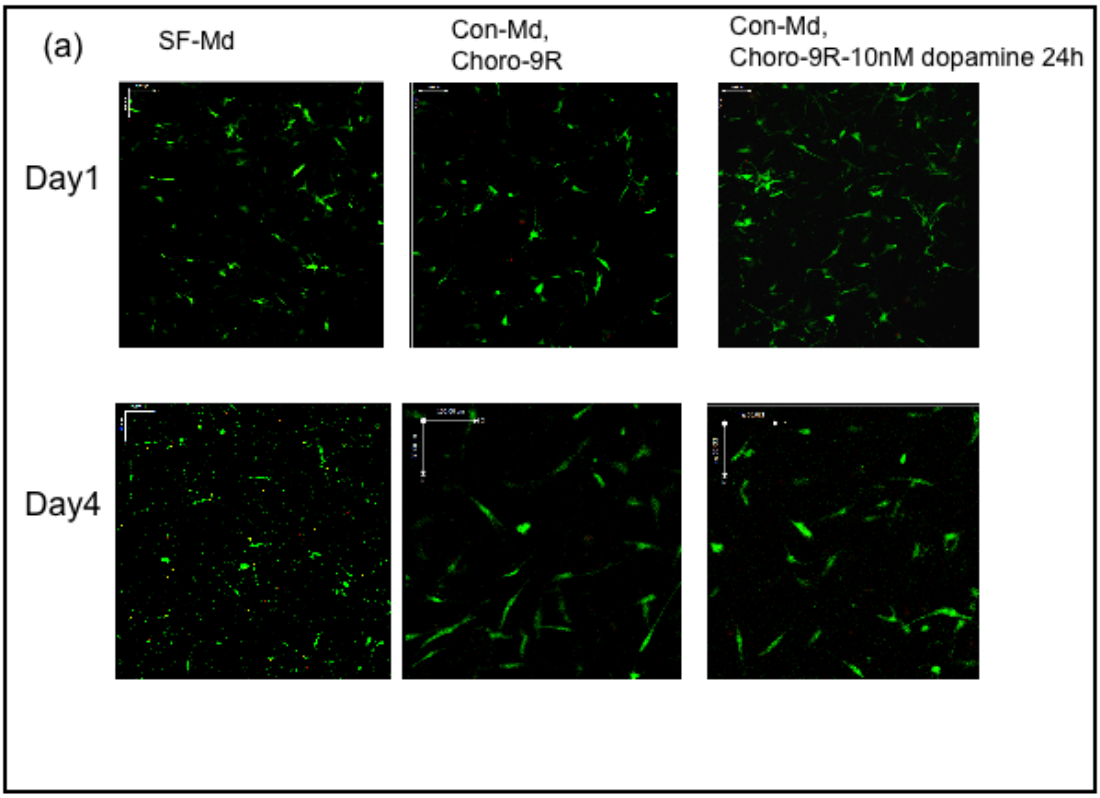

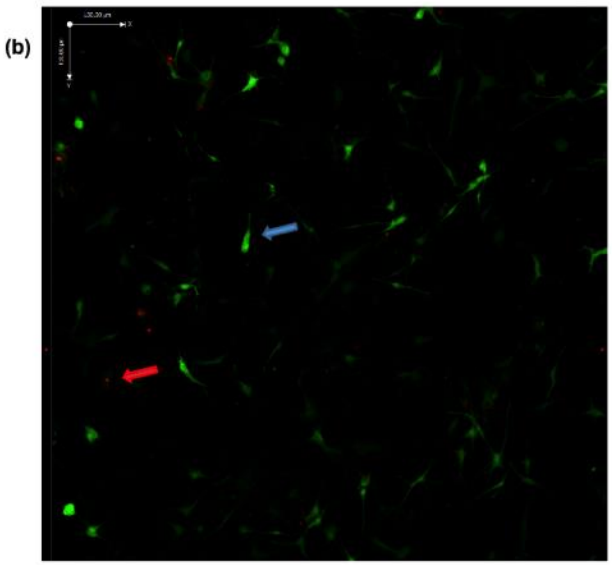

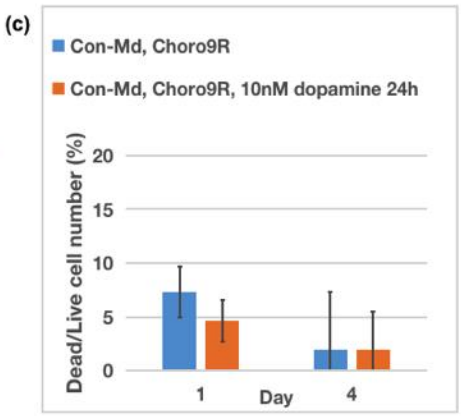

Figure 22. “Post dopamine conditioned medium did not affect sclera fibroblast viability in collagen gels. (a). Representative gel images of scleral fibroblasts (HSF9-P) in three different conditions of medium, with confocal LSM700 by Live/Dead assay, scale bar = 130um, on

the top left side of the image. (b). The representative image of scleral fibroblasts (HSF9-P) shows dead and live cells. The blue arrow indicates a live cell, the red arrow indicates a dead cell. The live/dead assay cell number analysis is mean +/-SD, the result of cell number percentage in the gel which conditioned medium from Choro-9R and Choro-9R-10nM dopamine 24h treatment on the day1, n=4; on the day4, the conditioned medium from Choro-9R group, n=5, Choro-9R-10nM dopamine 24h treatment group, n=6.

4. Developing a biomimetic model of the scleral and choroid interface.

To validate our studies in an environment that more faithfully recapitulates the sclera-choroid cell interplay, we developed a 3D sclera-choroid interface using collagen gels of different stiffness to mimic each layer of eye tissues. We developed the biomimetic model with 2 layers attached and established tensional homeostasis for cells. We compressed the bottom gel layer containing scleral fibroblasts by plastic compression for a stiffer environment, and placed a standard soft gel layer containing choroid cells on the top, attached to the Mattek dish well (*Figure 23a*). In this preliminary result, we found that scleral fibroblasts and choroid cells could be maintained for at least three weeks without noticeable cell damage (*Figure 23b,c*). However, it was hard to distinguish the two different layers in this set since they were a bit squashed when we mounted them between slide and coverslip for imaging on an upright confocal (Confocal LSM700).

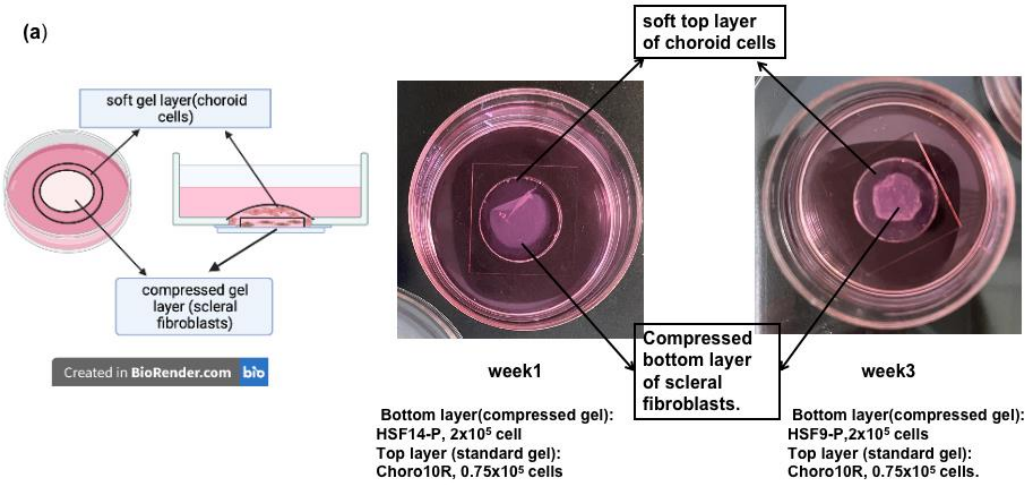
(a)
soft gel layer(choroid cells)
compressed gel layer (scleral fibroblasts)
Created in BioRender.com
soft top layer of choroid cells
Compressed bottom layer of scleral fibroblasts.
week1
week3
Bottom layer(compressed gel): HSF14-P, 2x10⁵ cell
Top layer (standard gel): Choro10R, 0.75x10⁵ cells
Bottom layer(compressed gel): HSF9-P,2x10⁵ cells
Top layer (standard gel): Choro10R, 0.75x10⁵ cells.

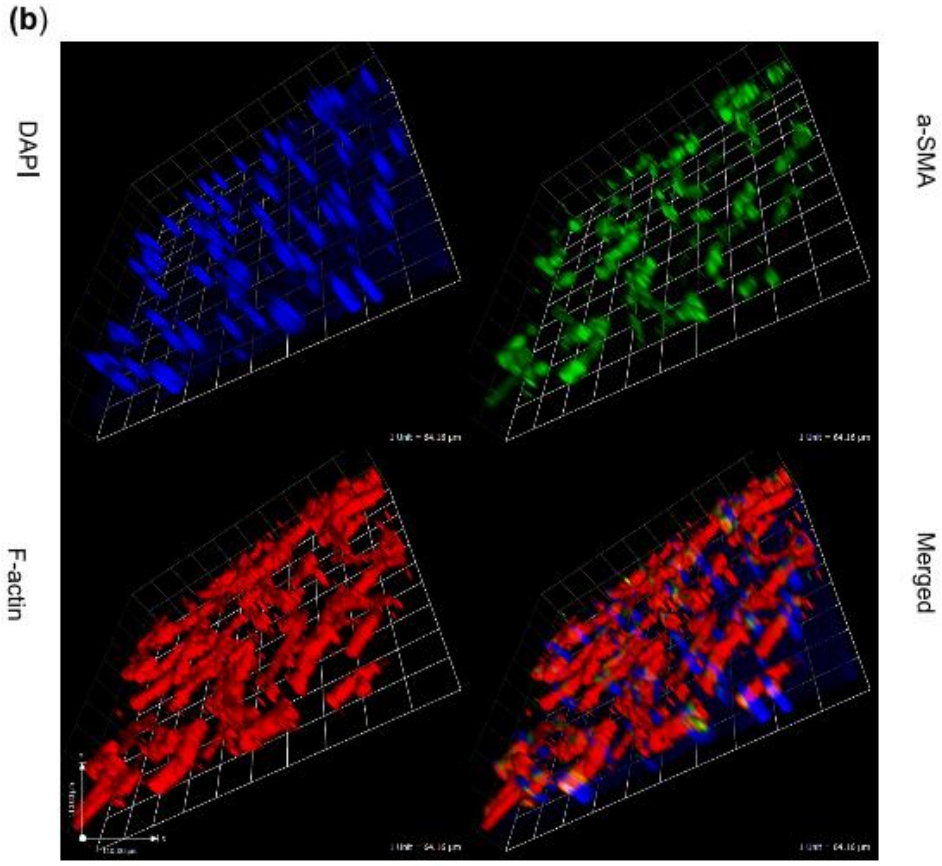
(b)
DAPI
a-SMA
F-actin
Merged

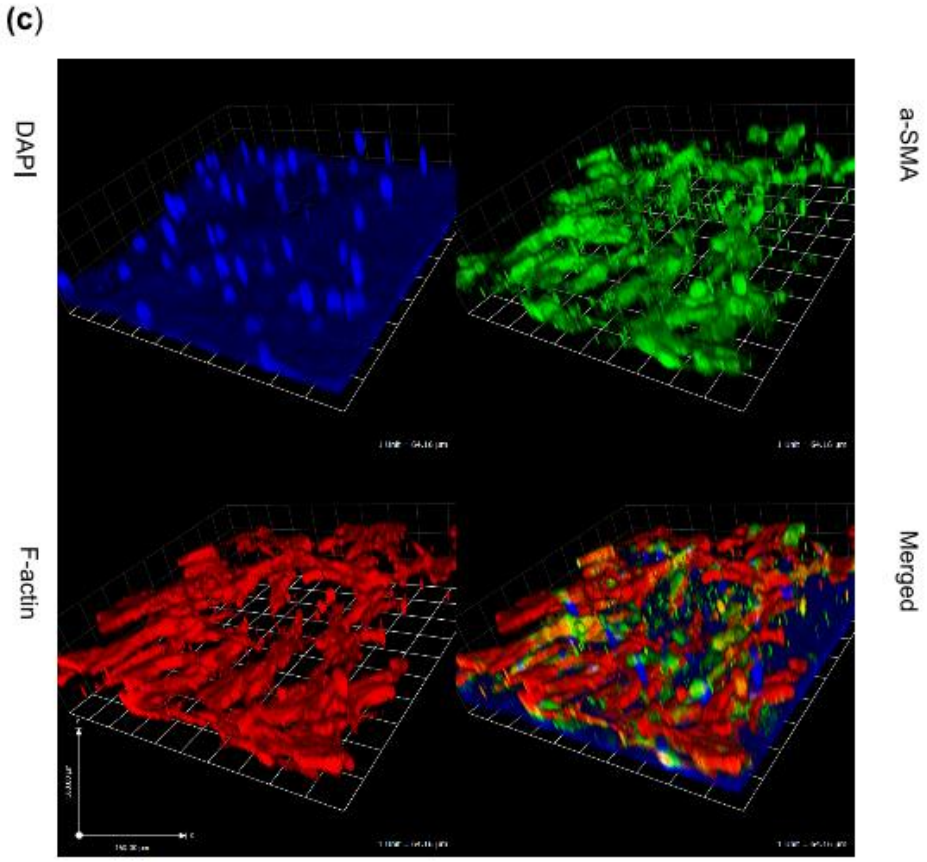

Figure 23(a-c). Physical weight-derived 2-layer biomimetic model (a). Schematic of Attached 2-layer biomimetic model in the Mattek dish on the Week3. The bottom layer (compressed gel) of HSF14-P seeded $2x10^5$ cells, Top layer (standard gel) of Choro10R seeded $0.75x10^5$ cells. Figure 16B. Attached 2-layer biomimetic model in the Mattek dish on week1. The bottom layer (compressed gel) of HSF14-P seeded $2x10^5$ cells. Top layer (standard gel) of Choro10R seeded $0.75x10^5$ cells. (b). 3D reconstruction of sclera-choroid layer after 1-week culture. The 2-layer tissue biomimetic was prepared with paediatric scleral fibroblasts (HSF14-P) and matching paediatric choroid cells (Choro-9). After a week, the bilayer was fixed and stained for F-actin (rhodamine-phalloidin), a-SMA (FITC) and DAPI (blue), and imaged on a Zeiss LSM700 confocal using a 10X non-immersion objective. Scale bar: 1 square unit =64 um. (c). 3D

reconstruction of the sclera layer from sclera-choroid layer after 3 weeks of culture. The 2-layer tissue biomimetic was prepared with paediatric scleral fibroblasts (HSF14-P) and matching paediatric choroid cells (Choro-9). After 3 weeks, the bilayer was fixed initially, but the layers separated during the staining process, allowing us to visualize the scleral layer on its own. F-actin (rhodamine-phalloidin), a-SMA (FITC) and DAPI (blue). Imaged on a Zeiss LSM700 confocal using a 10X non-immersion objective. Scale bar: 1 square unit =64 um.

To simplify the plastic compression process and make it more reproducible while facilitating the setting of the gels in an attached configuration, and also tried to achieve the actual stiff layer of the sclera, we used the RAFT 3D Cell Culture System with absorber technology to create the compressed layer with the scleral fibroblasts (*Figure 24a.b*). The gels with sclera fibroblasts were made and compressed directly in 24-well plates, and the soft gel with the choroid cells was set on top. Using this set, we were able to develop a 3-layer biomimetic model with a compressed bottom gel layer of scleral fibroblasts, a middle soft gel layer of choroid cells, and a top monolayer of IPSC-derived differentiated Retinal Pigment Epithelial (RPE) cells (provided by Dr Victoria Tovell, Professor Pete Coffey's lab, Institute of Ophthalmology UCL). This 3-layer biomimetic model enabled us to make a complete back of the eye biomimetic, mimicking the back layers of the human eye. This RAFT-derived biomimetic model was imaged on an inverted confocal microscope (Leica Stellaris5). We found that three layers could be distinguished clearly (*Figure 24c-f*), recapitulating the three outermost layers at the back of the eye. In addition, the cell density

in the scleral layer appeared very similar to what was published for the mouse tissue (Oglesby et al. 2016), as well as the cell shape. It suggested that our model recapitulated a “physiological” sclera, and thus would be helpful in understanding the interactions between the choroid and scleral cells.

(a)

RAFT Absorbers for creating RAFT Cultures in 24-well plates

(b)

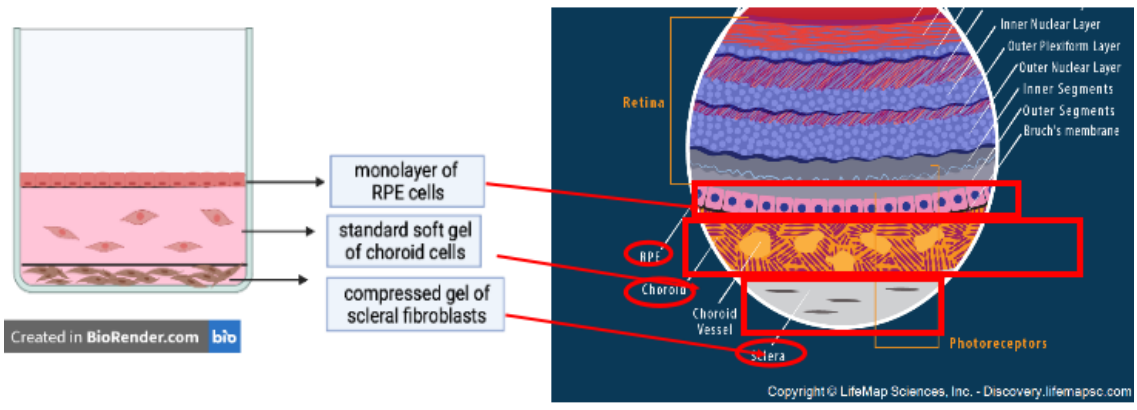

Anatomy of the eye layers

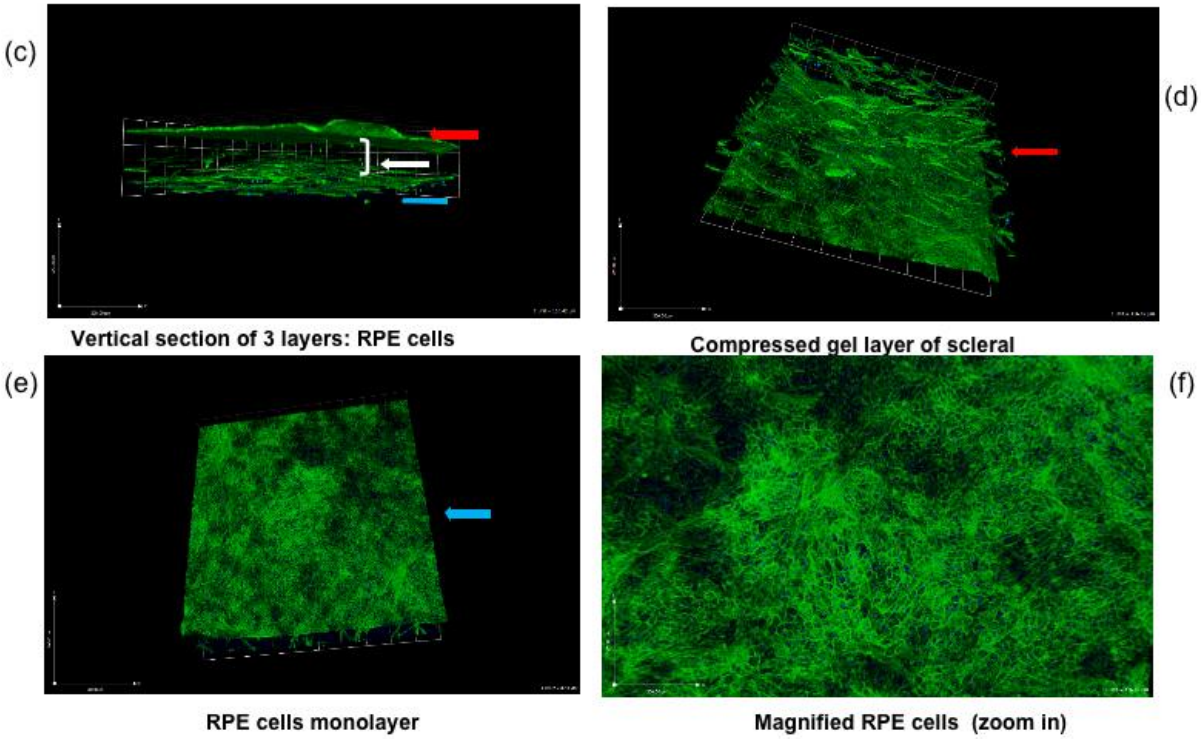

Figure 24. RAFT-derived 3-layer 3D model (a). Diagram of RAFT system. (b) Schematic of RAFT-derived 3-layer biomimetic of the back of the eye: sclera, choroid and RPE layers. (c).3D reconstruction of 3 layers, REP cell layer, standard gel layer of choroid cells, compressed gel layer of scleral fibroblasts. (d). Reconstruction rotated to show the compressed gel layer of scleral fibroblasts. (e). Reconstruction rotated to show the RPE monolayer on top. (f), Reconstruction rotated to show the RPE monolayer on top by zooming in. The Blue arrow shows the scleral layer, the white arrow shows the middle choroid layer, and the red arrow shows the monolayer of RPE cells. Reconstruction rotated to show the RPE monolayer on top. The 3 layers were fixed and stained for F-actin (rhodamin-phalloidin, the colour changed to green for better viewing)

and DAPI (blue), and imaged on a Stellaris5 confocal using a 10X non-immersion objective. Scale bar: 1 square unit =116 um.

Discussion

To the best of my knowledge, this is the first study *in vitro* using primary human scleral fibroblasts and choroid cells that presents the discovery: choroid cell-secreted factors promote scleral fibroblast contractility, and this stimulatory effect could be inhibited by dopamine applied to choroid cells. These findings will be discussed in detail in the subsequent section.

1. Scleral fibroblast contractility

Fibroblasts play an essential role in extracellular matrix (ECM) remodelling, fibroblast contraction commonly occurs in wound healing and tissue remodelling (Bainbridge 2013). Tissue contraction is a dynamic state characterised by both intracellular and extracellular events. With extracellular mechanical tension, scleral fibroblasts generate cell force to maintain tensional homeostasis, presenting fibroblasts contraction (He and Grinnell 1994; Brown et al. 1998). To describe this process in detail, microfilaments (composed of the contractile protein called actin) contract with stimuli, such as extracellular mechanical tension stimulation, and lead to an organized actin cytoskeleton in cooperation with microtubules (composed of subunits of the protein tubulin) which present as a “balanced space frame” to maintain cell shape, generating intracellular force (Tomasek et al. 1992; Brown et al. 1996). The contractility of scleral fibroblast is one parameter of scleral biomechanics, and we have found scleral fibroblast contractility was stimulated by choroid secreted factors. In our preliminary result, although PRELP was linked to myopia progression, we have found

the PRELP was unlikely a molecular marker that linked to the scleral fibroblasts contraction, as it negatively regulated scleral fibroblasts contractility. However, we found scleral fibroblast contractility presented age and antero-posterior position differences, and a-SMA expression exhibited discrepancy in age and antero-posterior position differences, which will be specifically discussed in the following subsections.

1.1. Scleral fibroblast contractility presents age and antero-posterior position differences

Collagen is the predominant component of the sclera, it cooperates with proteoglycan to play a critical role in determining scleral biomechanical properties, and dermatan sulfate proteoglycan ties fibrils, restricting their movement for organising collagen (Bailey 1987). In this study, we used rat tail collagen to embed scleral fibroblasts for the collagen gel contraction assay, which was a proxy for cell force measurement. We found the contractility of human scleral fibroblasts was overall greater in paediatric age than in older ages, regardless of antero-position differences, which suggested that paediatric fibroblasts can develop more cell force than adult ones. In addition, the geometry of collagen fibres changes with aging, the cross-sectional area of the scleral collagen molecule is increased in older age, whilst the lower degree of fibre alignment with advanced age (Coudrillier et al. 2015; Keeley, Morin, and Vesely 1984). Therefore, the scleral matrix presents in age differences exhibits different collagen geometry. The a-SMA is not only a classic marker for contraction, but also a classical link to fore (Wang, Zohar, and McCulloch 2006; Chen et al. 2007). Hence, it is essential to determine which molecular components in the scleral fibroblasts exhibited age differences, such as a-SMA.

The sclera presents ultrastructural differences in antero-posterior position differences. For example, in the rabbit model, the thickness of the anterior sclera is less than that in the posterior position, and the anterior sclera presents a higher concentration of collagen-related amino acids (such as hydroxyproline, hydroxylysine and proline), more glycosaminoglycans, and a larger mean diameter of collagen fibrils than posterior ones (Trier et al. 1999). Moreover, the scleral fibres also exhibited antero-posterior position differences, they are more circumferential in the posterior position but less aligned than those in the anterior position (Girard et al. 2011). During myopia progression, scleral thickness is reported to decrease, especially the posterior one (Moriyama et al. 2011), suggesting posterior sclera may exhibit different biomechanical property changes from anterior one during this process. In our study, we found human anterior scleral fibroblasts had greater contractility than posterior ones in the absence of serum, particularly in the paediatric scleral fibroblasts. It suggested that the scleral fibroblasts are indeed different in anterior and posterior sections, and their differences in antero-posterior positions are possible in response to the ultrastructural differences in the anterior and posterior positions, as scleral fibroblasts are the key factors that regulate scleral ECM remodelling.

The contractility differences of human scleral fibroblasts in antero-posterior position might also be due to scleral proliferation rate difference, as the more cell numbers, the more cell force could be generated to have greater contractility. In the 2D cell culture environment, we found that in the presence of serum, anterior fibroblasts overall proliferated faster than posterior ones. Similarly, differences with respect to the antero-posterior position presented in the 3D collagen gels as well, anterior scleral fibroblasts exhibited higher OD values than posterior ones in the same condition with the

CCK8 proliferation assay. The CCK8 assay is based on dehydrogenase activity detection in viable cells, chemicals or conditions that affect dehydrogenase activity in viable cells may cause discrepancy, thereby the proliferation difference of scleral fibroblasts in antero-posterior position difference determined by the CCK8 assay could be either actual proliferation discrepancy, or conditions affect dehydrogenase activity, such as metabolism. Although the metabolic activities of the anterior and posterior sclera are unclear, the posterior scleral thickness was reported to decrease more predominantly than that in the anterior position during myopia progression (Moriyama et al. 2011), which suggests that posterior fibroblasts behaved differently from anterior ones. In addition, quiescent human foreskin fibroblasts were found to have higher metabolic activity than proliferating ones (Lemons et al. 2010; Chen et al. 2012). Similarly, anterior scleral fibroblasts also proliferate differently from posterior ones, suggesting scleral fibroblasts in anterior and posterior positions might present proliferating differently like foreskin fibroblasts with different metabolism. Hence, the proliferation rate and/or metabolic differences in antero-posterior positions in the 3D, and anterior fibroblasts proliferated faster than the posterior ones in the 2D, suggesting proliferation discrepancy of fibroblasts in anterior and posterior positions may exhibit different contractility. However, it is also essential to determine the molecular component level differences of scleral fibroblasts in antero-posterior position differences.

In this study, there are some limitations as in the 2D cell growth rate experiments, we initially did not pay attention to the passage number of the cells tested, and some of the " paediatric" scleral fibroblasts used for the experiments were actually tested at higher passage numbers (up to passage 14). It is possible that the

difference seen is due to an artefact of the cells being in culture for too long, as we have noticed that some of the cells start growing slower after more than 9 passages in vitro. However, there was no difference in proliferation between adult and paediatric scleral fibroblasts, just differences between anterior and posterior ones. If cell passage issue was affecting paediatric scleral fibroblasts, it would have affect both paediatric and adult ones, suggesting cell passage issue is unlikely the key factor to exhibit antero-posterior differences in proliferation.

1.2. a-SMA role in scleral fibroblasts contractility

In fibroblast, a critical component of the cytoplasmic cytoskeleton - actin, plays a critical role in contraction in association with protein myosin. In fibroblasts contraction, myosin light chain (MLC) phosphorylation has a direct effect to regulate its contraction by activating MLC kinase (MLCK) (Ehrlich et al. 1991). Alpha-smooth muscle actin (a-SMA) is one of six tissue-specific actin isoforms in the mammalian actin gene family, playing a critical role in the tissue contraction (Khaitlina 2001). In the fibrotic tissue, the a-SMA expression in fibroblasts was found to be typically increased compared to healthy fibroblasts, which leads to increased contractility and cellular morphological change (Chadli et al. 2019). Moreover, myofibroblasts are typically differentiated from fibroblasts in fibrosis, which usually presents excessive remodelling and ECM accumulation (Bonnans, Chou, and Werb 2014). Myofibroblasts employ assumed actin-based motors to generate cell force to mediate extracellular matrix (ECM) remodelling by traction, and typically express a-SMA in strong actin filament bundles (Arora, Narani, and McCulloch 1999; Tomasek et al. 2002). Previous studies also reported that a-SMA expression upregulated fibroblast

contractile activity, and the proportion of myofibroblasts increased in this promoted contraction progression (Hinz et al. 2001; Zhang et al. 2016; Shinde, Humeres, and Frangogiannis 2017). Hence, the a-SMA is usually regarded as a marker for enhanced contractility.

In our study, we also found choroid cells showed high contractile ability in the 3D collagen gel contraction assay, their a-SMA expression levels are quite high (not true for one of them), and choroid cell populations contained typical myofibroblasts cells, suggesting that upregulated a-SMA expression level and increased myofibroblast numbers leads to increased contractility in choroid cells. In addition, the a-SMA expression in scleral fibroblasts increased during myopia progression, and myopia onset exclusively occurred in childhood, suggesting a-SMA is possibly relevant to scleral fibroblasts activation with age differences. In our study, paediatric scleral fibroblasts had an overall higher expression level of a-SMA than adult ones, while paediatric scleral fibroblasts had greater contractility than adult ones, suggesting a-SMA expression is associated with age differences and responsible for scleral fibroblasts contractility.

Moreover, scleral thickness is reduced during myopia progression, particularly in the posterior position, suggesting posterior scleral fibroblasts might present different biomechanisms than anterior ones. We firstly found human posterior scleral fibroblasts overall expressed a higher level of a-SMA than anterior ones regardless of age, this a-SMA distribution diversity in different antero-posterior positions was consistent with scleral fibroblast contractility discrepancy, particularly in paediatric scleral fibroblasts. However, the posterior scleral fibroblasts isolated from paediatric donor tissue had the higher expression level of a-SMA in our results, and they exhibited lower contractility than anterior ones, which is contrary to

that upregulated a-SMA expression increased the contractility of fibroblasts. It is possibly suggested that the a-SMA is not the only factor in response to the scleral fibroblast antero-posterior position differences. However, it is more possibly because our results of paediatric scleral fibroblasts in the anterior position contracted more than those in the posterior position in the absence of serum, but the scleral fibroblasts were used for a-SMA expression level tests were cultured in the presence of serum. Fibroblasts under these two conditions were significantly different with serum stimulation, but the serum is a critical factor to increase fibroblast contractility dramatically (Li et al. 2014). Therefore, our result of the a-SMA expression level of scleral fibroblasts with serum stimulation cannot directly indicate scleral fibroblast contractility in the absence of serum.

To sum up, although our study found the discrepancy of a-SMA expression level in scleral fibroblasts positioned in different antero-posterior sections and ages, less a-SMA expression in anterior section exhibited greater contractile ability than posterior one, suggesting that a-SMA is unlikely a possible hallmark for scleral fibroblast contractility.

2. The effect of choroid cell-secreted factors on scleral fibroblast contractility

The choroid is generally accepted to regulate scleral metabolism during visual signal-guided eye growth, and a number of choroid cell-secreted factors are associated with scleral remodelling, such as TGF-β, bFGF, FGF-2, MMPs and TIMPs. In the chick model *in vivo,* proteoglycan in the form-deprivation myopic sclera was increased as compared with the normal sclera (Rada et al. 1992). In the chick model *in vitro*, co-culture of isolated normal sclera with normal

choroid revealed inhibition of proteoglycan synthesis in the sclera, but co-co-culture normal sclera with myopic choroid (form-deprivation myopia) showed relatively increased proteoglycan synthesis in the sclera comparing to normal condition (Marzani and Wallman 1997). Similarly, our study *in vitro* also found that human choroid cell-secreted factors could affect the sclera, as they increased the contractility. The following subsections will discuss how scleral fibroblasts are affected by cell-secreted factors in our study.

2.1. Choroid cell-secreted factors promote scleral fibroblast contractility

Previous studies have shown that the choroid could secrete a number of growth factors that not only regulate choroid development and growth but also adjacent tissues. For example, choroid-secreted factors in the chick eye were found to have an impact on its adjacent tissue, ciliary body. In the chick choroid *in vitro*, choroid cells were found to secrete soluble macromolecule (>10kDa) to stimulate somatostatin expression in choroidal ciliary neurons, which provided support for ciliary neurons differentiation and development *(Coulombe and Nishi 1991)*. The adjacent tissue of choroid includes not only the ciliary body but also the sclera, as the choroid anteriorly connects to the ciliary body and posteriorly connects to the sclera. The choroid is relevant to the synthesis of multiple growth factors, such as VEGF, bFGF FGF-2, HGF, MMPs, TIMPs, and TGF-β, and some of these growth factors also play an important role in the scleral ECM remodelling (Saint-Geniez, Maldonado, and D'Amore 2006; Frank et al. 1996; Grierson et al. 2000; Steen et al. 1998; Ogata et al. 1996; Strauss 2005). Here, we starved choroid cells in the serum-free medium to generate the choroid conditioned medium, which

served as a “soup” which contained choroid cells-secreted factors in the medium. We found that contractility of scleral fibroblast was overall promoted upon stimulation with choroid conditioned medium, and the proliferation rates of scleral fibroblasts did not change with stimulation of choroid conditioned medium in 3D collagen gels under the same conditions. It suggested that choroid cell-secreted factors indeed promoted the contractility of scleral fibroblasts through changing molecular components of scleral fibroblasts rather than proliferation. To determine which cell populations in the choroid cells consisted in our study that possibly secreted growth factors, we also characterised primary choroid cells isolated from donor tissue that used in our experiments. We found those choroid cells were a mix cell population included fibroblasts, “active” fibroblasts – myofibroblasts, and smooth muscle cells, but without endothelial cells and pericytes. Thereby, growth factors that are secreted by choroidal fibroblasts, choroidal myofibroblasts and smooth muscle cells, such as bFGF, FDF-2, MMPs, TIMPs, and TGF-β, possibly affect scleral ECM remodelling, rather than VEGF as it synthesized by endothelial cells (Coultas, Chawengsaksophak, and Rossant 2005).

2.2. a-SMA role in scleral fibroblasts contractility upon stimulation of choroid cell-secreted factors

It is generally accepted that serum is a key factor that promotes fibroblast contractility (Li et al. 2014; Shinde, Humeres, and Frangogiannis 2017), and our preliminary experiments also ensured serum stimulation increased contractility of scleral fibroblasts that primarily isolated from donor tissue in our study. We used serum to resuspend scleral fibroblasts suspension for collagen mixture that was ultimately cultured in 10% serum medium, and the same volume

of 10% serum medium to resuspend scleral fibroblasts suspension for collagen mixture ultimately cultured in the other three mediums without serum, see *Figure 25*. In our study, we also found scleral fibroblasts contractility was promoted upon stimulation of choroid cell-secreted factors in 3D collagen gel, which is similar to the serum stimulation to increase the contractility of scleral fibroblasts. On the one hand, the fetal bovine serum is abundant with TGF-β, which is a key factor that potentially promotes fibroblasts differentiated to the myofibroblasts (Li, Huang, and Zhou 2009; Oida and Weiner 2010). Also, a-SMA is involved in the serum-induced contraction of fibroblasts, and a-SMA is typically presented in the myofibroblasts (Shinde, Humeres, and Frangogiannis 2017). On the other hand, the actin isoforms encoding genes have multiple promoters, the a-SMA promoter contains multiple regulatory elements, such as TATA and CArG boxes that consists of general sequence motifs TATATAA and CC(A/T-rich)6GG (Hautmann et al. 1998; Mack and Owens 1999). The CArG box is the core sequence of the serum response element (SRE) in the early-response gene, and the CArG element is essential for the transient transcriptional response of a-SMA gene with serum or other growth factor stimulation (Shore and Sharrocks 1995; Reecy et al. 1998). Hence, we sought to determine whether the growth factors secreted by choroid cells promoted scleral fibroblasts contractility that affected a-SMA expression level like serum stimulation. We cultured paediatric scleral fibroblasts in the pair of anterior and posterior positions in the choroid conditioned medium for 24 hours in 2D cell culture substrates, but no significant difference in the expression level of a-SMA was found in the scleral fibroblasts upon choroid cell-secreted factors stimulation. However, Shinde and colleagues demonstrated that when mouse cardiac fibroblasts were embedded in the collagen gel, the serum increased the contractility

of fibroblasts but a-SMA expression was reduced, which was opposite to that increased a-SMA usually promoted fibroblast contractility, suggesting serum-induced fibroblasts contraction in the collagen gel was not simply regulated by a-SMA expression and/or myofibroblasts transdifferentiation (Shinde, Humeres, and Frangogiannis 2017). Therefore, there are two possibilities for the a-SMA expression level of scleral fibroblasts not to change upon choroid-secreted factors stimulation. Firstly, it is possible that in the standard 2D cell culture environment, the a-SMA expression level of the scleral fibroblasts with choroid conditioned medium stimulation was inaccurate in indicating its actual expression in the 3D collagen gel. Mechanical tension plays a critical role in transdifferentiating fibroblasts to the myofibroblasts (Dobaczewski, de Haan, and Frangogiannis 2012), thereby when fibroblasts are embedded in the collagen gel, their transdifferentiation might be different from those cultured in the 2D plate, and subsequently have different a-SMA expression level between the 2D plate and 3D collagen gel due to subpopulation of fibroblasts. Secondly, it is possible that choroid-secreted factors that induced fibroblasts contraction in the collagen gel were not simply regulated by a-SMA expression and/or myofibroblasts transdifferentiation, but some other molecular components need to be determined in the future.

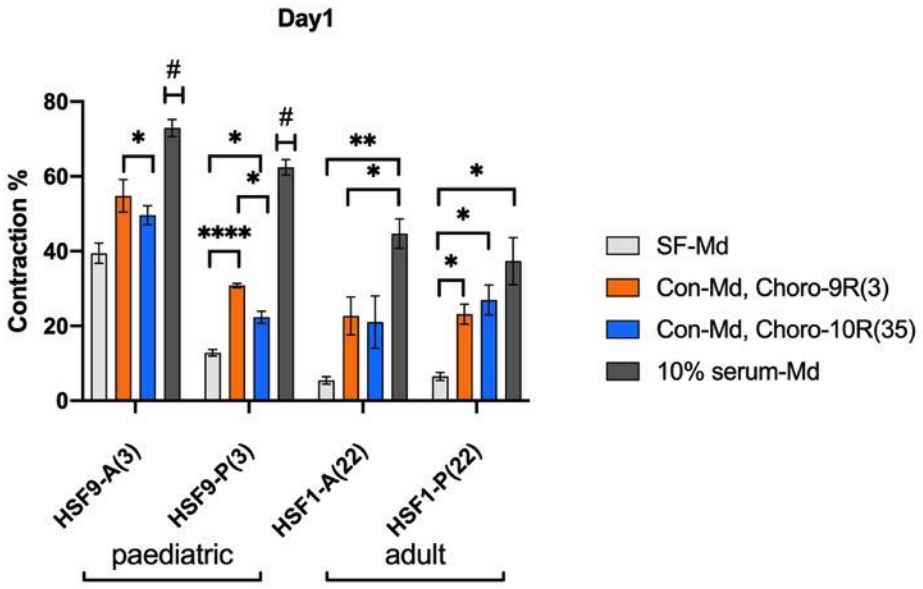

Figure 25. Serum stimulated scleral fibroblasts contractility. One set of paediatric (HSF9) and adult (HSF1) scleral fibroblasts were used. Scleral fibroblasts were embedded in collagen gels and contraction was measured after 1 day in the presence of serum-free medium, choroid conditioned medium or 10% serum medium. Shown is the mean contraction percent +/- SEM, in adult scleral fibroblasts (HSF1), “SF-Md”, n=6, “Con-Md-Choro-9R(3)”, “Con-Md-Choro-10R(35)”,and “10% serum-Md”, n=3. Shown is the mean contraction percent +/- SEM, in paediatric scleral fibroblasts (HSF9), “SF-Md”, n=6, “Con-Md-Choro-9R(3)” and “Con-Md-Choro-10R(35)”, n=3; shown is mean contraction percent +/- SD, in paediatric scleral fibroblasts (HSF9), “10% serum-Md”, n=1. The number in the bracket shows the tissue donor age. * P<0.05, ** P<0.01, **** P<0.0001, t test. “#” indicates n=1 only.

2.3. Dopamine inhibits the stimulatory effect of choroid-cell secreted factors on scleral fibroblast contractility

Dopamine is a chemical compound of the catecholamine and phenethylamine families, and it has a role in sending signals from neurons to other nerve cells as a neurotransmitter. Tyrosine

hydroxylase is a rate-limiting enzyme that associates with the synthesis of dopamine. Iuvone and colleagues found with light stimulation, tyrosine hydroxylase concomitantly activated *in vitro*, tyrosine hydroxylase was found to limit dopamine synthesis to maintain dopamine storage in the steady state, but dopamine concentration of the retina was increased which suggested that dopamine release was indeed increased with light stimulation (Kramer 1971; Iuvone et al. 1978). In the eye, dopamine is released by amacrine and interplexiform cells, D1 and D2 dopamine receptors are distributed in the retina, playing an important role in receiving and sending chemical signals for light adaption (Witkovsky 2004; Dowling and Ehinger 1978). Previous studies have shown dopamine prevented form-deprivation myopia in animal models. For example, intravitreal dopamine injections prevented FDM in guinea pigs and rabbits, and dopamine agonists successfully prevented FDM in chicken, guinea pigs, monkeys and mice (Mao et al. 2010; Gao et al. 2006; Rohrer, Spira, and Stell 1993; Stone et al. 1989; Dong et al. 2011; Iuvone et al. 1991; Yan et al. 2015), suggesting dopamine had great potential for maintaining normal eye growth as FDM was prevented. Moreover, in the FDM animal models, increased collagen fibril diameter in the sclera and increased scleral thickness were reported with the intravitreal injection of dopamine (Lin et al. 2008; Zhou et al. 2017). Although choroid thickness in the FDM model has been found to transiently increase with intravitreal injection of some dopamine agonists (apomorphine and quinpirole), we firstly applied dopamine directly to choroid cells, and used subsequent choroid cell-secreted factors upon this dopamine stimulation to culture scleral fibroblasts and measured their contractility. In our study, we found that dopamine critically and preferentially abrogated the paediatric choroid cells' ability to stimulate the contractility of scleral

fibroblasts. Firstly, our results showed that dopamine was not toxic to paediatric choroid cells. Secondly, to determine if this abrogation was due to cytotoxicity of the conditioned medium generated from dopamine-treated paediatric choroid cells (dopamine-CCM), we used three different methods to measure the viable cell numbers of scleral fibroblasts under different conditions of the culture medium. And we found that dopamine-CCM was not toxic to scleral fibroblasts, which confirmed that the prevention of scleral fibroblast contractility was because dopamine affected choroid cells to secrete growth factors rather than cytotoxicity of dopamine-CCM.

However, there were some results that need to be discussed in detail due to their limitations. Firstly, when we tested the dopamine-CCM effect on scleral fibroblasts, we used both serum-free medium and choroid-conditioned medium (CCM) as controls. When they were redone and served as controls in the dopamine-CCM testing, the contraction percentage of scleral fibroblasts (HSF9-P) was close to 20% with the CCM generated from paediatric choroid cells (Choro-9R), while it was about 30% with the CCM generated from adult choroid cells (Choro-10R). However, the results were inverted in the initial standard collagen gel contraction assay when we performed them to determine choroid-secreted factors promoted contractility of scleral fibroblasts, as paediatric choroid cells (Choro-9R) promoted scleral fibroblasts contraction more than adult choroid cells (Choro-10R). These contrary results might be due to the artefact of cells being in culture for too many passages, as the scleral fibroblasts were used from passage 8 to 10 for paediatric choroid cells (Choro-9R) and passage 7 to 9 for adult choroid cells (Choro-10R) when served as controls in the experiments to test the effect of dopamine-CCM. However, only passage 7 and 8 of scleral fibroblasts were used in the initial standard collagen gel contraction assay when they

were used to determine the effect of choroid-secreted factors on scleral fibroblast contractility. In addition, there was also a limitation of live/dead assay in our results to show cytotoxicity of dopamine-CCM culturing scleral fibroblasts embedded in the collagen gel. In our study, we used the live/dead assay reagent to stain the scleral fibroblasts embedded in the collagen gels, and used a confocal microscope to image them. After one-day culturing with serum-free medium, CCM and dopamine-CCM, the viability of scleral fibroblasts in the collagen gel was not changed significantly, which was consistently confirmed by three different methods including CCK8 proliferation assay, direct cell counting by hemocytometer after digesting gel, and live/dead assay. Although viable cell numbers under each conditioned medium remained no different, which suggested dopamine-CCM was not toxic to scleral fibroblasts. However, these three different methods showed overall different results after the gels (embedded with scleral fibroblasts) were cultured for 4 days. Those gel images did not show an increased proportion of dead cells in the gel on day4. In contrast, CCK8 proliferation assay and direct cell counting found the cell numbers of scleral fibroblasts decreased under the same condition. This contrary was possible because gels have contracted and fields were different, thereby decreasing cell numbers cannot be seen on images.

3. Conclusion remarks and outlook

3.1. Final remark

In this study, we investigated the effect of choroid cell-secreted factors on biomechanical properties of scleral fibroblasts, and how this is affected by biochemical stimulation (dopamine) applied to choroid cells.

Our work firstly demonstrated choroid cell-secreted factors promoted scleral fibroblasts contractility using primary human choroid cells and scleral fibroblasts *in vitro*. The contractility of scleral fibroblasts exhibited age and antero-posterior position differences, and they overall exhibited contractility promotion upon stimulation with choroid cell-secreted factors. Moreover, we confirmed that this scleral fibroblast contractility stimulation was not determined by scleral fibroblasts proliferation, but possibly relevant to a-SMA expression level change. Our work also firstly demonstrated that dopamine effectively inhibited the stimulatory effect of choroid-cell secreted factors on scleral fibroblast contractility, and confirmed that this inhibition was not determined by cytotoxicity of choroid cell-secreted factors post dopamine treatment. In addition, although we preliminarily engineered a functional 3D biomimetic RPE layer (retina), choroid and sclera interface to mimic an actual back of the human eye, this biomimetic model has a great potential to be optimised for supporting us in further exploring cellular components interactions in the future.

This study verified our hypothesis that signals from the choroid are crucial to the regulation of scleral biomechanics, dopamine applied to the choroid stimulates the synthesis of choroidal secreted factors, which play an inhibition role in scleral growth, exhibiting a negative biochemical signal to stop eye growth.

3.2. Future work

3.2.1. Investigating markers of scleral biomechanics activation

Our work has elucidated that a-SMA expression level is diverse in different ages and antero-posterior positions, and the contractility of scleral fibroblasts also exhibited discrepancy in different ages and antero-posterior positions. However, it is still unclear which

molecular components are responsible to these discrepancies of scleral fibroblast contractility, as anterior scleral fibroblasts contracted more than posterior ones but had less a-SMA expression. Therefore, it is essential to expand identification to other contractility relevant molecular markers. In addition, it is also unclear that if the a-SMA expression level of scleral fibroblasts in 3D collagen gels changes upon stimulation of choroid cell-secreted factors. It will be worthwhile to determine the role of a-SMA expression in the sclera with choroid cell-secreted factors stimulation, to have a readout for the functional changes we see in the contraction assay. Moreover, expanding identification to other biomechanical properties relevant to marker molecular expression, as well as myopia involvement markers, and mechanoregulatory pathways are also worthwhile to do in the future work.

1). a-SMA (Jobling et al. 2009; Harper and Summers 2015): using WB and RT-qPCR to determine whether exposure to choroid-conditioned medium alters aSMA expression in gel contraction.

2). Type1 collagen, TGF-β, Integrin a1 and a2 (Jobling et al. 2009; Gentle et al. 2003; Ma et al. 2014; Mo et al. 2016; Zhou et al. 2012; Hu et al. 2011; McBrien, Jobling, and Gentle 2009; Backhouse and Gentle 2018): these markers are linked to fibroblasts contraction potential and are decreased during myopia progression, using RT-qPCR to investigate changes in expression.

3). Proteoglycan, MMPs (Rada, Nickla, and Troilo 2000; Hayashi et al. 2013; Harper and Summers 2015; Metlapally and Wildsoet 2015; Liu et al. 2017): these markers are linked to scleral ECM remodelling, and involved in myopia progression, using RT-qPCR to investigate changes in expression.

4). YAP, MRTF, SMAD3 (Ma et al. 2014; Panciera et al. 2017; Piersma, Bank, and Boersema 2015; Eritja et al. 2017): YAP/

SMAD3 and MRTF regulate tissue stiffness and tissue homeostasis, using RT-qPCR to evaluate expression changes as well as immunofluorescence to determine changes in cytoplasmic/nuclear localization.

3.2.2. Investigating how biomechanical properties of scleral fibroblasts are affected by mechanical stimulation (stretching) applied to choroid cells

Our results showed that choroid cells secreted factors could significantly promote paediatric sclera fibroblasts (growing sclera) contractility, we hypothesise that the choroid normally stimulates eye growth. During accommodation, the eye changes optical power to focus on an object as its distance varies. The choroid becomes thinner during this process (Woodman-Pieterse et al. 2015; Read et al. 2019), which is similar to being stretched mechanically. Thus, we hypothesize that the choroid response to mechanical stretch will amplify the release of mediators of positive signal to eye growth, oppositely to dopamine stimulation served as negative signal to eye growth *(Figure 26, Figure 27*). Flexcell system (*Figure 27*) could be used to stretch choroid cells and then test the effect of the stretching on the ability of the choroid condition medium to stimulate scleral fibroblast contraction (or marker activation as identified in Discussion section 3.2.1 above).

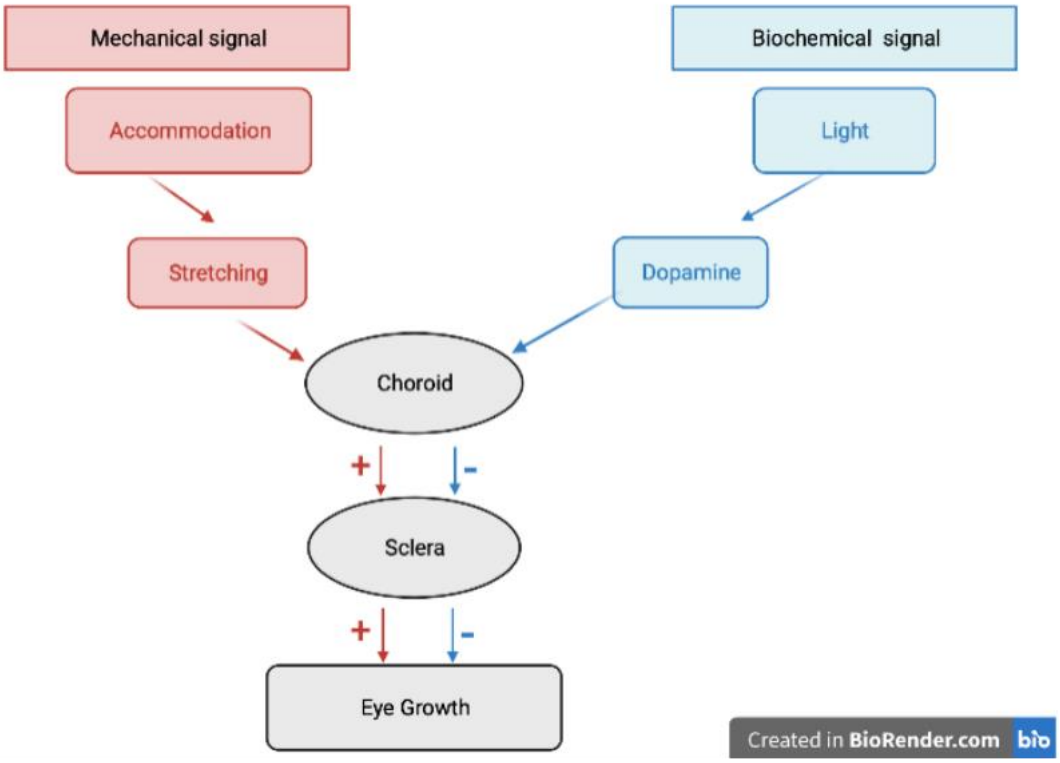

Figure 26. Schematic of hypothesis on how choroid signals regulate sclera biomechanics and eye growth. Accommodation leading to mechanical stretching of the choroid is the positive signal for the sclera to promote eye growth. Light-mediated dopamine released from the retina acts on the choroid to inhibit/counteract the growth promoting signals. Redline, positive signal pathway. Blue line, negative signal pathway.

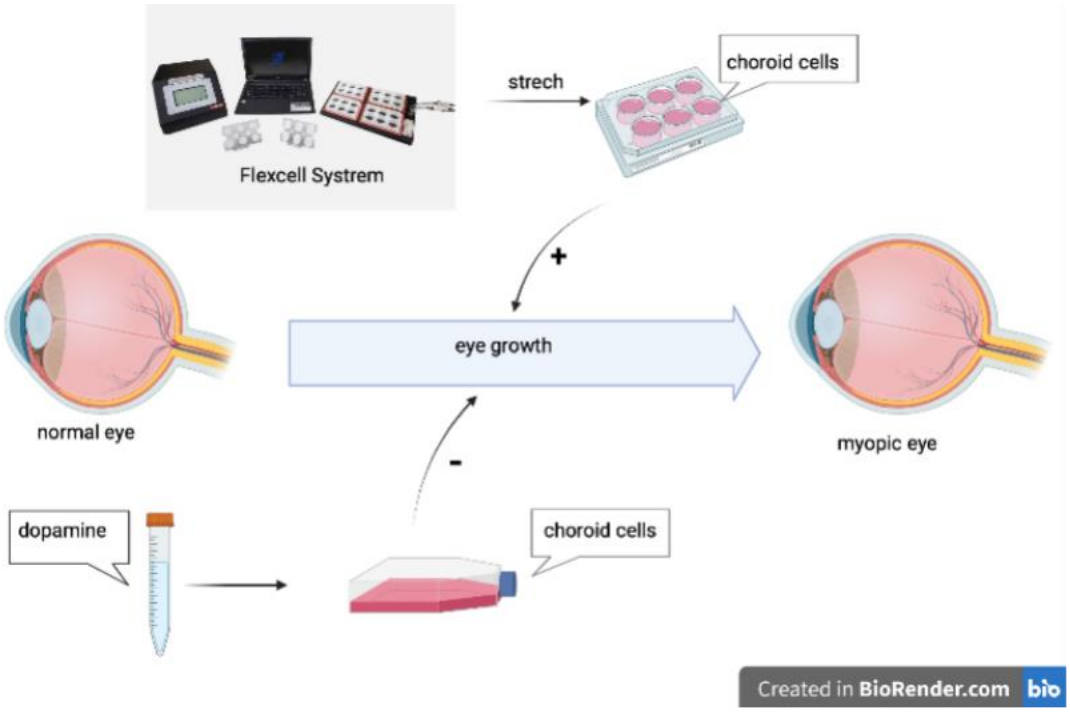

Figure 27. Diagram of hypothesis on choroid response to dopamine negative signal and mechanical stretching positive signal to eye growth.

3.2.3. Identifying choroid cell-secreted factors that regulate scleral biomechanics

It is critical to identify the optimal stimuli regulating choroid cell-secreted factors that modulate scleral biomechanics, RNA sequencing could be used to identify the choroid cell-secreted factors involved in the choroid conditioned medium by comparing optimal dopamine stimulation (negative signal to the eye growth) and/or mechanical stretching (positive signal to the eye growth) applied on choroid cells, to the condition of choroid cells without stimulations. Upon identification, individual secreted factors could be directly used for testing their ability to modulate scleral biomechanics, siRNA could be subsequently used for confirming those factors which effectively changed scleral biomechanics by depleting their

expression in choroid cells, and effective down-regulation of the targets could be assessed by RT-qPCR or Western blot.

3.2.4. Optimising the engineered retina, choroid and sclera biomimetic model

Our RAFT-derived biomimetic model was engineered only one time, and this biomimetic model is highly possibly less stiff than the actual sclera layer. Also, it is essential to optimize cell numbers in each layer to mimic the actual human eye. After optimisation, this model could be used to validate the optimal choroid stimuli identified in the studies and observe directly the effect of scleral cell behaviour. Immunofluorescence could be used to validate specific markers of scleral fibroblasts activation, confocal microscopy could be used to assess matrix remodelling. Ultimately, this engineered retina, choroid and sclera biomimetic model may be used to screen drugs for potential myopia prevention and treatment in the future.

Bibliography

Anstice, N. S., and J. R. Phillips. 2011. 'Effect of dual-focus soft contact lens wear on axial myopia progression in children', *Ophthalmology*, 118: 1152-61.

AOA. 2022. 'Eye Health for life', *American Optometric Association*

Arora, P. D., N. Narani, and C. A. McCulloch. 1999. 'The compliance of collagen gels regulates transforming growth factor-beta induction of alpha-smooth muscle actin in fibroblasts', *Am J Pathol*, 154: 871-82.

Asejczyk-Widlicka, M., D. W. Sródka, H. Kasprzak, and B. K. Pierscionek. 2007. 'Modelling the elastic properties of the anterior eye and their contribution to maintenance of image quality: the role of the limbus', *Eye (Lond)*, 21: 1087-94.

Backhouse, S., and J. R. Phillips. 2010. 'Effect of induced myopia on scleral myofibroblasts and in vivo ocular biomechanical compliance in the guinea pig', *Invest Ophthalmol Vis Sci*, 51: 6162-71.

Backhouse, Simon, and Alex Gentle. 2018. 'Scleral remodelling in myopia and its manipulation: a review of recent advances in scleral strengthening and myopia control', *Annals of Eye Science*, 3: 5.

Bailey, A. J. 1987. 'Structure, function and ageing of the collagens of the eye', *Eye (Lond)*, 1 (Pt 2): 175-83.

Bainbridge, P. 2013. 'Wound healing and the role of fibroblasts', *J Wound Care*, 22: 407-8, 10-12.

Baird, P. N., S. M. Saw, C. Lanca, J. A. Guggenheim, E. L. Smith Iii, X. Zhou, K. O. Matsui, P. C. Wu, P. Sankaridurg, A. Chia, M. Rosman, E. L. Lamoureux, R. Man, and M. He. 2020. 'Myopia', *Nat Rev Dis Primers*, 6: 99.

Bhardwaj, V., and G. P. Rajeshbhai. 2013. 'Axial length, anterior chamber depth-a study in different age groups and refractive errors', *J Clin Diagn Res*, 7: 2211-2.

Bonnans, C., J. Chou, and Z. Werb. 2014. 'Remodelling the extracellular matrix in development and disease', *Nat Rev Mol Cell Biol*, 15: 786-801.

Braun, A., H. Xu, F. Hu, P. Kocherlakota, D. Siegel, P. Chander, Z. Ungvari, A. Csiszar, M. Nedergaard, and P. Ballabh. 2007. 'Paucity of pericytes in germinal matrix vasculature of premature infants', *J Neurosci*, 27: 12012-24.

Breslin, K. M., L. O'Donoghue, and K. J. Saunders. 2013. 'A prospective study of spherical refractive error and ocular components among Northern Irish schoolchildren (the NICER study)', *Invest Ophthalmol Vis Sci*, 54: 4843-50.

Brown, R. A., R. Prajapati, D. A. McGrouther, I. V. Yannas, and M. Eastwood. 1998. 'Tensional homeostasis in dermal fibroblasts: mechanical responses to mechanical loading in three-dimensional substrates', *J Cell Physiol*, 175: 323-32.

Brown, R. A., G. Talas, R. A. Porter, D. A. McGrouther, and M. Eastwood. 1996. 'Balanced mechanical forces and microtubule contribution to fibroblast contraction', *J Cell Physiol*, 169: 439-47.

Buckhurst, H., B. Gilmartin, R. P. Cubbidge, M. Nagra, and N. S. Logan. 2013. 'Ocular biometric correlates of ciliary muscle thickness in human myopia', *Ophthalmic Physiol Opt*, 33: 294-304.

Chadli, L., B. Sotthewes, K. Li, S. N. Andersen, E. Cahir-McFarland, M. Cheung, P. Cullen, A. Dorjée, J. K. de Vries-Bouwstra, T. W. J. Huizinga, D. F. Fischer, J. DeGroot, J. L. Viney, T. S. Zheng,

J. Aarbiou, and A. Gardet. 2019. 'Identification of regulators of the myofibroblast phenotype of primary dermal fibroblasts from early diffuse systemic sclerosis patients', *Sci Rep*, 9: 4521.

Chamberlain, P., A. Bradley, B. Arumugam, D. Hammond, J. McNally, N. S. Logan, D. Jones, C. Ngo, S. C. Peixoto-de-Matos, C. Hunt, and G. Young. 2022. 'Long-term Effect of Dual-focus Contact Lenses on Myopia Progression in Children: A 6-year Multicenter Clinical Trial', *Optom Vis Sci*, 99: 204-12.

Chamberlain, P., P. Lazon de la Jara, B. Arumugam, and M. A. Bullimore. 2021. 'Axial length targets for myopia control', *Ophthalmic Physiol Opt*, 41: 523-31.

Chaurasia, S. S., H. Kaur, F. W. de Medeiros, S. D. Smith, and S. E. Wilson. 2009. 'Dynamics of the expression of intermediate filaments vimentin and desmin during myofibroblast differentiation after corneal injury', *Exp Eye Res*, 89: 133-9.

Chen, B. R., H. H. Cheng, W. C. Lin, K. H. Wang, J. Y. Liou, P. F. Chen, and K. K. Wu. 2012. 'Quiescent fibroblasts are more active in mounting robust inflammatory responses than proliferative fibroblasts', *PLoS One*, 7: e49232.

Chen, J., H. Li, N. SundarRaj, and J. H. Wang. 2007. 'Alpha-smooth muscle actin expression enhances cell traction force', *Cell Motil Cytoskeleton*, 64: 248-57.

Chen, Y., B. Drobe, C. Zhang, N. Singh, D. P. Spiegel, H. Chen, J. Bao, and F. Lu. 2020. 'Accommodation is unrelated to myopia progression in Chinese myopic children', *Sci Rep*, 10: 12056.

Coudrillier, B., J. Pijanka, J. Jefferys, T. Sorensen, H. A. Quigley, C. Boote, and T. D. Nguyen. 2015. 'Collagen structure and mechanical properties of the human sclera: analysis for the effects of age', *J Biomech Eng*, 137: 041006.

Coulombe, J. N., and R. Nishi. 1991. 'Stimulation of somatostatin expression in developing ciliary ganglion neurons by cells of the choroid layer', *J Neurosci*, 11: 553-62.

Coultas, L., K. Chawengsaksophak, and J. Rossant. 2005. 'Endothelial cells and VEGF in vascular development', *Nature*, 438: 937-45.

Dahlmann-Noor, A. H., B. Martin-Martin, M. Eastwood, P. T. Khaw, and M. Bailly. 2007. 'Dynamic protrusive cell behaviour generates force and drives early matrix contraction by fibroblasts', *Exp Cell Res*, 313: 4158-69.

Daniel, M. C., A. M. Dubis, A. Quartilho, H. Al-Hayouti, S. P. T. Khaw, M. Theodorou, and A. Dahlmann-Noor. 2018. 'Dynamic Changes in Schlemm Canal and Iridocorneal Angle Morphology During Accommodation in Children With Healthy Eyes: A Cross-Sectional Cohort Study', *Invest Ophthalmol Vis Sci*, 59: 3497-502.

Di Girolamo, N., A. Lloyd, P. McCluskey, M. Filipic, and D. Wakefield. 1997. 'Increased expression of matrix metalloproteinases in vivo in scleritis tissue and in vitro in cultured human scleral fibroblasts', *Am J Pathol*, 150: 653-66.

Dick, M. K., J. H. Miao, and F. Limaiem. 2022. 'Histology, Fibroblast.' in, *StatPearls* (StatPearls Publishing

Copyright © 2022, StatPearls Publishing LLC.: Treasure Island (FL)).

Dobaczewski, M., J. J. de Haan, and N. G. Frangogiannis. 2012. 'The extracellular matrix modulates fibroblast phenotype and function in the infarcted myocardium', *J Cardiovasc Transl Res*, 5: 837-47.

Domkin, D., M. Forsman, and H. O. Richter. 2019. 'Effect of ciliary-muscle contraction force on

trapezius muscle activity during computer mouse work', *Eur J Appl Physiol*, 119: 389-97.

Dong, F., Z. Zhi, M. Pan, R. Xie, X. Qin, R. Lu, X. Mao, J. F. Chen, M. D. Willcox, J. Qu, and X. Zhou. 2011. 'Inhibition of experimental myopia by a dopamine agonist: different effectiveness between form deprivation and hyperopic defocus in guinea pigs', *Mol Vis*, 17: 2824-34.

Dowling, J. E., and B. Ehinger. 1978. 'The interplexiform cell system. I. Synapses of the dopaminergic neurons of the goldfish retina', *Proc R Soc Lond B Biol Sci*, 201: 7-26.

Duffy, H. S. 2011. 'Fibroblasts, myofibroblasts, and fibrosis: fact, fiction, and the future', *J Cardiovasc Pharmacol*, 57: 373-5.

Ehrlich, H. P., W. B. Rockwell, T. L. Cornwell, and J. B. Rajaratnam. 1991. 'Demonstration of a direct role for myosin light chain kinase in fibroblast-populated collagen lattice contraction', *J Cell Physiol*, 146: 1-7.

El-Shazly, A. A., Y. A. Farweez, M. E. ElSebaay, and W. M. A. El-Zawahry. 2017. 'Correlation between choroidal thickness and degree of myopia assessed with enhanced depth imaging optical coherence tomography', *Eur J Ophthalmol*, 27: 577-84.

Eritja, N., I. Felip, M. A. Dosil, L. Vigezzi, C. Mirantes, A. Yeramian, R. Navaridas, M. Santacana, D. Llobet-Navas, A. Yoshimura, M. Nomura, M. Encinas, X. Matias-Guiu, and X. Dolcet. 2017. 'A Smad3-PTEN regulatory loop controls proliferation and apoptotic responses to TGF-β in mouse endometrium', *Cell Death Differ*, 24: 1443-58.

Espinosa-Heidmann, D. G., M. A. Reinoso, Y. Pina, K. G. Csaky, A. Caicedo, and S. W. Cousins. 2005. 'Quantitative enumeration of vascular smooth muscle cells and endothelial cells derived from bone marrow precursors in experimental choroidal neovascularization', *Exp Eye Res*, 80: 369-78.

Feldkaemper, M., and F. Schaeffel. 2013. 'An updated view on the role of dopamine in myopia', *Exp Eye Res*, 114: 106-19.

Feng, H. Z., H. Wang, K. Takahashi, and J. P. Jin. 2019. 'Double deletion of calponin 1 and calponin 2 in mice decreases systemic blood pressure with blunted length-tension response of aortic smooth muscle', *J Mol Cell Cardiol*, 129: 49-57.

Ferrara, M., G. Lugano, M. T. Sandinha, V. R. Kearns, B. Geraghty, and D. H. W. Steel. 2021. 'Biomechanical properties of retina and choroid: a comprehensive review of techniques and translational relevance', *Eye (Lond)*, 35: 1818-32.

Fisher, R. F. 1977. 'The force of contraction of the human ciliary muscle during accommodation', *J Physiol*, 270: 51-74.

Flores-Nascimento, M. C., A. M. Alessio, F. L. de Andrade Orsi, and J. M. Annichino-Bizzacchi. 2015. 'CD144, CD146 and VEGFR-2 properly identify circulating endothelial cell', *Rev Bras Hematol Hemoter*, 37: 98-102.

Frank, R. N., R. H. Amin, D. Eliott, J. E. Puklin, and G. W. Abrams. 1996. 'Basic fibroblast growth factor and vascular endothelial growth factor are present in epiretinal and choroidal neovascular membranes', *Am J Ophthalmol*, 122: 393-403.

Frederick, J. M., M. E. Rayborn, A. M. Laties, D. M. Lam, and J. G. Hollyfield. 1982. 'Dopaminergic neurons in the human retina', *J Comp Neurol*, 210: 65-79.

Friberg, T. R., and J. W. Lace. 1988. 'A comparison of the elastic properties of human choroid and sclera', *Exp Eye Res*, 47: 429-36.

Fu, A., F. Stapleton, L. Wei, W. Wang, B. Zhao, K. Watt, N. Ji, and Y. Lyu. 2020. 'Effect of low-dose atropine on myopia progression, pupil diameter and accommodative amplitude: low-

dose atropine and myopia progression', *Br J Ophthalmol*, 104: 1535-41.

Gao, Q., Q. Liu, P. Ma, X. Zhong, J. Wu, and J. Ge. 2006. 'Effects of direct intravitreal dopamine injections on the development of lid-suture induced myopia in rabbits', *Graefes Arch Clin Exp Ophthalmol*, 244: 1329-35.

Gentle, A., Y. Liu, J. E. Martin, G. L. Conti, and N. A. McBrien. 2003. 'Collagen gene expression and the altered accumulation of scleral collagen during the development of high myopia', *J Biol Chem*, 278: 16587-94.

Girard, M. J., A. Dahlmann-Noor, S. Rayapureddi, J. A. Bechara, B. M. Bertin, H. Jones, J. Albon, P. T. Khaw, and C. R. Ethier. 2011. 'Quantitative mapping of scleral fiber orientation in normal rat eyes', *Invest Ophthalmol Vis Sci*, 52: 9684-93.

Grierson, I., L. Heathcote, P. Hiscott, P. Hogg, M. Briggs, and S. Hagan. 2000. 'Hepatocyte growth factor/scatter factor in the eye', *Prog Retin Eye Res*, 19: 779-802.

Guggenheim, J. A., and N. A. McBrien. 1996. 'Form-deprivation myopia induces activation of scleral matrix metalloproteinase-2 in tree shrew', *Invest Ophthalmol Vis Sci*, 37: 1380-95.

Gwiazda, J. E., L. Hyman, T. T. Norton, M. E. Hussein, W. Marsh-Tootle, R. Manny, Y. Wang, and D. Everett. 2004. 'Accommodation and related risk factors associated with myopia progression and their interaction with treatment in COMET children', *Invest Ophthalmol Vis Sci*, 45: 2143-51.

Haarman, A. E. G., C. A. Enthoven, J. W. L. Tideman, M. S. Tedja, V. J. M. Verhoeven, and C. C. W. Klaver. 2020. 'The Complications of Myopia: A Review and Meta-Analysis', *Invest Ophthalmol Vis Sci*, 61: 49.

Harper, A. R., and J. A. Summers. 2015. 'The dynamic sclera: extracellular matrix remodeling in normal ocular growth and myopia development', *Exp Eye Res*, 133: 100-11.

Hautmann, M. B., C. S. Madsen, C. P. Mack, and G. K. Owens. 1998. 'Substitution of the degenerate smooth muscle (SM) alpha-actin CC(A/T-rich)6GG elements with c-fos serum response elements results in increased basal expression but relaxed SM cell specificity and reduced angiotensin II inducibility', *J Biol Chem*, 273: 8398-406.

Hayashi, M., Y. Ito, A. Takahashi, K. Kawano, and H. Terasaki. 2013. 'Scleral thickness in highly myopic eyes measured by enhanced depth imaging optical coherence tomography', *Eye (Lond)*, 27: 410-7.

He, Y., and F. Grinnell. 1994. 'Stress relaxation of fibroblasts activates a cyclic AMP signaling pathway', *J Cell Biol*, 126: 457-64.

Hinz, B., G. Celetta, J. J. Tomasek, G. Gabbiani, and C. Chaponnier. 2001. 'Alpha-smooth muscle actin expression upregulates fibroblast contractile activity', *Mol Biol Cell*, 12: 2730-41.

Holden, B. A., T. R. Fricke, D. A. Wilson, M. Jong, K. S. Naidoo, P. Sankaridurg, T. Y. Wong, T. J. Naduvilath, and S. Resnikoff. 2016. 'Global Prevalence of Myopia and High Myopia and Temporal Trends from 2000 through 2050', *Ophthalmology*, 123: 1036-42.

Hu, S., D. Cui, X. Yang, J. Hu, W. Wan, and J. Zeng. 2011. 'The crucial role of collagen-binding integrins in maintaining the mechanical properties of human scleral fibroblasts-seeded collagen matrix', *Mol Vis*, 17: 1334-42.

Huang, J., D. Wen, Q. Wang, C. McAlinden, I. Flitcroft, H. Chen, S. M. Saw, H. Chen, F. Bao, Y. Zhao, L. Hu, X. Li, R. Gao, W. Lu, Y. Du, Z. Jinag, A. Yu, H. Lian, Q. Jiang, Y. Yu, and J. Qu. 2016. 'Efficacy Comparison of 16 Interventions for Myopia Control in Children: A Network

Meta-analysis', *Ophthalmology*, 123: 697-708.

Hussain, R. N., F. Shahid, and G. Woodruff. 2014. 'Axial length in apparently normal pediatric eyes', *Eur J Ophthalmol*, 24: 120-3.

Iuvone, P. M., C. L. Galli, C. K. Garrison-Gund, and N. H. Neff. 1978. 'Light stimulates tyrosine hydroxylase activity and dopamine synthesis in retinal amacrine neurons', *Science*, 202: 901-2.

Iuvone, P. M., M. Tigges, A. Fernandes, and J. Tigges. 1989. 'Dopamine synthesis and metabolism in rhesus monkey retina: development, aging, and the effects of monocular visual deprivation', *Vis Neurosci*, 2: 465-71.

Iuvone, P. M., M. Tigges, R. A. Stone, S. Lambert, and A. M. Laties. 1991. 'Effects of apomorphine, a dopamine receptor agonist, on ocular refraction and axial elongation in a primate model of myopia', *Invest Ophthalmol Vis Sci*, 32: 1674-7.

Jeon, S., W. K. Lee, K. Lee, and N. J. Moon. 2012. 'Diminished ciliary muscle movement on accommodation in myopia', *Exp Eye Res*, 105: 9-14.

Jobling, A. I., A. Gentle, R. Metlapally, B. J. McGowan, and N. A. McBrien. 2009. 'Regulation of scleral cell contraction by transforming growth factor-beta and stress: competing roles in myopic eye growth', *J Biol Chem*, 284: 2072-9.

Jobling, A. I., M. Nguyen, A. Gentle, and N. A. McBrien. 2004. 'Isoform-specific changes in scleral transforming growth factor-beta expression and the regulation of collagen synthesis during myopia progression', *J Biol Chem*, 279: 18121-6.

Karouta, C., and R. S. Ashby. 2014. 'Correlation between light levels and the development of deprivation myopia', *Invest Ophthalmol Vis Sci*, 56: 299-309.

Keeley, F. W., J. D. Morin, and S. Vesely. 1984. 'Characterization of collagen from normal human sclera', *Exp Eye Res*, 39: 533-42.

Khaitlina, S. Y. 2001. 'Functional specificity of actin isoforms', *Int Rev Cytol*, 202: 35-98.

Khanal, S., and J. R. Phillips. 2020. 'Which low-dose atropine for myopia control?', *Clin Exp Optom*, 103: 230-32.

Kozdon, K., B. Caridi, I. Duru, D. G. Ezra, J. B. Phillips, and M. Bailly. 2020. 'A Tenon's capsule/bulbar conjunctiva interface biomimetic to model fibrosis and local drug delivery', *PLoS One*, 15: e0241569.

Kozdon, K., C. Fitchett, G. E. Rose, D. G. Ezra, and M. Bailly. 2015. 'Mesenchymal Stem Cell-Like Properties of Orbital Fibroblasts in Graves' Orbitopathy', *Invest Ophthalmol Vis Sci*, 56: 5743-50.

Kramer, S. G. 1971. 'Dopamine: A retinal neurotransmitter. I. Retinal uptake, storage, and light-stimulated release of H3-dopamine in vivo', *Invest Ophthalmol*, 10: 438-52.

Kur, J., E. A. Newman, and T. Chan-Ling. 2012. 'Cellular and physiological mechanisms underlying blood flow regulation in the retina and choroid in health and disease', *Prog Retin Eye Res*, 31: 377-406.

Kureshi, A. K., M. Dziasko, J. L. Funderburgh, and J. T. Daniels. 2015. 'Human corneal stromal stem cells support limbal epithelial cells cultured on RAFT tissue equivalents', *Sci Rep*, 5: 16186.

Lee, Y. C., J. H. Wang, and C. J. Chiu. 2017. 'Effect of Orthokeratology on myopia progression: twelve-year results of a retrospective cohort study', *BMC Ophthalmol*, 17: 243.

Lemons, J. M., X. J. Feng, B. D. Bennett, A. Legesse-Miller, E. L. Johnson, I. Raitman, E. A. Pollina,

H. A. Rabitz, J. D. Rabinowitz, and H. A. Coller. 2010. 'Quiescent fibroblasts exhibit high metabolic activity', *PLoS Biol*, 8: e1000514.

Li, H., C. Fitchett, K. Kozdon, H. Jayaram, G. E. Rose, M. Bailly, and D. G. Ezra. 2014. 'Independent adipogenic and contractile properties of fibroblasts in Graves' orbitopathy: an in vitro model for the evaluation of treatments', *PLoS One*, 9: e95586.

Li, Q., W. Huang, and X. Zhou. 2009. 'Expression of CD34, alpha-smooth muscle actin and transforming growth factor-beta1 in squamous intraepithelial lesions and squamous cell carcinoma of the cervix', *J Int Med Res*, 37: 446-54.

Lin, Z., X. Chen, J. Ge, D. Cui, J. Wu, F. Tang, J. Tan, X. Zhong, and Q. Gao. 2008. 'Effects of direct intravitreal dopamine injection on sclera and retina in form-deprived myopic rabbits', *J Ocul Pharmacol Ther*, 24: 543-50.

Liu, H., B. Chen, and B. Lilly. 2008. 'Fibroblasts potentiate blood vessel formation partially through secreted factor TIMP-1', *Angiogenesis*, 11: 223-34.

Liu, H. H., M. S. Kenning, A. I. Jobling, N. A. McBrien, and A. Gentle. 2017. 'Reduced Scleral TIMP-2 Expression Is Associated With Myopia Development: TIMP-2 Supplementation Stabilizes Scleral Biomarkers of Myopia and Limits Myopia Development', *Invest Ophthalmol Vis Sci*, 58: 1971-81.

Liu, R., and J. P. Jin. 2016. 'Calponin isoforms CNN1, CNN2 and CNN3: Regulators for actin cytoskeleton functions in smooth muscle and non-muscle cells', *Gene*, 585: 143-53.

Ma, M., Z. Zhang, E. Du, W. Zheng, Q. Gu, X. Xu, and B. Ke. 2014. 'Wnt signaling in form deprivation myopia of the mice retina', *PLoS One*, 9: e91086.

Mack, C. P., and G. K. Owens. 1999. 'Regulation of smooth muscle alpha-actin expression in vivo is dependent on CArG elements within the 5' and first intron promoter regions', *Circ Res*, 84: 852-61.

Majava, M., P. N. Bishop, P. Hägg, P. G. Scott, A. Rice, C. Inglehearn, C. J. Hammond, T. D. Spector, L. Ala-Kokko, and M. Männikkö. 2007. 'Novel mutations in the small leucine-rich repeat protein/proteoglycan (SLRP) genes in high myopia', *Hum Mutat*, 28: 336-44.

Mao, J., S. Liu, W. Qin, F. Li, X. Wu, and Q. Tan. 2010. 'Levodopa inhibits the development of form-deprivation myopia in guinea pigs', *Optom Vis Sci*, 87: 53-60.

Marzani, D., and J. Wallman. 1997. 'Growth of the two layers of the chick sclera is modulated reciprocally by visual conditions', *Invest Ophthalmol Vis Sci*, 38: 1726-39.

McBrien, N. A., A. I. Jobling, and A. Gentle. 2009. 'Biomechanics of the sclera in myopia: extracellular and cellular factors', *Optom Vis Sci*, 86: E23-30.

McBrien, N. A., P. Lawlor, and A. Gentle. 2000. 'Scleral remodeling during the development of and recovery from axial myopia in the tree shrew', *Invest Ophthalmol Vis Sci*, 41: 3713-9.

McCullough, S. J., L. O'Donoghue, and K. J. Saunders. 2016. 'Six Year Refractive Change among White Children and Young Adults: Evidence for Significant Increase in Myopia among White UK Children', *PLoS One*, 11: e0146332.

Megaw, P. L., I. G. Morgan, and M. K. Boelen. 1997. 'Dopaminergic behaviour in chicken retina and the effect of form deprivation', *Aust N Z J Ophthalmol*, 25 Suppl 1: S76-8.

Metlapally, R., and C. F. Wildsoet. 2015. 'Scleral Mechanisms Underlying Ocular Growth and Myopia', *Prog Mol Biol Transl Sci*, 134: 241-8.

Mo, Ya, Yi Wang, Bin Cao, Jiajia Zhang, Guoting Ren, and Ting Yang. 2016. 'Scleral TGF-β1 and Smad3 expression is altered by TCM Bu Jing Yi Shi Tablets in guinea pigs with form-

deprivation myopia', *Journal of Traditional Chinese Medical Sciences*, 3: 124-32.

Morgan, I. G., R. S. Ashby, and D. L. Nickla. 2013. 'Form deprivation and lens-induced myopia: are they different?', *Ophthalmic Physiol Opt*, 33: 355-61.

Morgan, I., and K. Rose. 2005. 'How genetic is school myopia?', *Prog Retin Eye Res*, 24: 1-38.

Moring, A. G., J. R. Baker, and T. T. Norton. 2007. 'Modulation of glycosaminoglycan levels in tree shrew sclera during lens-induced myopia development and recovery', *Invest Ophthalmol Vis Sci*, 48: 2947-56.

Moriyama, M., K. Ohno-Matsui, K. Hayashi, N. Shimada, T. Yoshida, T. Tokoro, and I. Morita. 2011. 'Topographic analyses of shape of eyes with pathologic myopia by high-resolution three-dimensional magnetic resonance imaging', *Ophthalmology*, 118: 1626-37.

Mutti, D. O., J. R. Hayes, G. L. Mitchell, L. A. Jones, M. L. Moeschberger, S. A. Cotter, R. N. Kleinstein, R. E. Manny, J. D. Twelker, and K. Zadnik. 2007. 'Refractive error, axial length, and relative peripheral refractive error before and after the onset of myopia', *Invest Ophthalmol Vis Sci*, 48: 2510-9.

Nickla, D. L., and J. Wallman. 2010. 'The multifunctional choroid', *Prog Retin Eye Res*, 29: 144-68.

Norman, R. E., J. G. Flanagan, S. M. Rausch, I. A. Sigal, I. Tertinegg, A. Eilaghi, S. Portnoy, J. G. Sled, and C. R. Ethier. 2010. 'Dimensions of the human sclera: Thickness measurement and regional changes with axial length', *Exp Eye Res*, 90: 277-84.

Norton, T. T., and J. A. Rada. 1995. 'Reduced extracellular matrix in mammalian sclera with induced myopia', *Vision Res*, 35: 1271-81.

Novais, E. A., E. Badaró, N. Allemann, M. S. Morales, E. B. Rodrigues, R. de Souza Lima, C. V. Regatieri, and R. Belfort, Jr. 2015. 'Correlation Between Choroidal Thickness and Ciliary Artery Blood Flow Velocity in Normal Subjects', *Ophthalmic Surg Lasers Imaging Retina*, 46: 920-4.

Ogata, N., M. Matsushima, Y. Takada, T. Tobe, K. Takahashi, X. Yi, C. Yamamoto, H. Yamada, and M. Uyama. 1996. 'Expression of basic fibroblast growth factor mRNA in developing choroidal neovascularization', *Curr Eye Res*, 15: 1008-18.

Oglesby, E. N., G. Tezel, E. Cone-Kimball, M. R. Steinhart, J. Jefferys, M. E. Pease, and H. A. Quigley. 2016. 'Scleral fibroblast response to experimental glaucoma in mice', *Mol Vis*, 22: 82-99.

Ohngemach, S., G. Hagel, and F. Schaeffel. 1997. 'Concentrations of biogenic amines in fundal layers in chickens with normal visual experience, deprivation, and after reserpine application', *Vis Neurosci*, 14: 493-505.

Ohno-Matsui, K., P. C. Wu, K. Yamashiro, K. Vutipongsatorn, Y. Fang, C. M. G. Cheung, T. Y. Y. Lai, Y. Ikuno, S. Y. Cohen, A. Gaudric, and J. B. Jonas. 2021. 'IMI Pathologic Myopia', *Invest Ophthalmol Vis Sci*, 62: 5.

Oida, T., and H. L. Weiner. 2010. 'Depletion of TGF-β from fetal bovine serum', *J Immunol Methods*, 362: 195-8.

Olsen, T. W., S. Y. Aaberg, D. H. Geroski, and H. F. Edelhauser. 1998. 'Human sclera: thickness and surface area', *Am J Ophthalmol*, 125: 237-41.

Ostrowska-Podhorodecka, Z., I. Ding, M. Norouzi, and C. A. McCulloch. 2022. 'Impact of Vimentin on Regulation of Cell Signaling and Matrix Remodeling', *Front Cell Dev Biol*, 10: 869069.

Panciera, T., L. Azzolin, M. Cordenonsi, and S. Piccolo. 2017. 'Mechanobiology of YAP and TAZ in physiology and disease', *Nat Rev Mol Cell Biol*, 18: 758-70.

Piersma, B., R. A. Bank, and M. Boersema. 2015. 'Signaling in Fibrosis: TGF-β, WNT, and YAP/TAZ

Converge', *Front Med (Lausanne)*, 2: 59.

Poukens, V., B. J. Glasgow, and J. L. Demer. 1998. 'Nonvascular contractile cells in sclera and choroid of humans and monkeys', *Invest Ophthalmol Vis Sci*, 39: 1765-74.

Qu, J., H. Chen, L. Zhu, N. Ambalavanan, C. A. Girkin, J. E. Murphy-Ullrich, J. C. Downs, and Y. Zhou. 2015. 'High-Magnitude and/or High-Frequency Mechanical Strain Promotes Peripapillary Scleral Myofibroblast Differentiation', *Invest Ophthalmol Vis Sci*, 56: 7821-30.

Rada, J. A., V. R. Achen, S. Penugonda, R. W. Schmidt, and B. A. Mount. 2000. 'Proteoglycan composition in the human sclera during growth and aging', *Invest Ophthalmol Vis Sci*, 41: 1639-48.

Rada, J. A., A. L. McFarland, P. K. Cornuet, and J. R. Hassell. 1992. 'Proteoglycan synthesis by scleral chondrocytes is modulated by a vision dependent mechanism', *Curr Eye Res*, 11: 767-82.

Rada, J. A., D. L. Nickla, and D. Troilo. 2000. 'Decreased proteoglycan synthesis associated with form deprivation myopia in mature primate eyes', *Invest Ophthalmol Vis Sci*, 41: 2050-8.

Rada, J. A., and L. Palmer. 2007. 'Choroidal regulation of scleral glycosaminoglycan synthesis during recovery from induced myopia', *Invest Ophthalmol Vis Sci*, 48: 2957-66.

Rada, J. A., R. A. Thoft, and J. R. Hassell. 1991. 'Increased aggrecan (cartilage proteoglycan) production in the sclera of myopic chicks', *Dev Biol*, 147: 303-12.

Read, S. A., D. Alonso-Caneiro, S. J. Vincent, A. Bremner, A. Fothergill, B. Ismail, R. McGraw, C. J. Quirk, and E. Wrigley. 2016. 'Anterior eye tissue morphology: Scleral and conjunctival thickness in children and young adults', *Sci Rep*, 6: 33796.

Read, S. A., M. J. Collins, and S. J. Vincent. 2015. 'Light Exposure and Eye Growth in Childhood', *Invest Ophthalmol Vis Sci*, 56: 6779-87.

Read, S. A., J. A. Fuss, S. J. Vincent, M. J. Collins, and D. Alonso-Caneiro. 2019. 'Choroidal changes in human myopia: insights from optical coherence tomography imaging', *Clin Exp Optom*, 102: 270-85.

Reecy, J. M., C. A. Bidwell, O. M. Andrisani, D. E. Gerrard, and A. L. Grant. 1998. 'Multiple regions of the porcine alpha-skeletal actin gene modulate muscle-specific expression in cell culture and directly injected skeletal muscle', *Anim Biotechnol*, 9: 101-20.

Reitsamer, H. A., C. Zawinka, and M. Branka. 2004. 'Dopaminergic vasodilation in the choroidal circulation by d1/d5 receptor activation', *Invest Ophthalmol Vis Sci*, 45: 900-5.

Rohrer, B., A. W. Spira, and W. K. Stell. 1993. 'Apomorphine blocks form-deprivation myopia in chickens by a dopamine D2-receptor mechanism acting in retina or pigmented epithelium', *Vis Neurosci*, 10: 447-53.

Rose, K. A., I. G. Morgan, J. Ip, A. Kifley, S. Huynh, W. Smith, and P. Mitchell. 2008. 'Outdoor activity reduces the prevalence of myopia in children', *Ophthalmology*, 115: 1279-85.

Saint-Geniez, M., A. E. Maldonado, and P. A. D'Amore. 2006. 'VEGF expression and receptor activation in the choroid during development and in the adult', *Invest Ophthalmol Vis Sci*, 47: 3135-42.

Saka, N., K. Ohno-Matsui, N. Shimada, S. Sueyoshi, N. Nagaoka, W. Hayashi, K. Hayashi, M. Moriyama, A. Kojima, K. Yasuzumi, T. Yoshida, T. Tokoro, and M. Mochizuki. 2010. 'Long-term changes in axial length in adult eyes with pathologic myopia', *Am J Ophthalmol*, 150: 562-68.e1.

Schache, M., and P. N. Baird. 2012. 'Assessment of the association of matrix metalloproteinases

with myopia, refractive error and ocular biometric measures in an Australian cohort', *PLoS One*, 7: e47181.

Schmid, G. F., G. I. Papastergiou, D. L. Nickla, C. E. Riva, T. Lin, R. A. Stone, and A. M. Laties. 1996. 'Validation of laser Doppler interferometric measurements in vivo of axial eye length and thickness of fundus layers in chicks', *Curr Eye Res*, 15: 691-6.

Scholfield, C. N., J. G. McGeown, and T. M. Curtis. 2007. 'Cellular physiology of retinal and choroidal arteriolar smooth muscle cells', *Microcirculation*, 14: 11-24.

Schultz, N., H. M. Nielsen, L. Minthon, and M. Wennström. 2014. 'Involvement of matrix metalloproteinase-9 in amyloid-β 1-42-induced shedding of the pericyte proteoglycan NG2', *J Neuropathol Exp Neurol*, 73: 684-92.

Seko, Y., N. Azuma, T. Yokoi, D. Kami, R. Ishii, S. Nishina, M. Toyoda, H. Shimokawa, and A. Umezawa. 2017. 'Anteroposterior Patterning of Gene Expression in the Human Infant Sclera: Chondrogenic Potential and Wnt Signaling', *Curr Eye Res*, 42: 145-54.

Sergienko, N. M., and I. Shargorogska. 2012. 'The scleral rigidity of eyes with different refractions', *Graefes Arch Clin Exp Ophthalmol*, 250: 1009-12.

Shelton, L., D. Troilo, M. R. Lerner, Y. Gusev, D. J. Brackett, and J. S. Rada. 2008. 'Microarray analysis of choroid/RPE gene expression in marmoset eyes undergoing changes in ocular growth and refraction', *Mol Vis*, 14: 1465-79.

Shi, X., L. Jiang, X. Zhao, B. Chen, W. Shi, Y. Cao, Y. Chen, X. Li, Y. He, C. Li, X. Liu, X. Li, H. Lu, C. Chen, and J. Liu. 2021. 'Adipose-Derived Stromal Cell-Sheets Sandwiched, Book-Shaped Acellular Dermal Matrix Capable of Sustained Release of Basic Fibroblast Growth Factor Promote Diabetic Wound Healing', *Front Cell Dev Biol*, 9: 646967.

Shinde, A. V., C. Humeres, and N. G. Frangogiannis. 2017. 'The role of α-smooth muscle actin in fibroblast-mediated matrix contraction and remodeling', *Biochim Biophys Acta Mol Basis Dis*, 1863: 298-309.

Shore, P., and A. D. Sharrocks. 1995. 'The MADS-box family of transcription factors', *Eur J Biochem*, 229: 1-13.

Siatkowski, R. M., S. Cotter, J. M. Miller, C. A. Scher, R. S. Crockett, and G. D. Novack. 2004. 'Safety and efficacy of 2% pirenzepine ophthalmic gel in children with myopia: a 1-year, multicenter, double-masked, placebo-controlled parallel study', *Arch Ophthalmol*, 122: 1667-74.

Sliogeryte, K., and N. Gavara. 2019. 'Vimentin Plays a Crucial Role in Fibroblast Ageing by Regulating Biophysical Properties and Cell Migration', *Cells*, 8.

Smith, E. L., 3rd, L. F. Hung, and B. Arumugam. 2014. 'Visual regulation of refractive development: insights from animal studies', *Eye (Lond)*, 28: 180-8.

Smith, E. L., 3rd, L. F. Hung, and J. Huang. 2012. 'Protective effects of high ambient lighting on the development of form-deprivation myopia in rhesus monkeys', *Invest Ophthalmol Vis Sci*, 53: 421-8.

Sohn, E. H., A. Khanna, B. A. Tucker, M. D. Abràmoff, E. M. Stone, and R. F. Mullins. 2014. 'Structural and biochemical analyses of choroidal thickness in human donor eyes', *Invest Ophthalmol Vis Sci*, 55: 1352-60.

Steen, B., S. Sejersen, L. Berglin, S. Seregard, and A. Kvanta. 1998. 'Matrix metalloproteinases and metalloproteinase inhibitors in choroidal neovascular membranes', *Invest Ophthalmol Vis Sci*, 39: 2194-200.

Sternlicht, M. D., and Z. Werb. 2001. 'How matrix metalloproteinases regulate cell behavior', *Annu Rev Cell Dev Biol*, 17: 463-516.

Stone, R. A., Y. Cohen, A. M. McGlinn, S. Davison, S. Casavant, J. Shaffer, T. S. Khurana, M. T. Pardue, and P. M. Iuvone. 2016. 'Development of Experimental Myopia in Chicks in a Natural Environment', *Invest Ophthalmol Vis Sci*, 57: 4779-89.

Stone, R. A., T. Lin, A. M. Laties, and P. M. Iuvone. 1989. 'Retinal dopamine and form-deprivation myopia', *Proc Natl Acad Sci U S A*, 86: 704-6.

Strauss, O. 2005. 'The retinal pigment epithelium in visual function', *Physiol Rev*, 85: 845-81.

Summers Rada, J. A., and L. R. Hollaway. 2011. 'Regulation of the biphasic decline in scleral proteoglycan synthesis during the recovery from induced myopia', *Exp Eye Res*, 92: 394-400.

Tomasek, J. J., G. Gabbiani, B. Hinz, C. Chaponnier, and R. A. Brown. 2002. 'Myofibroblasts and mechano-regulation of connective tissue remodelling', *Nat Rev Mol Cell Biol*, 3: 349-63.

Tomasek, J. J., C. J. Haaksma, R. J. Eddy, and M. B. Vaughan. 1992. 'Fibroblast contraction occurs on release of tension in attached collagen lattices: dependency on an organized actin cytoskeleton and serum', *Anat Rec*, 232: 359-68.

Trier, K., E. B. Olsen, T. Kobayashi, and S. M. Ribel-Madsen. 1999. 'Biochemical and ultrastructural changes in rabbit sclera after treatment with 7-methylxanthine, theobromine, acetazolamide, or L-ornithine', *Br J Ophthalmol*, 83: 1370-5.

Troilo, D., E. L. Smith, 3rd, D. L. Nickla, R. Ashby, A. V. Tkatchenko, L. A. Ostrin, T. J. Gawne, M. T. Pardue, J. A. Summers, C. S. Kee, F. Schroedl, S. Wahl, and L. Jones. 2019. 'IMI - Report on Experimental Models of Emmetropization and Myopia', *Invest Ophthalmol Vis Sci*, 60: M31-m88.

Troilo, D., and J. Wallman. 1991. 'The regulation of eye growth and refractive state: an experimental study of emmetropization', *Vision Res*, 31: 1237-50.

Upadhyay, A., and R. W. Beuerman. 2020. 'Biological Mechanisms of Atropine Control of Myopia', *Eye Contact Lens*, 46: 129-35.

Wallman, J., C. Wildsoet, A. Xu, M. D. Gottlieb, D. L. Nickla, L. Marran, W. Krebs, and A. M. Christensen. 1995. 'Moving the retina: choroidal modulation of refractive state', *Vision Res*, 35: 37-50.

Wang, B., Y. Hua, B. L. Brazile, B. Yang, and I. A. Sigal. 2020. 'Collagen fiber interweaving is central to sclera stiffness', *Acta Biomater*, 113: 429-37.

Wang, J., R. Zohar, and C. A. McCulloch. 2006. 'Multiple roles of alpha-smooth muscle actin in mechanotransduction', *Exp Cell Res*, 312: 205-14.

Watson, P. G., and R. D. Young. 2004. 'Scleral structure, organisation and disease. A review', *Exp Eye Res*, 78: 609-23.

Wildsoet, C., and J. Wallman. 1995. 'Choroidal and scleral mechanisms of compensation for spectacle lenses in chicks', *Vision Res*, 35: 1175-94.

Williams, K. M., G. Bertelsen, P. Cumberland, C. Wolfram, V. J. Verhoeven, E. Anastasopoulos, G. H. Buitendijk, A. Cougnard-Grégoire, C. Creuzot-Garcher, M. G. Erke, R. Hogg, R. Höhn, P. Hysi, A. P. Khawaja, J. F. Korobelnik, J. Ried, J. R. Vingerling, A. Bron, J. F. Dartigues, A. Fletcher, A. Hofman, R. W. Kuijpers, R. N. Luben, K. Oxele, F. Topouzis, T. von Hanno, A. Mirshahi, P. J. Foster, C. M. van Duijn, N. Pfeiffer, C. Delcourt, C. C. Klaver, J. Rahi, and C. J. Hammond. 2015. 'Increasing Prevalence of Myopia in Europe and the Impact of

Education', *Ophthalmology*, 122: 1489-97.

Witkovsky, P. 2004. 'Dopamine and retinal function', *Doc Ophthalmol*, 108: 17-40.

Witkovsky, P., C. Nicholson, M. E. Rice, K. Bohmaker, and E. Meller. 1993. 'Extracellular dopamine concentration in the retina of the clawed frog, Xenopus laevis', *Proc Natl Acad Sci U S A*, 90: 5667-71.

Woodman-Pieterse, E. C., S. A. Read, M. J. Collins, and D. Alonso-Caneiro. 2015. 'Regional Changes in Choroidal Thickness Associated With Accommodation', *Invest Ophthalmol Vis Sci*, 56: 6414-22.

Wu, H., W. Chen, F. Zhao, Q. Zhou, P. S. Reinach, L. Deng, L. Ma, S. Luo, N. Srinivasalu, M. Pan, Y. Hu, X. Pei, J. Sun, R. Ren, Y. Xiong, Z. Zhou, S. Zhang, G. Tian, J. Fang, L. Zhang, J. Lang, D. Wu, C. Zeng, J. Qu, and X. Zhou. 2018. 'Scleral hypoxia is a target for myopia control', *Proc Natl Acad Sci U S A*, 115: E7091-e100.

Wu, P. C., C. T. Chen, K. K. Lin, C. C. Sun, C. N. Kuo, H. M. Huang, Y. C. Poon, M. L. Yang, C. Y. Chen, J. C. Huang, P. C. Wu, I. H. Yang, H. J. Yu, P. C. Fang, C. L. Tsai, S. T. Chiou, and Y. H. Yang. 2018. 'Myopia Prevention and Outdoor Light Intensity in a School-Based Cluster Randomized Trial', *Ophthalmology*, 125: 1239-50.

Wu, P. C., M. N. Chuang, J. Choi, H. Chen, G. Wu, K. Ohno-Matsui, J. B. Jonas, and C. M. G. Cheung. 2019. 'Update in myopia and treatment strategy of atropine use in myopia control', *Eye (Lond)*, 33: 3-13.

Wu, P. C., H. M. Huang, H. J. Yu, P. C. Fang, and C. T. Chen. 2016. 'Epidemiology of Myopia', *Asia Pac J Ophthalmol (Phila)*, 5: 386-93.

Xi, L. Y., S. P. Yip, S. W. Shan, J. Summers-Rada, and C. S. Kee. 2017. 'Region-specific differential corneal and scleral mRNA expressions of MMP2, TIMP2, and TGFB2 in highly myopic-astigmatic chicks', *Sci Rep*, 7: 11423.

Yan, T., W. Xiong, F. Huang, F. Zheng, H. Ying, J. F. Chen, J. Qu, and X. Zhou. 2015. 'Daily Injection But Not Continuous Infusion of Apomorphine Inhibits Form-Deprivation Myopia in Mice', *Invest Ophthalmol Vis Sci*, 56: 2475-85.

Yang, I. H., G. E. Rose, D. G. Ezra, and M. Bailly. 2019. 'Macrophages promote a profibrotic phenotype in orbital fibroblasts through increased hyaluronic acid production and cell contractility', *Sci Rep*, 9: 9622.

Yuan, Y., M. Li, C. H. To, T. C. Lam, P. Wang, Y. Yu, Q. Chen, X. Hu, and B. Ke. 2018. 'The Role of the RhoA/ROCK Signaling Pathway in Mechanical Strain-Induced Scleral Myofibroblast Differentiation', *Invest Ophthalmol Vis Sci*, 59: 3619-29.

Zhang, Q., J. Duan, M. Olson, A. Fazleabas, and S. W. Guo. 2016. 'Cellular Changes Consistent With Epithelial-Mesenchymal Transition and Fibroblast-to-Myofibroblast Transdifferentiation in the Progression of Experimental Endometriosis in Baboons', *Reprod Sci*, 23: 1409-21.

Zhang, S., G. Zhang, X. Zhou, R. Xu, S. Wang, Z. Guan, J. Lu, N. Srinivasalu, M. Shen, Z. Jin, J. Qu, and X. Zhou. 2019. 'Changes in Choroidal Thickness and Choroidal Blood Perfusion in Guinea Pig Myopia', *Invest Ophthalmol Vis Sci*, 60: 3074-83.

Zhang, Y., and C. F. Wildsoet. 2015. 'RPE and Choroid Mechanisms Underlying Ocular Growth and Myopia', *Prog Mol Biol Transl Sci*, 134: 221-40.

Zhou, X., F. Ji, J. An, F. Zhao, F. Shi, F. Huang, Y. Li, S. Jiao, D. Yan, X. Chen, J. Chen, and J. Qu. 2012. 'Experimental murine myopia induces collagen type Iα1 (COL1A1) DNA methylation and altered COL1A1 messenger RNA expression in sclera', *Mol Vis*, 18: 1312-24.

Zhou, X., M. T. Pardue, P. M. Iuvone, and J. Qu. 2017. 'Dopamine signaling and myopia development: What are the key challenges', *Prog Retin Eye Res*, 61: 60-71.